JOURNAL OF CAVE AND KARST STUDIES

August 2009
Volume 71, Number 2
ISSN 1090-6924
A Publication of the National Speleological Society

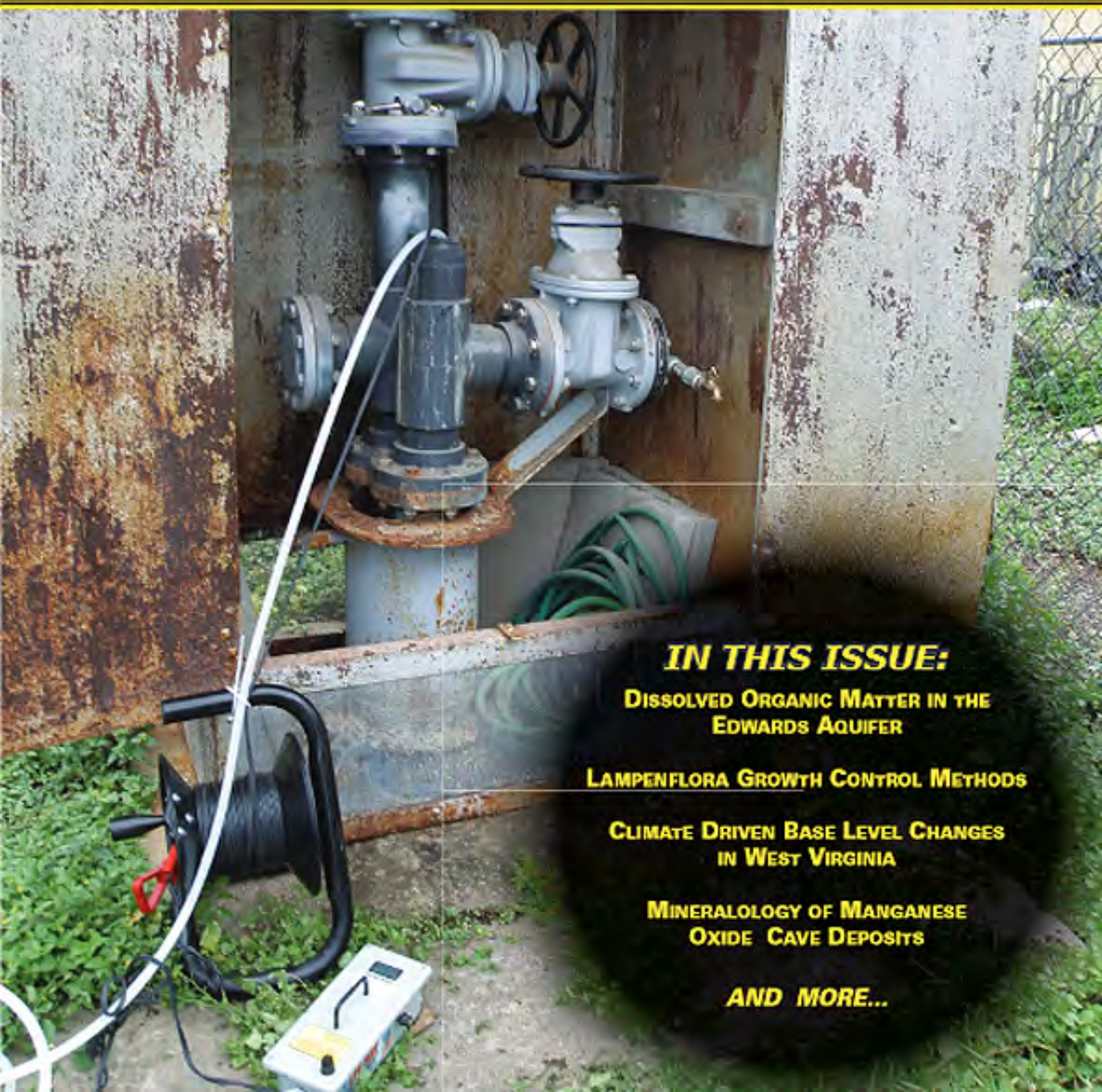

IN THIS ISSUE:

Published By
The National Speleological Society

The *Journal of Cave and Karst Studies* (ISSN 1090-6924, CPM Number 40016956) is a multi-disciplinary, refereed journal published three times a year by the National Speleological Society, 2813 Cave Avenue, Huntsville, Alabama 35810-4431 USA; Phone (256) 852-1300; Fax (256) 851-9241, email: nss@caves.org; World Wide Web: http://www.caves.org/pub/journal/.
Check the Journal website for subscription rates. Back issues and cumulative indexes are available from the NSS office.

POSTMASTER: send address changes to the *Journal of Cave and Karst Studies*, 2813 Cave Avenue, Huntsville, Alabama 35810-4431 USA.

The *Journal of Cave and Karst Studies* is covered by the following: ISI Thomson Services Science Citation Index Expanded, ISI Alerting Services, and Current Contents/Physical, Chemical, and Earth Sciences.

Front cover: Wellhead of typical artesian well in Edwards Aquifer Hail Water Zone, Texas, see Birdwell and Engel in this volume. Photo by A. S. Engel.

LAMPENFLORA ALGAE AND METHODS OF GROWTH CONTROL

JANEZ MULEC[1] AND GORAZD KOSI[2]

Abstract: Karst caves are unique natural features and habitats where specialized organisms live. Some caves are also important as cultural heritage sites. In recent decades, many caves have experienced intensified tourist visits. To attract visitors, artificial illumination was installed that changed conditions in the caves. As a result, communities of organisms called lampenflora develop in close and remote proximity to lights. These phototrophic organisms are inappropriate from an aesthetic point of view and cause the degradation of colonized substrata, which is a particular problem in caves with prehistoric art. Key factors that allow lampenflora to grow are light and moisture. Illuminated spots in caves can be quickly colonized by algae, some of which have broad tolerances for different substrata. Several phototrophs can survive in caves even at photon flux densities lower than the photosynthetic compensation point. In this paper, the pros and cons of physical, chemical, and biological methods to control phototrophic growth are reviewed and discussed. Experiences in show caves can be helpful in controlling undesirable algal growth in other environments.

INTRODUCTION

Caves have a special place in human history. Early in prehistory, humans discovered that caves can provide suitable temporary or permanent shelters. Later, man developed a different relation with caves, not only as shelter but also for their natural beauty and inspiration. In many caves around the globe, remnants of prehistoric man are found. Especially interesting are those caves with paintings. Many caves of natural and cultural importance are listed on the United Nations Educational, Scientific, and Cultural Organization (UNESCO) World Heritage List. Cave tourism is considered to be one of the oldest forms of tourism.

In recent decades, many caves have experienced intensified tourist visits. To attract visitors, artificial illumination was installed. Illuminated areas such as rocky surfaces, sediments, and artificial materials around lamps quickly become colonized by phototrophic organisms. This complex community of autotrophic photosynthetic organisms is called lampenflora and develops in natural and artificial caves around artificial light sources (Dobat, 1998). In this lampenflora community, various aerophytic algae, as well as some mosses and ferns dominate, and are usually strongly adhered to the substratum. Mosses and ferns, also part of lampenflora, are not discussed further because in the early phase of colonization and succession, algae, both prokaryotic cyanobacteria and eukaryotic algae, usually play the most important role, while mosses and ferns appear later in the succession. Vascular plants are sometimes found, but almost always as germinating shoots (Martinčič et al., 1981). Lampenflora is, relative to the aerophytic phototrophs from the cave entrances, completely independent of sunlight and other external climatic factors. In comparison with sunlight, artificial light sources show no oscillations in light intensity. Dobat (1972) named spots with growing lampenflora ecosystems in formation.

One of the characteristics of the natural cave environment is low nutrient input (Simon et al., 2007) that is changed with the introduction of light energy. Such drastic changes to the cave ecosystem directly and indirectly influence cave fauna. Higher nutrient input in cave environments enables newcomers to be more competitive than the originally present troglomorphic organisms. Consequently obligate cave-dwelling organisms are threatened and may become extinct without restoration of previous natural conditions (Pipan, 2005).

In the last few years, many different views about unwanted phototrophs in caves have appeared, but the main question was not what these green cave dwellers are, but how to prevent their growth (Planina 1974; Ash et al., 1975; Caumartin, 1977; Caumartin, 1986; Iliopoulou-Georgoudaki et al., 1993; Gurnee, 1994; Byoung-woo, 2002; Hazslinszky, 2002; Lochner, 2002; Olson, 2002; Merdenisianos, 2005). An important problem occurs when lampenflora becomes covered with $CaCO_3$, irrespective of whether this carbonate is a result of abiotic or biotic precipitation. Such an amorphous mix of dead phototrophs and $CaCO_3$ irreversibly destroys the natural heritage of speleothems or other objects of cultural value (Mulec, 2005). Loss of historic paintings and objects in caves due to biological activities is becoming an important problem. The purpose of this paper is to review various methods to control lampenflora growth and to select the most appropriate one.

[1] Karst Research Institute, Scientific Research Centre of the Slovenian Academy of Sciences and Arts, Titov trg 2, SI-6230 Postojna, Slovenia, janez.mulec@guest.arnes.si
[2] National Institute of Biology, Večna pot 111, SI-1000 Ljubljana, Slovenia, gorazd.kosi@nib.si

ALGAE OF THE LAMPENFLORA COMMUNITY

Biodiversity of lampenflora is low compared to the flora from cave entrances where cyanobacteria are dominant (Palik, 1964; Golubić, 1967; Buczkó and Rajczy, 1989; Vinogradova et al., 1995; Vinogradova et al., 1998; Asencio and Aboal, 2000a, b; Uher and Kováčik, 2002; Mulec et al., 2008). Mulec et al. (2008) demonstrated that the concentration of chlorophyll *a* per unit surface area of lampenflora algae was slightly higher (max. 2.44 μg cm^{-2}) compared to the epilithic algae from the cave entrance (max. 1.71 μg cm^{-2}). This difference can be explained due to the different light regimes in both microhabitats (i.e., changing light quality and irradiance levels during the day in the cave entrance), different periods of illumination, different *in situ* moisture levels, and different species composition. Generally speaking, areas around lamps have more stable conditions because they are deeper in the constant zone of the cave (Mulec et al., 2008).

As reported by Garbacki et al. (1999) in Belgian caves, Cyanobacteria made up 54% of the phototrophic organisms, Chrysophyta 30%, and Chlorophyta 16%. Dobat (1970) and Chang and Chang-Schneider (1991) recorded the percentages of phototrophs in German caves; Cyanobacteria 55%, Chrysophyta 14%, and Chlorophyta 31%. Cyanobacteria also prevailed in Slovenian caves with 51%, followed by Chrysophyta 27%, and Chlorophyta 22% (Dobat, 1973; Martinčič et al., 1981; Krivograd-Klemenčič and Vrhovšek, 2005; Mulec, 2005; Mulec et al., 2008). It was shown that cyanobacteria, *Aphanothece castagnei* and *Gloeocapsa sanguinea*, and green alga, *Stichococcus bacillaris*, were part of lampenflora in all three countries. Other species that appeared with high frequency included *Aphanocapsa grevillei*, *A. muscicola*, *Chondrocystis dermochroa*, *Chroococcus varius*, *C. westii*, *Gloeocapsa atrata*, *G. compacta*, *G. rupestris*, *Gloeothece rupestris*, *Leptolyngbya lurida*, *L. perelegans*, *Phormidium retzii*, *Schizothrix calcicola*, *Scytonema julianum* (Cyanobacteria), *Achnanthes* sp., *A. lanceolata*, *Elipsoidon oocystoides*, *Navicula contenta*, *Pinnularia borealis* (Chrysophyta), *Chlorella miniata*, *Gloeocystis polydermatica*, *Klebshormidium flaccidum*, *Pleurococus vulgaris*, and *Trentepohlia aurea* (Chlorophyta).

As soon as a lampenflora community is established, these phototrophic organisms start to colonize new, not yet established substrates. Although cyanobacteria are the most adaptable phototrophs to extreme environments, in habitats with less environmental stress, like illuminated spots around lamps, they are easily overgrown by fast-growing eukaryotic algae (Mulec, 2005). In a growth experiment, after 25 days of cultivation under cave conditions, the green alga *Chlorella* sp. had a 10-times greater increase in cell count when compared to the cyanobacterium *Chroococcus minutes* (Mulec et al., 2008). The two organisms are two common phototrophs that are found in subaerophytic habitats in caves. In the mature stage of species succession in the lampenflora community, cyanobacteria become much more abundant, and thus, community composition becomes more similar to the community from a cave entrance where cyanobacteria dominate (Mulec et al., 2008).

In another experiment, limestone disks placed around lamps in show caves were colonized by the following phototrophs: *Apatococcus lobatus*, *Chlorella* sp., *Lyngbya* sp., *Nostoc* sp., *Navicula mutica*, and *Trentepohlia aurea*. Similar composition of the algal community was observed when limestone disks were covered with Jaworski agar (Mulec, 2005), a culture medium commonly used in algology (Warren et al., 1997). Organisms identified on disks covered with agar were: *Apatococcus* cf. *lobatus*, *Chlorella* sp., *Lyngbya* sp., *Stichococcus bacillaris*, and *Trentepohlia aurea*. This later experiment confirmed that eukaryotic microalgae successfully and quickly colonize new stony surfaces around lamps. Fast-growing phototrophs can quickly re-colonize former niches, even with a high frequency of cleaning of rocky surfaces with biocides. Microscopic observations of scrapes from disk surfaces showed that disks covered with agar were colonized to a greater extent by bacteria and fungi when compared to the disks without agar covering (Mulec, 2005). Nevertheless, lampenflora algae are usually ubiquitous, fast reproducing, and adaptable soil algae (Rajczy, 1989). Existence of algae and other higher plants (i.e., ferns and mosses deep in show caves) demonstrates effective transport of viable propagules from outside the caves.

KEY ENVIRONMENTAL FACTORS THAT INFLUENCE LAMPENFLORA GROWTH

Three modes of transport of viable propagules into the karst underground can be distinguished: air currents, water flow, and introduction by animals and humans. (Dobat, 1970; Vegh, 1989). Conditions deep in the cave are usually very stable, but that can be changed when high amounts of energy are introduced. An important factor in the spreading of lampenflora and other organisms is local air currents caused by warm air in the proximity of strong lamps, especially halogen ones (500–1000 W) (Vegh, 1989). Increased temperature notably influences algal growth. Pulido-Bosch et al. (1997) used an incandescent lamp and found that at a distance of 50 cm from the light source the temperature was 8 °C higher than elsewhere. Even low energy lamps can change the cave climate. Mulec (2005) showed that relative humidity 20 cm from a 108 W lamp dropped from normal cave relative humidity of 95% to only 73% relative humidity (Fig. 1). Frequency of switching lights on and off affects relative humidity and temperature. At the point where the highest drop of relative humidity was observed, Mulec (2005) measured a temperature increase of 1.6 °C. Lampenflora do not develop in the immediate vicinity of strong lights due to very high temperature that kills the organisms. Visitors can

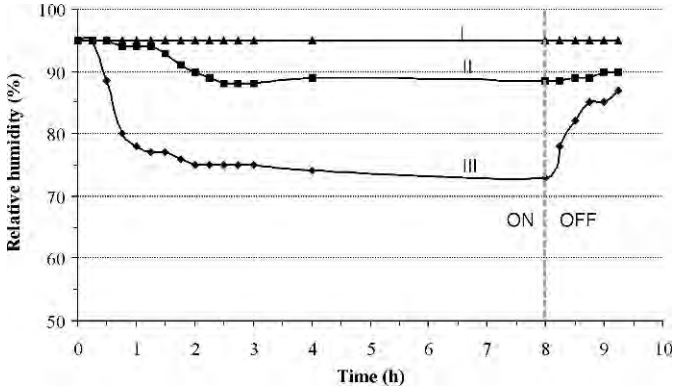

Figure 1. Changes in relative humidity are dependent on distance to the lamp at selected light intensities (I – 0 μmol photons m^{-2} s^{-1} (450 cm); II – 50 μmol photons m^{-2} s^{-1} (48 cm); III – 100 μmol photons m^{-2} s^{-1} (20 cm)) when the lamp was on and after it was switched off.

also increase cave temperatures. Mais (2004) reported that the presence of visitors in ice caves can start to melt the ice. As a consequence of mass tourism in caves, CO_2 concentration can exceed 5000 ppm (Pulido-Bosch et al., 1997). In addition to the natural corrosion processes in caves, the combined effect of an increase in CO_2 concentration and temperature variations induced by visitors can directly affect the intensity, and even the development, of wall corrosion processes. As shown by Sánchez-Moral et al. (1999) in a case study of Altamira Cave (Spain), the corrosion induced by visitors can be up to 78 times greater than the corrosion arising from natural processes.

Aerophytic algae can survive in the environment only when humidity is high enough. Generally, the presence of running and seeping water accelerates growth of plants in caves (Martinčič et al., 1981). Another important ecological parameter that affects algal growth is the type of substratum and the presence of sediment (Martinčič et al., 1981; Chang and Chang-Schneider, 1991). Shade acclimated algae (e.g., from caves) have high photosynthetic efficiencies and low light saturation (Grobbelaar et al., 2000). Some lampenflora algae can survive and reproduce even at light intensities that are lower than the photosynthesis compensation point (i.e., light intensity at which the amount of CO_2 fixed in sugars during photosynthesis is equal to the CO_2 released during respiration). In Slovenian show caves, growth of algae can appear in a light intensity as low as 0.33 μmol photons m^{-2} s^{-1} (Mulec, 2005). Martinčič et al. (1981) showed that algae in caves can survive at photon flux densities in the range of 0.5 to 1 μmol photons m^{-2} s^{-1}. Cyanobacteria and diatoms have an average compensation point between 5 and 6 μmol photons m^{-2} s^{-1}, while for green algae, it is generally around 21 μmol photons m^{-2} s^{-1} (Hill, 1996). In caves, heterotrophy must then play an important role, which is the case for many planktonic and benthic algae (Tuchman, 1996).

Interaction of Phototrophs with Substratum

Complex microbial communities can be found not only as an epilithion, but also inside the rock endolithion. For successful colonization, epilithic organisms must develop in a close interaction with the substratum. A substratum and its characteristics at the micro-level are one of the key factors for aerophytic algae, which were demonstrated with the absence of correlation between photon irradiance and chlorophyll *a* concentrations (Mulec et al., 2008). Epilithic algae also take up essential elements for growth from the base on which they are adhered (Warscheid and Braams, 2000; Hoffmann, 2002). In some cases, a substratum may not support, or can even inhibit, growth of organisms.

Organisms have developed several strategies to take up minerals by utilizing biogenic organic acids and siderophores (Warscheid and Braams, 2000). The often anionic exopolymers strongly absorb cations and dissolves organic molecules from the underlying minerals (Hoffmann, 2002). During the process of mechanical destruction of the rock, the cyanobacterial sheath and various polymers of the outer cell layers play an important role because they can absorb and release huge quantities of water. Such extension and contraction can mechanically destroy the substratum, which is even more evident when water freezes (Asencio and Aboal, 2001). All these biological activities lead to bio-oxidation of minerals and changes in the mineral structure of the rock, which leads to destruction, weathering, and increased porosity and permeability of water deep into the rock (Warscheid and Braams, 2000). Using pH electrodes at the micro-level, Albertano (1993) and Hoffmann (2002) demonstrated photosynthesis linked alkalization of the surrounding milieu, simultaneously with acidification from CO_2 released during fermentation and respiration. Alkalization during illumination induces precipitation of mineral mixtures (Albertano et al., 2000).

In poorly illuminated cave environments, the cyanobacteria *Geitleria calcarea* and *Scytonema julianum* are frequent cave dwellers. For both species, deposition of calcite on cell filaments at a thickness of up to 30 μm was observed. Incrustation of *G. calcarea* is probably controlled by the organism itself (Pentecost and Whitton, 2000). On the outer cell layers of *Leptolyngbya* and *Dischereella*, a huge amount of $CaCO_3$ was also observed (Albertano, 1997). Precipitation of mineral particles on sheaths causes epilithic strains to become endolithic (Asencio and Aboal, 2001). In caves, *G. calcarea*, *S. julianum*, *Loriella osteophila*, and *Herpyzonema pulverulentum* are the best characterized organisms that are able to mobilize calcium ions from the carbonate substrata (Hernandez-Marine and Canals, 1994; Hernandez-Marine et al., 1999).

Biodeterioration processes are undesirable in caves of special cultural or natural heritage. A thick biofilm composed of phototrophs responsible for calcite precipitation and bio-corrosion growing on illuminated prehistoric and more recent cave paintings has been identified by Pietrini and Ricci (1993), Asencio and Aboal (2001), and Cañaveras et al. (2001). It seems that light intensity influences the change of the organisms from epilithic to the endolithic phase (Asencio and Aboal, 2001). When illumination is too high, some epilithic algae simply switch to the endolithic phase. Depending upon the growth as epilithic or endolithic, some species can change their cell size (Asencio and Aboal, 2000b). However, once the substratum is colonized by these organisms and precipitation of $CaCO_3$ starts, the deposited carbonate can act as protection against excessively high photon-flux intensity. Extremely strong illumination causes other changes on the substratum to appear. In Castelana Cave (Italy), it was observed that at a distance of 50 cm from a 1000 W lamp, aragonite crystals started to grow over calcite stalagmites (Hill and Forti, 1997).

CONTROL OF GROWTH OF PHOTOTROPHS IN CAVES

As previously discussed, the lampenflora has various negative effects on the cave environment and in caves with important cultural heritage. Problems connected with illumination and phototrophic biofilms are usually not properly solved. The main obstacle is because the cause (i.e., light) remains on the site and the proper way of preventing lampenflora growth is still missing. The simplest solution to preventing lampenflora growth in a cave would be complete removal of existing phototrophic communities, cessation of the illumination, and abolition of tourist visits, which of course, is not acceptable to the cave management.

Some algae can tolerate the absence of illumination for short or longer periods of time (Dalby, 1966). Once visible lampenflora appears it should be removed. Hazslinszky (2002) reported that in Baradla Cave (Hungary) without any intervention, lampenflora spread quickly, doubling from 1977 to 1984.

Many approaches to lampenflora control in caves have already been tested, including physical, chemical, and biological control.

PHYSICAL METHODS

Cleaning of speleothems overgrown by algae with water and brush is not recommended because the infestation can be more easily dispersed throughout the cave (Rajczy, 1989; Hazslinszky, 2002). The mechanical removal of lampenflora with water and brushes damages the fragile crystals structure of speleothems. Cleaning with high pressure vapour destroys tiny flowstone forms (Ash et al., 1975).

The simplest way to restrict lampenflora growth is time limited illumination of the caves with an automatic switch system to shut down the lighting whenever the user is absent. Planina (1974) estimated that lampenflora cannot develop to a great extent if illumination in the cave does not exceed 100 h yr^{-1}. Growth and spread is further limited if illumination of damp surfaces is avoided (Rajczy, 1989). Byoung-woo (2002) recommended increasing the illumination distance between speleothems and light source by more than two meters.

Growth of phototrophs can be notably diminished by the reduction of light intensity (Gurnee, 1994) and by using special lamps that emit light at wavelengths which do not support maximum absorption of the main photosynthetic pigments (Caumartin, 1986). In Mammoth Cave (USA), Olson (2002) used light-emitting diodes (LEDs) to control lampenflora. Yellow-light (595 nm) LEDs at an intensity of 49.5 lx prevented growth for 1.5 years after complete lampenflora removal. Despite the yellowish light, the LEDs still gave a natural appearance to the cave (Olson, 2002). Quantitative analyses of biofilms formed by the cyanobacterium, *Gloeothece membranacea*, and green alga, *Chlorella sorokiniana*, illuminated exclusively with white or green light suggested that illumination by green light can be a possible treatment for preventing photosynthetic biofilm growth (Roldán et al., 2006). Lochner (2002) determined that using ozone producing lamps did not significantly diminish the lampenflora in Saalfelder Feengrotten Cave (Germany). Suppression of the lampenflora can be achieved using UV irradiation due to its known germicidal effect, but it was shown that it has only a transitory suppressing effect (Dobat, 1998). Lampenflora does not develop, or it develops very slowly, if a dispersed mode of illumination is used, as was done at the speleotherapy station for patients with pulmonary diseases of Sežana Hospital (Slovenia) (Mulec, 2005). Several health centers around the world use speleotherapy to heal bronchial, allergic, and rheumatic diseases. The healing effect is attributed to special properties of air in the subterranean spaces, stability of the temperature, humidity, pressure, and content of gaseous components. The ions in aerosols have not only local disinfectant and anti-inflammatory effect, but they also stimulate the human immune system (Jirka, 1999).

More attention should be applied to planning the illumination system in newly opened show caves and to renovation of systems in existing show caves. An important step in controlling lampenflora growth is appropriate installation of lamps and housings and modes of illumination. In caves with previously installed lamps, lighting of individual sectors with automatic switch systems must be implemented as soon as possible. Reducing the intensity and period of illumination also brings a benefit in reduced energy costs. Light spectra of lamps must be carefully considered. Illuminated places and spots that would be interesting for tourists must be carefully selected, especially places with dripping and seeping water. Lighting sediments and mud should be avoided. Touching of speleothems by

visitors with clothes, fingers, or other materials should be reduced as much as possible, because this results in introduction of nutrients and microbes into caves and cessation of carbonate deposition. Finally, placement of lamps in areas with strong air circulation should be thoroughly considered due to possible increases in lampenflora dispersion.

CHEMICAL METHODS

Chemical substances which would be suitable to control lampenflora growth must fulfill the criteria of minimum side effects on the cave environment and organisms while providing humans with high efficacy in suppressing phototrophs. These biocides should have long lasting effects without any negative influences on cave rocks, speleothems, and electro-installation materials.

Use of DCMU (diuron, N-3, 4-dichlorophenyl-N′-dimetil urea) and bromine compounds as suggested by Caumartin (1977) are absolutely inappropriate due to toxicity. Selective herbicides such as Atrazine (6-Chloro-N-ethyl-N′-(1methylethyl)-1,3,5-triazine-2,4-diamine) and Simazine (6-Chloro-N,N′-diethyl-1,3,5-triazine-2,4-diamine) are not suitable for widespread use in caves since the green coloring on the karst formations persists (Grobbelaar, 2000).

Effective and less toxic biocides are sodium hypochlorite (NaOCl) (Zelinka et al., 2002) or calcium hypochlorite ($Ca(OCl)_2$) (Iliopoulou-Georgoudaki et al., 1993), but some filamentous cyanobacteria, such as *Scytonema julianum* and *Leptolyngbya* spp. trapped in the pores of bedrock, can still survive and later reproduce (Iliopoulou-Georgoudaki et al., 1993). Other authors have suggested formalin (Cubbon, 1976; Caumartin, 1986; Merdenisianos, 2005), cupric ammoniac solution (Merdenisianos, 2005), or butyl alcohol (Hill and Forti, 1997). Sodium hypochlorite successfully restricts growth of lampenflora in caves, but it represents a large burden for the cave environment. From the hypochlorite solution, gaseous chlorine can be released. In the reaction of hypochlorite with ammonia and other nitrogenous compounds, toxic chloramines and even carcinogenic trihalomethanes are released. Low chlorine concentration in the cave environment can kill microbiota, which represents an important source of nutrients for cave-dwelling organisms. Chlorine causes lowering of the pH and thus dissolves calcite (Faimon et al., 2003). Even $Ca(OCl)_2$ is a quite efficient biocide, but it is, like NaOCl, responsible for reddish coloration of carbonate substrata due to the oxidation of Fe^{2+} into Fe^{3+} that precipitates as an amorphous iron hydroxide ($Fe(OH)_3$) (Iliopoulou-Georgoudaki et al., 1993).

For suppressing lampenflora growth, Faimon et al. (2003) suggested use of hydrogen peroxide (H_2O_2) instead of an aggressive 5% aqueous solution of NaOCl. The key question regarding using H_2O_2 is what concentration is high enough to destroy the lampenflora and yet does not have a deteriorating effect on speleothems. A 15% solution of H_2O_2 is sufficient to kill phototrophic organisms if it is applied three times over two to three weeks. However, even a 15% solution of H_2O_2 attacks carbonate bedrock more aggressively than karst water (Faimon et al., 2003). Grobbellar (2000) suggested the following procedure to eradicate lampenflora: application of 200–500 mg L^{-1} H_2O_2 and after 5–30 minutes washing and collecting of the wash water. If lampenflora persists, the application can be repeated or UV-C radiation can be applied, or the area can be sprayed with 20–50 m L^{-1} of Atrazine. Grobbellar (2000) experienced that spraying with H_2O_2 and washing is only required once every six months to a year due to the slow growth rates of the algae. In practice, in order to kill lampenflora in show caves, other commercially available biocides are also applied.

In some caves, lampenflora becomes progressively covered with flowstone and it turns slowly into an amorphous greenish mass of dead biomass. Yellowish-green speleothems remain preserved in caves for years, because the main photosynthetic pigment chlorophyll *a* is not water soluble and carbonate depositing dripping water cannot simply rinse it away (Mulec, 2005). To remove the green color from flowstone, one should use a solution in which chlorophyll *a* is soluble and that has minimal effects on the cave environment. As eligible substances, several non-polar solvents can be used, including alcohols, dietyl-ether, benzene, or acetone (Meeks, 1974). Procedures with minimal negative effects on the environment should be developed. In any case, the porosity and permeability of each flowstone should be taken into consideration, which further complicates the procedure.

BIOLOGICAL METHODS

To date, no studies on the use of biological methods to control lampenflora have been done. One possible way to restrict lampenflora growth is the use of biological antagonists like genetically modified viruses[1]. Another approach would be inactivation of those factors which are crucial for development and establishment of lampenflora community, such as cell signalling molecules, or molecules which are necessary for metabolism of iron (Albertano, 2003).

CONCLUSIONS

Caves are important for humans because they represent geomorphologic, geologic, biologic, historical, archaeological, and paleontological laboratories. Caves are sometimes the only source of information of past geological events. People visit caves due to esthetical, recreational, educational, health, and religious purposes. Anthropogenic influences in fragile cave environments have many consequences; and therefore, everything should be conducted in

[1] Editor's Note: Introducing exotic species to selected areas for the purpose of controlling other unwanted species often results in new, unexpected, and typically much worse environmental problems.

ways that minimize these effects (Boston et al., 2004). In artificially illuminated caves, lighting results in temperature and relative humidity changes in the cave environment. Lampenflora growth as a result of this interference must be restricted. To control its growth, several physical, chemical, and biological methods can be adopted. However, at the moment, there is no ideal solution. The most suitable method, or combinations of methods, are still under investigation.

Cave management should not open new parts of a cave or new caves to the public without careful study, and cave management should not show everything in the brightest way to the tourists. Rather, it should be done in such a way so that some natural or cultural heritage remains in dim aspect of admiring beauty, as it was at the beginning of cave tourism.

ACKNOWLEDGEMENTS

Some results included in this paper were accomplished in the framework of the project no. Z6-7072 "Role and significance of microorganisms in karst processes" supported by the Slovenian Research Agency. The authors are grateful to David C. Culver for helpful comments on an earlier version of the manuscript and revision of the English text.

REFERENCES

Albertano, P., 1993, Epilithic algal communities in hypogean environments: Giornale Botanico Italiano, v. 127, no. 3, p. 386–392.

Albertano, P., 1997, Elemental mapping as tool in the understanding of microorganisms-substrate interactions: Journal of Computer-Assisted Microscopy, v. 9, no. 2, p. 81–84.

Albertano, P., Bruno, L., D'Ottavi, D., Moscone, D., and Palleschi, G., 2000, Effect of photosynthesis on pH variation in cyanobacterial biofilms from Roman catacombs: Journal of Applied Phycology, v. 12, p. 279–384.

Albertano, P., 2003, Methodological approaches to the study of stone alteration caused by cyanobacterial biofilms in hypogean environments, *in* Koestler, R.J., Koestler, V.R., Charola, A.E., and Nieto-Fernandez, F.E., eds., Art, Biology, and Conservation: Biodeterioration of Works of Art, New York, The Metropolitan Museum of Art, p. 302–315.

Asencio, A.D., and Aboal, M., 2000a, Algae from La Serreta cave (Murcia, SE Spain) and their environmental conditions: Archiv für Hydrobiologie: Supplementband, Algological Studies, v. 131, no. 96, p. 59–78.

Asencio, A.D., and Aboal, M., 2000b, A contribution to knowledge of chasmoenolithic algae in cave-like environments: Archiv für Hydrobiologie: Supplementband, Algological Studies, v. 133, no. 98, p. 133–151.

Asencio, A.D., and Aboal, M., 2001, Biodeterioration of wall paintings in caves of Murcia (SE Spain) by epilithic and chasmoendolithic microalgae: Archiv für Hydrobiologie: Supplementband, Algological Studies, v. 140, no. 103, p. 131–142.

Ash, J., Ashton, K., Bonny, A., Dimond, P., Hendy, C., May, B., Nelson, C., Wheeler, D., and Williams, P., 1975, Report on the conservation of Waitomo caves: New Zealand Speleological Bulletin, v. 5, no. 93, p. 373–396.

Boston, P.J., Northup, D., and Lavoie, K.H., 2004, Protecting microbial habitats: preserving the unseen, *in* Hildreth-Werker, V., and Werker, J.C., eds., Cave conservation and restoration, Huntsville, AL., National Speleological Society, p. 67–88.

Buczkó, K., and Rajczy, M., 1989, Contributions to the flora of the Hungarian caves II. Flora of the three caves near Beremend, Hungary: Studia Botanica Hungarica (Antea: Fragmenta Botanica), v. 21, p. 13–26.

Byoung-woo, K., 2002, Ecological study for the control of green contamination in Korean show caves, *in* Proceedings, 4th Samcheok International Cave Symposium, Samcheok City, South Korea, Kangwon Development Research Institute, p. 74–76.

Cañaveras, J.C., Sanchez-Moral, S., Soler, V., and Saiz-Jimenez, C., 2001, Microorganisms and microbially induced fabrics in cave walls: Geomicrobiology Journal, v. 18, no. 3, p. 223–240.

Caumartin, V., 1977, Conservation des cavernes aménagées. Resultats obtenus dans quelques pays d'Europe occidentale, *in* Ford, T.D., ed., Proceedings of the 7th International Congress of Speleology, Sheffield, U.K., University of Leicester, p. 96–98.

Caumartin, V., 1986, La conservation des concrétions dans les cavernes aménagées, *in* Proceedings, 9° congreso international de espeleología, Barcelona, Spain, Comisión Organizadora del IX Congreso International de Espeleología, v. 2, p. 223–225.

Chang, T.P., and Chang-Schneider, H., 1991, Algen in vier süddeutschen Höhlen: Berichte der Bayerischen Botanischhen Gesellschaft, v. 62, p. 221–229.

Cubbon, B.D., 1976, Cave flora, *in* Ford, T.D., and Cullingford, C.H.D., eds., The science of speleology, London, U.K., Academic Press, p. 423–452.

Dalby, D.H., 1966, The growth of plants under reduced light: Studies in Speleology, v. 1, no. 4, p. 193–203.

Dobat, K., 1970, Considérations sur la végétation cryptogamique des grottes du Jura Souabe (sud-ouest de l'Allemagne): Annales de Spéléologie, v. 25, no. 4, p. 872–907.

Dobat, K., 1972, Ein Ökosystem in Aufbau: Die "Lampenflora Schauhöhlen": Umschau in Wissenschaft und Technik, v. 72, no. 15, p. 493–494.

Dobat, K., 1973, Ein Beitrag zur eingangs–, Lampen– und Pilzflora der Postojnska jama ("Adelsberger Grotte" bei Postojna, Jugoslawien): Razprave, Slovenska akademija znanosti in umetnosti, v. 16, no. 2, p. 123–143.

Dobat, K., 1998, Flore de la lumiére artificiélle (lampenflora-maladie verte), *in* Juberthie, C., and Decu, V., eds., Encyclopaedia Biospeleologica, Tome 2, Société de Biospéologie, Moulis-Bucarest, p. 1325–1335.

Faimon, J., Štelcl, J., Kubešová, S., and Zimák, J., 2003, Environmentally acceptable effect of hydrogen peroxide on cave "lamp-flora", calcite speleothems and limestones: Environmental Pollution, v. 122, p. 417–422.

Garbacki, N., Ector, L., Kostikov, I., and Hoffmann, L., 1999, Contribution à l'étude de la flore des grottes de Belgique: Belgian Journal of Botany, v. 132, no. 1, p. 43–76.

Golubić, S., 1967, Algenvegetation der Felsen: Eine ökologische Algenstudie im dinarischen Karstgebiet, *in* Elster, H.J., and Ohle, W., eds., Die Binnengewässer, Stuttgart, Germany, Band XXIII, E. Schweizerbart'sche Verlagsbuchhandlung, 183 p.

Grobbelaar, J.U., 2000, Lithophytic algae: A major threat to the karst formation of show caves: Journal of Applied Phycology, v. 12, p. 309–315.

Gurnee, J., 1994, Management of some unusual features in the show caves in the United States: International Journal of Speleology, v. 23, no. 1–2, p. 13–17.

Hazslinszky, T., 2002, Übersicht der Lampenflorabekämpfung in Ungarn, *in* Hazslinszky, T., ed., International Conference on Cave Lighting, Budapest, Hungary, Hungarian Speleological Society, p. 41–50.

Hernandéz-Mariné, M., Asencio, A.D., Canals, A., Ariño, X., Aboal, M., and Hoffmann, L., 1999, Discovery of population of the lime-incrusting genus *Loriella* (Stigonematales) in Spanish caves: Archiv für Hydrobiologie: Supplementband, Algological Studies, v. 129, no. 94, p. 121–138.

Hernandéz-Mariné, M., and Canals, T., 1994, *Herpyzonema pulverulentum* (Mastigocladaceae), a new cavernicolous atmophytic and lime-incrusted cyanophyte: Archiv für Hydrobiologie: Supplementband, Algological Studies, v. 105, no. 75, p. 123–136.

Hill, C., and Forti, P., 1997, Cave Minerals of the World, 2nd edition, Huntsville, AL., National Speleological Society, 463 p.

Hill, W.R., 1996, Effects of light, *in* Stevenson, R.J., Bothwell, M.L., and Lowe, R.L., eds., Algal ecology: freshwater benthic ecosystems, San Diego, Academic Press, p. 121–144.

Hoffmann, L., 2002, Caves and other low-light environments: aerophitic photoautotrophic microorganisms, *in* Bitton, G., ed., Encyclopedia of environmental microbiology, New York, John Wiley & Sons, p. 835–843.

Jirka, Z., 1999, Introduction, *in* 11th International Symposium of Speleotherapy Zlaté Hory, International Union of Speleology, Permanent International Commission of Speleotherapy, Zlaté Hory, p. 5–6.

Krivograd-Klemenčič, A., and Vrhovšek, D., 2005, Algal flora of Krška jama cave, Slovenia, Sborník Národního Muzea v Praze, Řada B, Přírodní Vědy: Historia Naturalis, v. 61, no. 1–2, p. 77–80.

Iliopoulou-Georgoudaki, J., Pantazidou, A., and Theoulakis, P., 1993, An assessment of cleaning photoautotropic microflora: The case of "Perama" cave, Ioannina Greece: Mémoires de Biospéologie, v. 20, p. 117–120.

Lochner, B., 2002, Extreme Lampenfloraentwicklung durch falsche Beleuchtung in den "Saalfelder Feengrotten", *in* Hazslinszky, T., ed., Proceedings, International Conference on Cave Lighting, Budapest, Hungary, Hungarian Speleological Society, p. 77–90.

Mais, K., 2004, The influence of visitors on alpine show caves, *in* Dvorščak, K., Kranjc, A., Mihevc, A., Paternost, S., Šajn, S., and Zupan-Hajna, N., eds., Proceedings, 4th International ISCA Congress, Postojna, Slovenia, Postojnska jama, turizem, d.d., p. 201–208.

Martinčič, A., Vrhovšek, D., and Batič, F., 1981, Flora v jamah z umetno osvetlitvijo: Biološki Vestnik, v. 29, no. 2, p. 27–56.

Meeks, J.C., 1974, Chlorophylls, *in* Stewart, W.D.P., ed., Algal physiology and biochemistry, Oxford, U.K., Blackwell Scientific Publications, p. 161–175.

Merdenisianos, C., 2005, The maladie verte (green disease) of the caves, *in* Proceedings, 14th International Congress of Speleology, Athens-Kalamos, Greece, Hellenic Speleological Society, p. 160–162.

Mulec, J., 2005, Algae in the karst caves of Slovenia [Ph.D. thesis], Ljubljana, Slovenia, University of Ljubljana, 149 p.

Mulec, J., Kosi, G., and Vrhovšek, D., 2008, Characterization of cave aerophytic algal communities and effects of irradiance levels on production of pigments: Journal of Cave and Karst Studies, v. 70, no. 1, p. 3–12.

Olson, R., 2002, Control of lamp flora in Mammoth Cave National Park, *in* Hazslinszky, T., ed., International Conference on Cave Lighting, Budapest, Hungary, Hungarian Speleological Society, p. 131–136.

Palik, P., 1964, Über die Algenwelt der Höhlen in Ungarn: International Journal of Speleology, v. 1, no. 1–2, p. 35–44.

Pentecost, A., and Whitton, B.A., 2000, Limestones, *in* Whitton, B.A., and Potts, M., eds., The ecology of cyanobacteria: Their diversity in time and space, Dordrecht, The Netherlands, Kluwer Academic Publishers, p. 257–279.

Pietrini, A.M., and Ricci, S., 1993, Occurence of a calcareous blue-green alga, *Scytonema julianum* (Kütz) Meneghini, on the frescoes of a church carved from the rock in Matera, Italy: Cryptogamic Botany, v. 3, p. 290–295.

Pipan, T., 2005, Epikarst—A promising habitat: copepod fauna, its diversity and ecology: A case study from Slovenia (Europe), Ljubljana, Slovenia, ZRC Publishing, 101 p.

Planina, T., 1974, Preprečevanje rasti vegetacije ob lučeh v turističnih jamah: Naše Jame, v. 16, p. 31–35.

Pulido-Bosch, A., Martin-Rosales, W., López-Chicano, M., Rodrigues-Navarro, C.M., and Vallejos, A., 1997, Human impact in a tourist karstic cave (Aracena, Spain): Environmental Geology, v. 31, no. 3–4, p. 142–149.

Rajczy, M., 1989, The flora of Hungarian caves, Karszt és Barlang, Special issue, p. 69–72.

Roldán, M., Oliva, F., Gónzales del Valle, M.A., Saiz-Jimenez, C., and Hernández-Mariné, M., 2006, Does green light influence the fluorescence properties and structure of phototrophic biofilms?: Applied and Environmental Microbiology, v. 72, no. 4, p. 3026–3031.

Sánchez-Moral, S., Soler, V., Cañaveras, J.C., Sanz-Rubio, E., Van Grieken, R., and Gysels, K., 1999, Inorganic deterioration affecting the Altamira Cave, N Spain: Quantitative approach to wall-corrosion (solutional etching) process induced by visitors: The Science of the Total Environment, v. 243–244, p. 67–84.

Simon, K.S., Pipan, T., and Culver, D.C., 2007, A conceptual model of the flow and distribution of organic carbon in caves: Journal of Cave and Karst Studies, v. 69, no. 2, p. 279–284.

Tuchman, N.C., 1996, The role of heterotrophy in algae, *in* Stevenson, R.J., Bothwell, M.L., and Lowe, R.L., eds., Algal Ecology: Freshwater Benthic Ecosystems, San Diego, Academic Press, p. 299–316.

Uher, B., and Kováčik, L., 2002, Epilithic cyanobacteria of subaerial habitats in National Park Slovak Paradise: Bulletin Slovenskej Botanickej Spoločnosti, v. 24, p. 25–29.

Vegh, Z., 1989, The problem of the lampflora in Baradla cave, *in* Proceedings of the 10th International Congress of Speleology, Budapest, Hungary, Hungarian Speleological Society, Budapest, p. 559–561.

Vinogradova, O.N., Kovalenko, O.V., Wasser, S., Nevo, E., Tsarenko, P.M., Stupina, V.V., and Kondratiuk, E.S., 1995, Algae of the Mount Carmel National Park (Israel): Algologia, v. 5, no. 2, p. 178–192.

Vinogradova, O.N., Kovalenko, O.V., Wasser, S.P., Nevo, E., and Weinstein-Evron, M., 1998, Species diversity gradient to darkness stress in blue–green algae/cyanobacteria: a microscale test in a prehistoric cave, Mount Carmel, Israel: Israel Journal of Plant Sciences, v. 46, p. 229–238.

Warren, A., Day, J.G., and Brown, S., 1997, Cultivation of algae and protozoa, *in* Hurst, C.J., Knudsen, G.R., McInerney, M.J., Stetzenbach, L.D., and Walter, M.V., eds., Manual of Environmental Microbiology, Washington, D.C., Washington, American Society for Microbiology, p. 61–71.

Warscheid, T., and Braams, J., 2000, Biodeterioration of stone: a review: International Biodeterioration and Biodegradation, v. 46, p. 343–368.

Zelinka, J., Hebelka, J., Fillo, M., and Novomeský, J., 2002, Illumination reconstruction in Slovakian show caves in relation to "lampflora" creation prevention, *in* Hazslinszky, T., ed., International Conference on Cave Lighting, Budapest, Hungary, Hungarian Speleological Society, p. 151–157.

J.A. Yoder, J.B. Benoit, B.S. Christensen, T.J. Croxall, and H.H. Hobbs III – Entomopathogenic fungi carried by the cave orb weaver spider, *Meta ovalis* (Araneae, Tetragnathidae), with implications for mycoflora transer to cave crickets. *Journal of Cave and Karst Studies,* v. 71, no. 2, p. 116–120.

ENTOMOPATHOGENIC FUNGI CARRIED BY THE CAVE ORB WEAVER SPIDER, *META OVALIS* (ARANEAE, TETRAGNATHIDAE), WITH IMPLICATIONS FOR MYCOFLORA TRANSER TO CAVE CRICKETS

Jay A. Yoder[1], Joshua B. Benoit[2], Brady S. Christensen[1], Travis J. Croxall[1], and Horton H. Hobbs III[1]

Abstract: We report the presence of the entomopathogenic fungi, *Beauveria* spp. and *Paecilomyces* spp., associated with female adults of the cave orb weaver spider, *Meta ovalis*, from Laurel Cave (Carter Cave State Resort Park, Carter Co., Kentucky). There was also an abundance of saprophytic *Aspergillus* spp., *Mucor* spp., *Penicillium* spp., *Rhizopus* spp., and to a lesser extent, *Absidia* spp., *Cladosporium* spp., *Mycelia sterilia*, and *Trichoderma* spp. These are mostly saprobes that reflect the mycoflora that are typical of the cave environment. Incubation at 25 °C resulted in increased growth of all fungi compared to growth at 12 °C (cave conditions) on each of four different kinds of culture media, indicating that the cave environment is suppressive for the growth of these fungi. Topically-applied inocula of *Beauveria* sp. and *Paecilomyces* sp. (spider isolates) were not pathogenic to *M. ovalis*, but these fungi were pathogenic to the cave cricket, *Hadenoecus cumberlandicus*. One possibility is that the *Beauveria* spp. and *Paecilomyces* spp. carried by *M. ovalis* could negatively impact the survival of cave crickets that co-occur with these spiders, thus possibly altering the ecological dynamics within the caves.

Introduction

A mycological survey of the cave orb weaver spider, *Meta ovalis*, was done to provide information related to factors that may influence spider population dynamics. We determined which fungi may be potential spider pathogens (internal mycoflora) and which may be spread to other cavernicolous invertebrates (external mycoflora), especially cave crickets. Our study was done in Laurel Cave (38° 22′ 30.8″ N, 83° 06′ 55.4″ W), in the cold, dry upper level (Pfeffer et al., 1981). This is a small cave (total length 1019 m) developed in Mississippian limestone and located in Carter Cave State Resort Park, Carter Co., Kentucky where these spiders have been found to be particularly abundant. *M. ovalis* occurs most commonly in the entrance and twilight zone of Laurel Cave and occasionally in the deeper parts of the cave. Whether migration occurs between cave and epigean environments is not known, but they can be found outside on occasion. We do not usually observe individuals of *M. ovalis* especially close to one another; they appear to be inactive most of the time, hanging attached to some part of the web, seemingly more on the periphery, but whether this is the preferred placement on the web is not known. Little, if any, information exists on their reproductive cycle or life history. They are not classic cave-adapted organisms that are K-strategists that produce a very small number of offspring (Hobbs, 1992); rather, they produce a sizeable egg case (exact number of eggs is not known) with numerous offspring, thus being more characteristic of r-strategists. Exact data on their longevity are lacking, but we speculate that they have a fairly long life (Lavoie et al., 2007).

In Laurel Cave, individuals of *M. ovalis* are virtually never found on the cave floor or low on cave walls and appear to prefer ceilings and upper walls in areas that are recessed (termed kettles or bells) and out of the desiccating impact of air currents. Often, these spiders are in close proximity to cave crickets (both *Ceuthophilus* spp. and *Hadenoecus* spp.), sometimes as close as several centimeters, with no apparent impact on crickets (Yoder et al., 2009) even though they are regarded as cricket predators. Millipedes, other spiders, and carabid beetles are other possible prey (Lavoie et al., 2007). *Hadenoecus* spp., in particular *H. cumberlandicus* in Laurel Cave, are notoriously found in caves and have importance as a keystone species by supplying food (guano) to an array of millipedes, flies, and beetles that reside under the cricket roost (Lavoie et al., 2007). Dense aggregations, consisting of up to hundreds of individuals, are the hallmark behavior of *Hadenoecus* spp. (Studier et al., 1986; Yoder et al., 2002). In Laurel Cave, *M. ovalis* is reliably found close by these cricket aggregations (Yoder et al. 2009), which makes *M. ovalis* relevant for influencing the cave ecosystem by impacting the cave crickets.

[1] Department of Biology, Wittenberg University, Ward Street at North Wittenberg Avenue, Springfield, OH 45501. jyoder@wittenberg.edu
[2] Department of Entomology, The Ohio State University, 318 West 12th Avenue, Columbus, OH 43210

Table 1. External mycoflora of cave orb weaver spider, *Meta ovalis*, from Laurel Cave (Carter County, Kentucky, USA). NA, nutrient agar; BA, blood agar; MMN, modified Melin-Norkrans agar; PDA, potato dextrose agar.

	No. external isolates from *Meta ovalis* (n = 40 spiders)					
Fungi	NA	BA	MMN	PDA	Total	%
Absidia spp.	1	0	2	1	4	8.3
Aspergillus spp.	1	1	5	4	11	22.9
Beauveria spp.	0	0	0	2	2[a]	4.2
Cladosporium spp.	1	0	1	0	2	4.2
Mucor spp.	1	2	2	2	7	14.6
Mycelia sterilia	0	0	2	2	4	8.3
Paecilomyces spp.	0	1	1	0	2[a]	4.2
Penicillium spp.	2	1	2	2	7[a]	14.6
Rhizopus spp.	2	1	3	2	8	16.7
Trichoderma spp.	0	0	1	0	1	2.1
Total	8	6	19	15	48	

[a] Fungus that was also isolated internally.

Methods

A total of 40 spiders were used; ten each for four different embedding media, with five being used for external isolations and five being used for internal isolations. The test group of 40 spiders represents several collecting trips, 2004–2007, to prevent depleting the population, but they were collected during the same time of year, August–November. The test groups were divided, one for growth at 12 °C and the other at 25 °C.

Standard aseptic technique was followed for spider collection, and specimens were plated less than 12 h after collection. Only female adults spiders were used (identified according to Ubick et al., 2005). Embedding media were blood agar-lyophilized bovine blood (BA), modified Melin-Norkrans agar (MMN), nutrient agar (NA) and potato dextrose agar (PDA) to maximize recovery of fungi that might be fastidious. Incubation conditions were 12 ± 1 °C (to mimic Laurel Cave; Hill, 2003) in total darkness.

Preparation of samples for external fungus recovery involved placing a spider into a Petri dish, covering with molten embedding media (one dead spider per dish), incubation, daily examination (100×) for hyphae (typically 5–10 days), excising a single hyphal tip by a scalpel (100×, tracing hypha to spider's body surface), placing the agar block containing tip on a fresh plate of solidified media, and daily examination until culture characteristics appeared for identification (criteria of Barnett and Hunter, 1998). Isolates that failed to produce identifiable structures were designated as *Mycelia sterilia*; sterility is common for cave fungi due to unchanging environmental conditions and darkness (Chapman, 1993).

The procedure for internal fungus recovery was similar, except the spider was washed (twice for 1 minute each) in sterile deionized (DI) water, then mild bleach solution (DI water-absolute ethanol-5.25% NaOCl; 18-1-1, v/v/v) followed by two DI water rinses, and the body was quartered (one body portion/plate) prior to embedding (Currah et al., 1997; Zettler, 1997; Yoder et al., 2003).

The radial growth rate of each fungus was determined using the trisecting line method as described by Currah et al. (1997). Three lines were drawn on the bottom of a Petri dish radiating from the center of the dish 40° from each other. The dish was filled with agar and allowed to solidify. A 1 cm^3 block of mycelium from an established culture was placed on the agar surface in the center over top of the point of intersection of the three lines and incubated (12 °C and 25 °C, darkness). Each day for the next five days, measurements were taken along each of the three lines as the mycelium spread over the agar surface. To calculate the radial growth rate (K_r), we used the equation $K_r = (R_1 - R_0)/(t_1 - t_0)$, where R_0 and R_1 are colony radii at initial (t_0) and elapsed (t_1) times between beginning of linear, t_0, and stationary, t_1, growth phases as described by Baldrian and Gabriel (2002). The radial growth rate was expressed as millimeters per hour. For each fungus, data are mean ± standard error (SE) of 45 measurements, 15 per plate, replicated three times each using mycelia selected randomly from ten separate pure cultures of a particular fungus. An analysis of variance (ANOVA) was used to compare data (SPSS 14.0 for Windows, Microsoft Excel and Minitab; Chicago, IL) as described by Sokal and Rohlf (1995).

Inocula were prepared from spider isolates *Beauveria* sp. and *Paecilomyces* sp. (Table 1), genera that are classified as entomopathogens (Barnett and Hunter, 1998), and tested to determine whether these fungi are infective to spiders and cave crickets, *H. cumberlandicus*. An aqueous inoculum was made by shaking a 1 cm^3 block of mycelium from established cultures in 5 ml phosphate-buffered saline (PBS, pH 7.5) overnight. Conidia concentration was adjusted to 6.8×10^8 conidia ml^{-1} (20 µl application) per individual (modified from Kirkland et al., 2004) using PBS based on 10 separate counts with a hemocytometer (AO Spencer Bright Line, St. Louis, MO)

and 0.1% trypan blue exclusion; PBS served as a control. Each fungus formulation (and PBS control) was applied topically to spiders ($n = 20$, 4 replicates of 5, with each replicate representing a different collecting trip) and crickets ($n = 30$, 5 replicates of 6, with each replicate representing a different collecting trip). Specimens were housed in individual clear 8000 cc plexiglass chambers at 12 $\pm$ 0.5 °C, 98 $\pm$ 2.0% relative humidity (RH) and darkness. The chamber was inverted so that crickets could be in an upside down position like they are in the cave. The criteria used to determine a dead or dying cricket or spider were lack of movement, failure to respond to mechanical stimuli, and inability to right and crawl five body lengths. Observations were made daily in red light. Data were compared using ANOVA.

RESULTS AND DISCUSSION

A listing of external and internal fungi associated with *M. ovalis* is presented in Table 1. The percentages represent the diversity and amount of fungi that may be found on a single individual spider at any one time. Fungi from ten genera were recovered from the spider's body surface, with *Aspergillus* spp., *Mucor* spp., *Penicillium* spp., and *Rhizopus* spp. as major isolates. All of the fungi in the spider's external mycoflora are common, naturally-occurring fungi present in soil, leaf litter, and organic debris, where they function as agents of decay (Cubbon, 1976; Rutherford and Huang, 1994; Reeves et al., 2000). Incubation at 12 °C, reminiscent of mean temperature in the interior of Laurel Cave, had a suppressive effect on growth/spread of the mycelium and delayed sporulation (production of conidia) of all of these fungi; that is, it took about twice as long compared to incubation at 25 °C for culture characteristics to appear. Radial growth rate (mean $\pm$ SE < 0.034) at 25 °C and at 12 °C dropped from 0.088 mm h^{-1} to 0.031 mm h^{-1} for *Aspergillus* sp.; 0.308 mm h^{-1} to 0.114 mm h^{-1} for *Mucor* sp.; 0.127 mm h^{-1} to 0.055 mm h^{-1} for *Penicillium* sp. and 0.367 mm h^{-1} to 0.208 mm h^{-1} for *Rhizopus* sp. as the predominate isolates on the spider's surface ($p < 0.05$). Less frequently recovered fungi from the spider's surface showed similar rate reductions in response to low temperature: 0.224 mm h^{-1} (25 °C) vs. 0.125 mm h^{-1} (12 °C) for *Absidia* sp., 0.197 mm h^{-1} (25 °C) vs. 0.073 mm h^{-1} (12 °C) for *Beauveria* sp.; 0.141 mm h^{-1} (25 °C) vs. 0.0884 mm h^{-1} (12 °C) for *Cladosporium* sp.; 0.239 mm h^{-1} (25 °C) vs. 0.118 mm h^{-1} (12 °C) for *Paecilomyces* sp.; and 0.313 mm h^{-1} (25 °C) vs. 0.146 mm h^{-1} (12 °C) for *Trichoderma* sp. The ubiquitous distribution of the fungi identified from the spiders is reflected by their ability to grow on a variety of different culture media (Table 1), showing no particular nutritional or pH requirement consistent with their ability to utilize a variety of substrates for growth and proliferation (Jennings and Lysek, 1999).

Noteworthy among the spider body surface isolates were *Beauveria* spp. and *Paecilomyces* spp. that are classified ecologically as facultative parasites, which under certain conditions can switch from saprobe to parasite (but classified as obligate parasites according to Samsinakova et al., 1974), and act as insect pathogens. *Beauveria* spp., in particular, is often used in biological control (Hajek and Butler, 2000; Strasser et al., 2000). *Trichoderma* spp. is commonly mycoparasitic (Jennings and Lysek, 1999). Because Laurel Cave is stable at low temperature (12 $\pm$ 1.1 °C) and high relative humidity (98.6–100% RH) (Hill, 2003), these conditions favor a small number of prolific fungal taxa, especially anamorphs, such as those isolated (Table 1), namely *Aspergillus* spp. and *Penicillium* spp. that consistently show high abundance in caves (Cubbon, 1976; Rutherford and Huang, 1994; Reeves et al., 2000). We observed no appreciable difference in mycoflora from spiders collected from different years (data not shown). Therefore, the fungi isolated from the body surface of *M. ovalis* are typical of a cave setting, all are accelerated conidia-producing genera allowing rapid dispersal, and a heavy, diverse fungus load can apparently be supported by the spider without any noticeable detrimental effects or changes in spider appearance or behavior.

Of special interest was the internal isolation, albeit low, of the entomopathogens *Beauveria* spp. and *Paecilomyces* spp. from within *M. ovalis* body contents, consistent with their parasitic nature (Table 1). Twenty-three percent of spiders (9 out of 40 spiders) were infected with *Beauveria* spp., and 10% of spiders (4 out of 40 spiders) were infected with *Paecilomyces* spp. As such, recovery of these fungi internally from tissues implies penetration of fungal hyphae, exploiting the spider internally and proliferating inside, presumably originating from the body surface where they were also isolated (Table 1). Gaining access to the inside of the spider's body likely occurs through the mouth, anus, genital, or glandular openings or directly through the cuticle by secretion of proteolytic and chitinolytic enzymes that characterize entomopathogenic infections (St. Leger et al., 1998). The other fungus that was isolated internally (1/40 spiders, 3%) was *Penicillium* spp., classified as a saprobe (Jennings and Lysek, 1999), and this fungus was probably present as a secondary invader or a contaminant; *Aspergillus* spp. and *Mucor* spp. also have this ability (Gliñski and Buczek, 2003), but neither of these fungi were detected in our study by internal fungus culture. Evidence from internal recovery from *M. ovalis* of known pathogenic fungi suggests that *Beauveria* spp. and *Paecilomyces* spp. may serve as natural regulators of spider populations in Laurel Cave. Another alternative is that the presence of these fungi internally may be contaminants that could have come from the digestive tract that is contiguous with the outside. Both *Beauveria* spp. and *Paecilomyces* spp., although both well-known insect pathogens, have been shown to be pathogenic to spiders on occasion, but results are inconsistent (i.e., that these fungi are pathogenic to spiders are from the observations of Muma (1975) and that they are not pathogenic to

spiders are from the observations of Baltensweiler and Cerutti (1986)).

In contrast, *Beauveria* spp. and *Paecilomyces* spp. have been shown to be lethal to the cave cricket, *Troglophilus neglectus* (Gunde-Cimerman et al., 1998). We attempted to clarify the parasitic nature of *Beauveria* spp. and *Paecilomyces* spp. in our pathogenic testing of these fungi on spiders and cave crickets as it applies to Laurel Cave. With regard to the spider (mean ± SE), *M. ovalis*, we observed 20 ± 3.2% mortality for spiders that had received a topical application of *Beauveria* sp.; 15 ± 4.4% mortality for spiders treated with *Paecilomyces* sp.; 30 ± 1.3% mortality for spiders treated with PBS; and 20 ± 2.7% mortality for spiders that received no treatment. No significant differences were noted between control spiders and spiders that had been treated with fungus (Abbott correction; $p > 0.05$) and no fungi (*Paecilomyces* spp. or *Beauveria* spp.) were recovered internally from those spiders that were dead.

Significant differences, however, were noted between controls and fungus formulation applications in the cricket *H. cumberlandicus* (Abbott correction; $p < 0.05$): 77 ± 5.3% were observed dead after treatment with *Beauveria* sp. and 90 ± 4.2% were killed with *Paecilomyces* sp., compared to 23 ± 2.9% mortality for crickets treated with PBS and 30 ± 6.4% mortality in untreated controls. *Beauveria* spp. and *Paecilomyces* spp. were recovered by internal fungus culture from the dead crickets. Prior to topical treatment with these entomopathogenic fungi, the crickets were in healthy conditions and showed no signs of disease, implying that they were not previously infected. Conceivably, the co-occurrence of *M. ovalis* with cave crickets (*H. cumberlandicus*) puts the crickets at potential elevated risk of becoming infected, and this is likely enhanced behaviorally by formation of cricket aggregations (enabling increased spread of conidia and exposure to a larger number of individuals at a time). Because these crickets are closely related (only parthenogenic population exists in Laurel cave; Hubbell and Norton, 1978), that may make them more prone to infection. Thus, it seems reasonable to suggest that given the close spider-cricket co-occurrence in Laurel Cave, there is a potential for cross-infection that poses a special risk for cave cricket populations (Benoit et al., 2004).

Conclusions

Adult females of the cave orb weaver spider, *Meta ovalis*, have fungi on their surfaces and have the potential to disperse fungal spores (conidia) throughout the cave environment. Fungi present are typical of those in a cave setting and most are common filamentous soil saprobes (listed in order of relative abundance): *Aspergillus* spp., *Rhizopus* spp., *Penicillium* spp. = *Mucor* spp., *Absidia* spp., *Beauveria* spp. = *Cladosporium* spp. = *Paecilomyces* spp., and *Trichoderma* spp. A topically-applied *Beauveria* sp. and *Paecilomyces* sp. (well known entomopathogenic fungi) isolated from these spiders were infective and killed adult cave crickets, *Hadenoecus cumberlandicus*, but these fungi were not pathogenic when applied to the spiders. The fact that *M. ovalis* and *H. cumberlandicus* readily co-occur in caves puts *H. cumberlandicus* at an elevated risk for disease by fungal pathogens.

References

Baldrian, P., and Gabriel, J., 2002, Intraspecific variability in growth response to cadmium of the wood-rotting fungus *Piptoporus betulinus*: Mycologia, v. 94, p. 428–436.

Baltensweiler, W., and Cerutti, F., 1986, Bericht über die Nebenwirkungen einer Bekämpfung des Maikäfer (*Melolontha melolotha* L.) mit dem Pilz *Beauveria brongniartii* (Sacc.) Petch auf die Arthropodenfauna des Waldrandes: Mitteilungen der Schweizerischen Entomologischen Gesellschaft, v. 59, p. 267–274.

Barnett, H.L., and Hunter, B.B., 1998, Illustrated genera of imperfect fungi, St. Paul, American Phytopathological Society Press, 166 p.

Benoit, J.B., Yoder, J.A., Zettler, L.W., and Hobbs, H.H. III., 2004, Mycoflora of a trogloxenic cave cricket, *Hadenoecus cumberlandicus* (Orthoptera: Rhaphidophoridae), from two small caves in Northeastern Kentucky: Annals of the Entomological Society of America, v. 97, p. 989–993.

Chapman, P., 1993, Caves and cave life, London, Harper Collins, 219 p.

Cubbon, B.D., 1976, Cave flora, *in* Ford, T.D., and Cullingford, C.H.D., eds., Science of speleology, London, Academic Press, p. 423–433.

Currah, R.S., Zettler, L.W., and McInnis, T.M., 1997, *Epulorhiza inquilina* sp. nov. from *Platanthera* (Orchidaceae) and key to *Epulorhiza* species: Mycotaxon, v. 61, p. 335–342.

Gliñski, Z., and Buczek, K., 2003, Response of the Apoidea to fungal infections: Apicata, v. 38, p. 183–189.

Gunde-Cimerman, N., Zalar, P., and Jeram, S., 1998, Mycoflora of cave cricket *Troglophilus neglectus* cadavers: Mycopathologia, v. 141, p. 111–114.

Hajek, A.E., and Butler, L., 2000, Predicting the host range of entomopathogenic fungi, *in* Follett, P.A., and Duan, J.J., eds., Nontarget effects of biological control, Rotterdam, The Netherlands, Kluwer, p. 263–276.

Hill, S.E., 2003, Examination of the movements of crickets in Laurel Cave, Carter County, Kentucky: Pholeos, v. 21, p. 24–28.

Hobbs, H.H. III., 1992, Caves and springs, *in* Hackney, C.T., Adams, S.M., and Martin, W.M., eds., Biodiversity of the southeastern United States: aquatic communities, London, Wiley, p. 59–131.

Hubbell, T.H., and Norton, R.M., 1978, The systematics and biology of the cave-crickets of the North American Tribe Hadenoecini (Orthoptera Saltatoria: Ensifera: Rhaphidophoridae: Dolichlpodinae): Miscellaneous Publications of the Museum of Zoology, v. 156, p. 1–124.

Jennings, D.H., and Lysek, G., 1999, Fungal biology: understanding the fungal lifestyle, New York, Springer, 166 p.

Kirkland, B.H., Westwood, G.S., and Keyhani, N.O., 2004, Pathogenicity of entomopathogenic fungi *Beauveria bassiana* and *Metarhizium anisopliae* to Ixodidae tick species *Dermacentor variabilis*, *Rhipicephalus sanguineus* and *Ixodes scapulari*: Journal of Medical Entomology, v. 41, p. 705–711.

Lavoie, K.H., Helf, K.L., and Poulson, T.L., 2007, The biology and ecology of North American cave crickets: Journal of Cave and Karst Studies, v. 69, p. 114–134.

Muma, M.H., 1975, Spiders in Florida citrus groves: The Florida Entomologist, v. 58, p. 83–90.

Pfeffer, N., Madigan, T.J., and Hobbs, H.H. III., 1981, Laurel Cave: Pholeos, v. 2, p. 10–13.

Reeves, W.K., Jensen, J.B., and Ozier, J.C., 2000, New faunal and fungal records from caves in Georgia, USA: Journal of Cave and Karst Studies, v. 62, p. 169–179.

Rutherford, J.M., and Huang, L.H., 1994, A study of fungi of remote sediments in West Virginia caves and a comparison with reported species in the literature: The National Speleological Society Bulletin, v. 56, p. 38–45.

Samsinakova, A., Kalalova, S., Daniel, M., Dusbabek, F., Honzakova, E., and Cerny, V., 1974, Entomogenous fungi associated with the tick *Ixodes ricinus* (L.): Folia Parasitologica, v. 21, p. 39–48.

Sokal, R.R., and Rohlf, F.J., 1995, Biometry: the principles and practice of statistics in biological research, San Francisco, W. H. Freeman and Company, 887 p.

St. Leger, R.J., Joshi, L., and Roberts, D., 1998, Ambient pH is a major determinant in the expression of cuticle-degrading enzymes and hydrophobin by *Metarhizium anisopliae*: Applied and Environmental Microbiology, v. 64, p. 709–713.

Strasser, H., Vey, A., and Butt, T.M., 2000, Are there any risks in using entomopathogenic fungi for pest control, with particular reference to the bioactive metabolites of *Metarhizium*, *Tolypocladium* and *Beauveria* species?: Biocontrol Science and Technology, v. 10, p. 717–735.

Studier, E.H., Lavoie, K.H., Wares, W.D. II, and Linn, J.A.M., 1986, Bioenergetics of the cave cricket, *Hadenoecus subterraneus*: Comparative Biochemistry and Physiology A, v. 84, p. 431–436.

Ubick, D., Paquin, P., Cushing, P.E., and Roth, V., 2005, Spiders of North America: an identification manual, American Arachnological Society, 377 p.

Yoder, J.A., Christensen, B.S., Croxall, T.J., Tank, J.L., and Hobbs, H.H. III., 2009, Aggregation pheromone in the cave cricket, *Hadenoecus cumberlandicus*, with an examination of this pheromone's capacity as a host cue (kairomone) to a predatory spider: Journal of Insect Science (in press).

Yoder, J.A., Hanson, P.E., Zettler, L.W., Benoit, J.B., Ghisays, F., and Piskin, K.A., 2003, Internal and external mycoflora of the American dog tick, *Dermacentor variabilis* (Acari:Ixodidae), and its ecological implications: Applied and Environmental Microbiology, v. 69, p. 4994–4996.

Yoder, J.A., Hobbs, H.H. III, and Hazelton, M.C., 2002, Aggregate protection against dehydration in adult females of the cave cricket, *Hadenoecus cumberlandicus* (Orthoptera, Rhaphidophoridae): Journal of Cave and Karst Studies, v. 64, p. 140–144.

Zettler, L.W., 1997, Terrestrial orchid conservation by symbiotic seed germination: Techniques and perspectives: Selbyana, v. 18, p. 188–194.

G.S. Springer, H.D. Rowe, B. Hardt, F.G. Cocina, R.L. Edwards, and H. Cheng – Climate driven changes in river channel morphology and base level during the Holocene and Late Pleistocene of southeastern West Virginia. *Journal of Cave and Karst Studies,* v. 71, no. 2, p. 121–129.

CLIMATE DRIVEN CHANGES IN RIVER CHANNEL MORPHOLOGY AND BASE LEVEL DURING THE HOLOCENE AND LATE PLEISTOCENE OF SOUTHEASTERN WEST VIRGINIA

Gregory S. Springer*[1], Harold D. Rowe[4], Ben Hardt[2], Frank G. Cocina[1,3], R. Lawrence Edwards[2], and Hai Cheng[2]

Abstract: Rivers commonly respond to climate change by aggrading or incising. This is well documented for North American rivers in arid and proglacial regions, but is also true of rivers in unglaciated, humid-temperate regions. Here, we present a record of Holocene hydroclimatology for a humid, temperate watershed in the Appalachian Mountains of eastern North America. We use stable isotope geochemistries of a stalagmite and clastic cave sediments to reconstruct Holocene climate and ecology in the Greenbrier River catchment (3,600 km^2) of southeastern West Virginia. Independently, we use river-deposited cave sediments to construct a history of incision, aggradation, and morphological change in the surface channel. The clastic cave deposits display enriched (less negative) values of sedimentary $\delta^{13}C_{org}$ during the Holocene Climatic Optimum (HCO), which regional pollen records indicate was warm compared to later climes. The river channel had aggraded by >4 m during or prior to the HCO and adopted an alluvial morphology, probably due to the mobilization of hillslope sediments accumulated during the colder, drier full-glacial conditions of the Late Pleistocene. As climate moistened during the Holocene, the Greenbrier River incised through channel-filling sediments and back onto bedrock, but not until ~3,500 cal. years B.P. Therefore, the bedrock morphology of many streams in the Appalachian Mountains may not have existed for much of the Holocene, which highlights the effect of climate variability on channel processes. The base-level rise is more evidence that bedrock incision by rivers is often episodic and that slow, long-term incision rates reported for Appalachian Rivers are probably not representative of short-term incision rates.

Introduction

Average global temperatures have been rising in recent time and climate change is expected to measurably affect stream hydrology (Kundzewicz et al., 2007). As such, societal interactions with rivers will change, including those related to flooding. The magnitudes and directions of these changes are uncertain and new, more quantitative data are needed to predict future responses and prepare society for the changes ahead (Wood et al., 2002; Maurer et al., 2004; Lettenmaier et al., 2006). High-resolution studies are especially needed because of the scale mismatch between climatic models and catchments, as the latter are the functional units of the terrestrial hydrosphere (Kundzewicz et al., 2007). Climate change affects a host of stream variables, including channel morphology, which is a good predictor of stream behaviors and processes (Montgomery and Buffington, 1997). In the simplest case, a decrease in net precipitation can cause channels to infill with sediment (aggrade) and change from an incised channel to a broader, shallower channel (Knighton, 1998). Conversely, an increase in precipitation, stream discharge, or gradient can also cause channels to infill if sediments stored on alluvial fans and valley bottoms are remobilized and transported into the stream (Schumm, 1973). In such a generalized scenario, channel aggradation raises base level, which leads to increased flooding on terraces and floodplains (e.g., Bull, 1988). However, corresponding changes in stream morphology may change stage-discharge relationships and thereby increase or decrease peak flood stages (e.g., Stover and Montgomery, 2001). Thus, predicting changes in base level and channel morphologies are important steps toward understanding future stream behaviors and risks.

Here, we reconstruct Holocene changes in channel morphology and base-level elevation in a mountainous watershed draining the Eastern Continental Divide (ECD) of North America (Fig. 1). The sedimentology of river-

* Corresponding author
[1] Department of Geological Sciences, Ohio University, Athens, OH, 45701, springeg@ohio.edu
[2] Department of Geology and Geophysics, University of Minnesota, Minneapolis, MN, 55455
[3] Present Address: Qinetiq North America, 1350 Central Ave. Los Alamos, NM, 87544
[4] Department of Geology, Box 19049, University of Texas at Arlington, Arlington, TX, 76019-0049

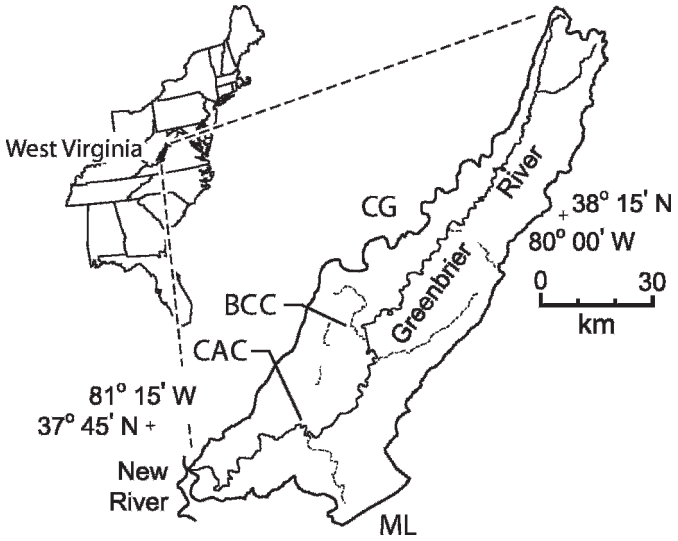

Figure 1. Colonial Acres Cave (CAC) and the associated surface channel are located along the Greenbrier River in southeastern West Virginia. The Greenbrier River watershed abuts the Eastern Continental Divide along its north and east boundaries. The CAC/Greenbrier River sedimentary record is compared to paleoclimate records drawn from Buckeye Creek Cave (BCC), Cranberry Glades (CG), and Mountain Lake, Virginia (ML).

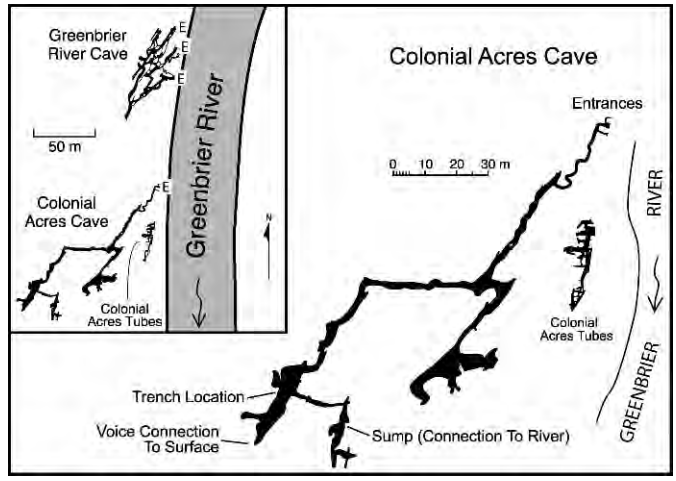

Figure 2. The examined stream reach contains three large caves developed in the river-right bank of the Greenbrier River (inset). Colonial Acres Tubes contain no usable sediments. Greenbrier River Cave (GRC) contains slackwater sediments deposited by historic and ancient floods, but no evidence of Holocene base level fluctuations has been found GRC. This probably reflects its vertical position relative to the river; much of GRC lies 7 m above the low water surface of the Greenbrier River. The slackwater sediments discussed in this study are from a modest-size room and excavated trench in Colonial Acres Cave (CAC). Greenbrier River floodwaters can reach the room from impassable pathways within a voice-transmitting collapse at the south end of the trench room, a series of tubular passages originating at three side-by-side entrances, and a small passage emanating from a sump hydrologically connected to the river (all shown).

deposited slackwater sediments is used to construct a history of stream hydrology and morphology, which is compared to a record of Holocene climates. We reconstruct climate using stalagmitic $\delta^{18}O_{calcite}$ and $\delta^{13}C_{calcite}$ values, bulk organic values of $\delta^{13}C_{org}$ in clastic cave sediments, and previously published palynological data. Ours is the first detailed simultaneous examination of the climate and river hydrology within the source region of large Appalachian rivers (Fig. 1).

METHODS AND SAMPLE LOCATIONS

STALAGMITE BCC-002

A calcite stalagmite (BCC-002) from Buckeye Creek Cave (BCC) (Fig. 1) is used to develop a stable isotope record of climate for interpretation of the causes of significant changes in slackwater stratigraphy in Colonial Acres Cave (CAC) (Fig. 2) (Springer et al., 2008). BCC is within the Greenbrier River watershed of southeastern West Virginia. The watershed is a major tributary of the westward-flowing New River and across the ECD from the eastward-flowing Potomac and James Rivers. The 200-mm-long stalagmite was fed by a soda straw stalactite with a slow, but incessant drip rate. Temperature and humidity are stable in the cave passage and air movement is slow. Springer et al. (2008) provide a picture of the sawn, polished stalagmite in their online supplemental material.

The $\delta^{18}O$ values in stalagmites vary with changes in the meteoric water (Hendy, 1971), which predictably varies in response to changes in temperature, precipitation amount, and moisture source (Dansgaard, 1964; Rozanski et al., 1993). While speleothems in tropical regions exhibit a dominant response to the amount effect (i.e., Wang et al., 2001), mid-latitude sites have a larger temperature component (i.e., Dorale et al., 1998). Here, we assume that 1) changes in $\delta^{18}O_{calcite}$ largely reflect past changes in above-cave air temperature and precipitation source, and 2) $\delta^{13}C_{calcite}$ and $\delta^{13}C_{org}$ are proxies for floral and soil community composition, productivity, and relative moisture levels (Kirby et al., 2002; McDermott, 2004). Post-2,000 cal. years B.P. values of $\delta^{13}C_{calcite}$ are not interpreted because of anthropogenic disturbances to the BCC watershed (White, 2007).

Fourteen $^{234}U/^{230}Th$ age estimates were obtained along the growth axis of BCC-002 using U/Th dating techniques developed for carbonates (Broecker, 1963) and adapted for measurement on a mass spectrometer (Edwards et al., 1987). Calcite powders were milled with a dental drill, dissolved, and spiked with a ^{233}U-^{236}U-^{229}Th tracer. Uranium and thorium were separated using anion exchange resin, and the clean U and Th were run separately

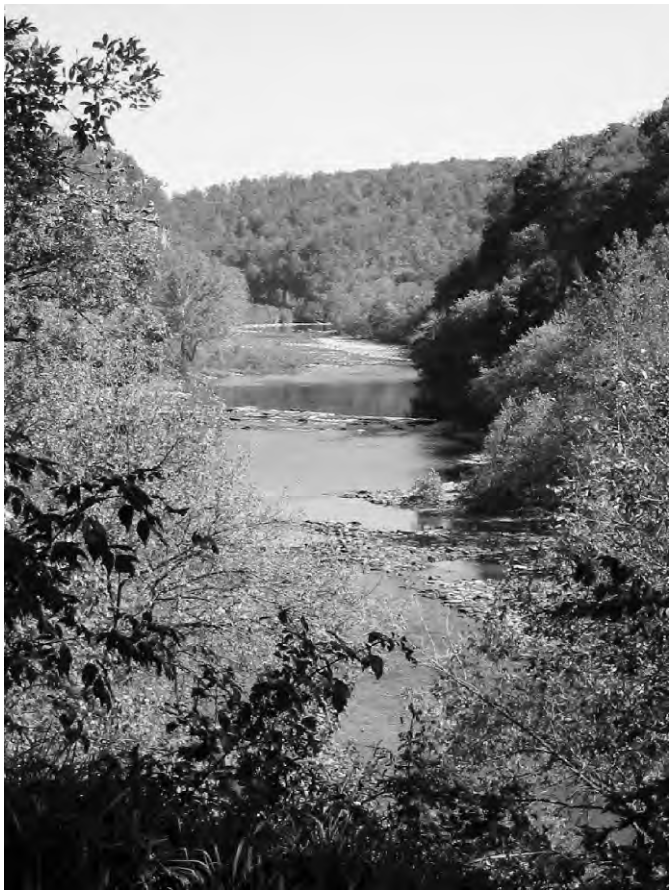

Figure 3. The Greenbrier River at Colonial Acres Cave (CAC) flows in a narrow valley containing narrow or no floodplains, but many limestone cliff banks. Flow is toward the viewer (out of the page). Channel morphology is pool-riffle or pool-rapid with boulders and large cobbles dominating bedload. Bedrock is exposed in many riffles and most pools. CAC lies 300 m downstream of the lower-right corner of this picture.

on an inductively coupled plasma mass spectrometer (Shen et al., 2002) along with a chemical blank. Ages were calculated using the decay constants determined by Cheng et al. (2000).

Clastic Slackwater Sediments

Clastic slackwater sediments deposited by the Greenbrier River in CAC are used to infer past hydrological relationships between the cave and river (Fig. 2). As demonstrated by Springer et al. (1997), Springer (2002), and Bosch and White (2003), the hydrological relationships are used to determine relative (to the cave) base-level elevations, paleoflood stages, and surface channel hydrologies. Presently, the surface channel has a bedrock morphology (>50% rock-lined), with coarse cobbles and small boulders composing the bedload (Fig. 3). The drainage area upstream of the cave is 3,600 km^2. There are no indications of significant subsurface piracy of the 60-m-wide river, which is perennial. Locally, mean annual discharge is 57 $m^3\ s^{-1}$ (n = 111) with a peak historic discharge of 2,600 $m^3\ s^{-1}$ (Springer, 2002).

CAC lies behind a vertical bank of the river. We examined a 2-m-thick package of slackwater sediments deposited by the river in a small room (Fig. 2). The room ends in collapse against the riverbank. Voices and, therefore, water readily pass through the collapse, although light does not. The Greenbrier River is the only significant source of water and sediment to CAC and completely fills the room during and above medium recurrence-interval floods. In addition to the collapse, floodwaters enter the cave room via a 210-m-long, 1.5-m-diameter passage originating at the cave entrance and via a 0.75-m-diameter passage connected to a sump (Fig. 2) that is a permanently flooded connection to the river. Sump depth varies with river stage.

A 2-m-deep trench was excavated in CAC slackwater sediments. Seven AMS-^{14}C dates were obtained from charcoal in the upper 70 cm of the trench. The ages of underlying sediments are extrapolated using a sedimentation rate calculated from the upper 70 cm (175 mm ka^{-1}). Only general conclusions are drawn from sediments below 70 cm because of age uncertainties. Each identifiable stratigraphic unit was sampled for grain size analysis (sieving). The sediments were contiguously sampled at a 2-cm interval for determination of bulk sedimentary $\delta^{13}C_{org}$. Herein, the fraction of sand present is reported and used to evaluate energy levels of the formative floodwaters. To obtain stable isotopic values for organic carbon ($\delta^{13}C_{org}$), dry sediment powders were weighed into silver capsules, repeatedly acidified with 6% sulfurous acid, and analyzed using a Costech 4010 elemental analyzer coupled via a Conflo III Device to a ThermoFinnigan DeltaPlusXP isotope-ratio mass spectrometer (IRMS). Values for $\delta^{13}C_{org}$ are reported relative to V-PDB, and precision for the isotopic standard (USGS-24) and unknowns is <0.1‰. Temporal variations in sedimentary $\delta^{13}C_{org}$ represent a watershed-integrated record of ecological change upstream of the deposit. The $\delta^{18}O_{calcite}$ and $\delta^{13}C_{calcite}$ were also determined using the ThermoFinnigan DeltaPlusXP isotope-ratio mass spectrometer, although standard carbonate sample preparations were performed.

Holocene Climate Of Greenbrier River Watershed

The $\delta^{18}O_{calcite}$ and $\delta^{13}C_{calcite}$ values from stalagmite BCC-002 show pronounced variations during the Holocene (Fig. 4A, B). The closest published palynological record is from Cranberry Glades (Watts, 1979), located 56 km north of BCC-002 and only 5 km from the Greenbrier River watershed (Fig. 1). The bog lies at an elevation of 1024 m, which is 350 m higher than the land surface above BCC-002. Comparing BCC-002 to the bog, $\delta^{18}O_{calcite}$ values are heaviest during the mid-Holocene when hardwood pollen abundance increases (notably *Carya* (hickory), *Fagus*

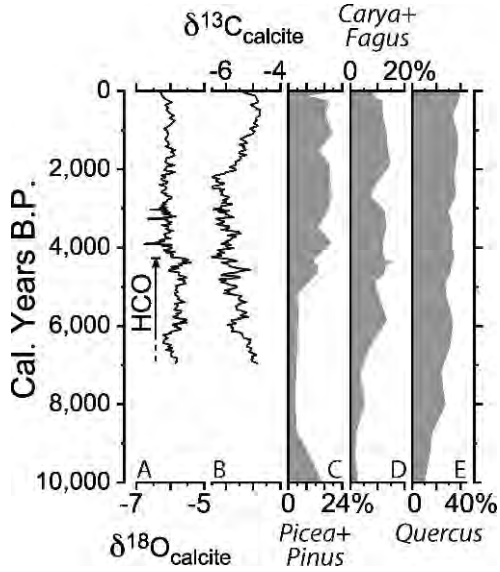

Figure 4. Slackwater stratigraphy is compared to independent paleoclimate proxies from Buckeye Creek Cave stalagmite BCC-002 (A and B; Springer et al., 2008) and Cranberry Glades pollen (C–E; Watts, 1979). The $\delta^{18}O_{calcite}$ values are heaviest (most enriched) between 4,200 and 7,000 cal. years B.P. At approximately the same time, Holocene temperatures peaked during what is known as the Holocene Climatic Optimum (HCO) (Kaplan and Wolfe, 2006). Locally, enriched $\delta^{18}O_{calcite}$ values record a warm HCO climate at BCC and Colonial Acres Caves (CAC). Declining $\delta^{18}O_{calcite}$ values after 4,200 cal. years B.P. record an abrupt cooling, after which temperatures were comparatively stable for the remainder of the Holocene (A). The $\delta^{13}C_{calcite}$ values decrease between 7,000 and 2,000 cal. years B.P., which records a general moistening or increasing precipitation (B). The abrupt enrichment of $\delta^{13}C_{calcite}$ values after 2,000 cal. years B.P. records landscape disturbances attributable to Native Americans (White, 2007; Springer et al., submitted). The warm temperatures inferred from $\delta^{18}O_{calcite}$ values are consistent with low spruce (*Picea*) and pine (*Pinus*) pollen abundances at that time (C). However, increasing abundances of hickory (*Carya*), beech (*Fagus*), and oak (*Quercus*) are attributable to the moistening recorded in the $\delta^{13}C_{calcite}$ record (D–E). Figure modified from Springer et al. (2008).

(beech), and *Quercus* (oak)), pollen abundance from subboreal trees (principally *Picea* (spruce)) reach a Holocene low (Fig. 4), and pollen counts of the moisture sensitive Family *Cyperaceae* (sedges) decline by several orders of magnitude and to zero for short intervals (not shown). Coincident with changes in *Cyperaceae* abundance is the appearance of *Nyssa* (tupelo) pollen in lacustrine sediments found 100 km to the east of BCC-002 (Watts, 1979; Kneller and Peteet, 1993). Tupelo prefers warm temperatures and is mostly absent from regional pollen records, except during the mid-Holocene, when values peak. Collectively, $\delta^{18}O_{calcite}$ values and pollen abundances indicate a warm mid-Holocene climate, which is recognized elsewhere as the Holocene Climatic Optimum (HCO) or Hypsithermal (Kaplan and Wolfe, 2006). The HCO began >6,500 cal. years B.P. and ended at 4,200 cal. years B.P. when $\delta^{18}O_{calcite}$ values abruptly decrease by 0.4‰ (Fig. 4A). Reported starting and ending dates of the HCO vary by region, but termination of the HCO at Buckeye Creek Cave coincides with purported mega-droughts and climatic shifts throughout the upper Midwest of the USA, northern Africa, the Middle East (see review by Booth et al., 2005), and New Jersey (Li et al., 2007).

Mid-Holocene values of $\delta^{13}C_{calcite}$ are enriched (less negative) (Fig. 4B), which suggests that soils overlying BCC-002 were drier or less productive than those of the Late Holocene (McDermott, 2004). In fact, clay mineralogies and weathering profiles of paleosols in the floodplain of a Greenbrier River tributary (41 km NNE of BCC-002) record warmer, drier conditions during the HCO (Driese et al., 2005). *Pinus* (pine) pollen abundances reach their Holocene low during the HCO, despite the existence of a strong, positive correlation between the percentage of *Pinus* pollen in modern, mid-Atlantic sediments and temperatures of the preceding January ($R^2 = 0.91$) (Willard et al., 2005). *Pinus* pollen abundances are also correlated with moisture and increase post-HCO, which is observed elsewhere along the eastern margin of North America and is attributed to a general moistening (Watts, 1979; Webb, 1987; Willard et al., 2005). Presumably, (seasonal?) soil moisture was the major HCO control on *Pinus* abundance or its pollen productivity. Post-HCO values of $\delta^{18}O_{calcite}$ and $\delta^{13}C_{calcite}$ are comparatively depleted (more negative) than those of the HCO, and the Cranberry Glades pollen record is dominated by tree species that favor cooler, wetter climates (Fig. 4C–E).

Summarizing the stalagmite, paleopedological, and palynological data, the HCO was warmer and (seasonally?) drier than the Late Holocene in the Greenbrier River watershed. Climate was comparatively stable throughout the Late Holocene (Fig. 4A), but Holocene values of $\delta^{13}C_{org}$ from alluvium in BCC and CAC are typical of forested landscapes (-24.5 ± 1‰) (White, 2007). Although forest composition evolves with time (Fig. 4C–E), $\delta^{13}C_{org}$ values indicate that the watershed remained heavily forested throughout the Mid- to Late-Holocene. Observed changes in $\delta^{13}C_{calcite}$ and $\delta^{13}C_{org}$ post-HCO are attributable to changes in soil productivity and respiration, but not attributable to major changes in C3 or C4 abundances (e.g., Dorale et al., 1998). However, the absence of pre-HCO data prevents interpretation of vegetation types during the Early Holocene and near the onset of the HCO.

HOLOCENE HYDROLOGY OF THE GREENBRIER RIVER

The Greenbrier River deposits slackwater sediments in CAC during intermittent floods. As a result, CAC contains a sedimentological record of stream hydrology. Sediments

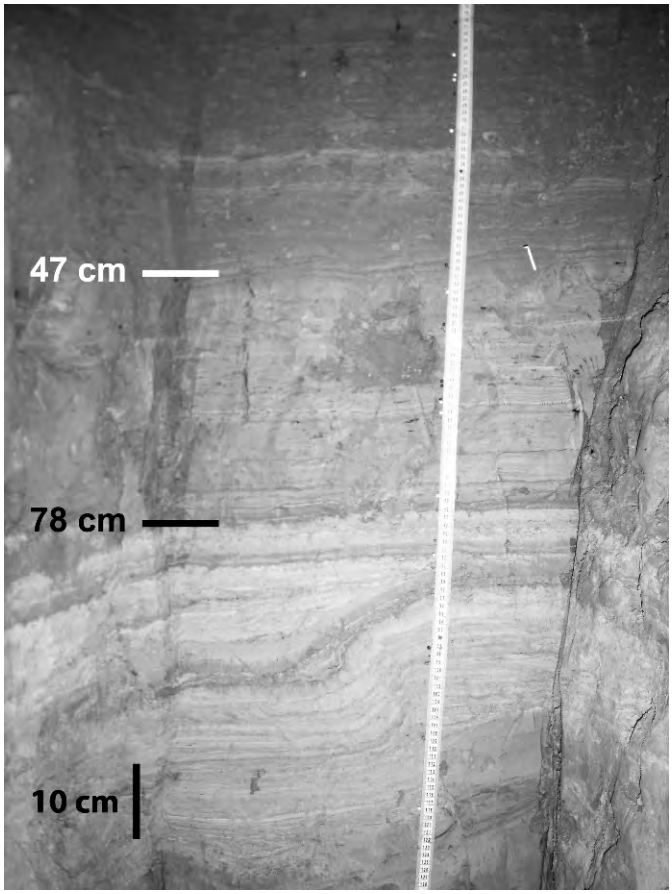

Figure 5. Three major units can be recognized in the slackwater sediments excavated in Colonial Acres Cave. These consist of sands (pale lower unit), which are overlain by dense, clayey silts (47 to 78 cm). The black, horizontal line indicates their contact. The white line highlights the contact between the clayey silts and overlying sandy silts and silty sands. All units are laminated and have undergone minimal bioturbation, although the lower sands underwent soft sediment deformation as they subsided into an underlying clay unit. The latter is not visible in this photograph. Contrast has been digitally enhanced to make the laminations and bed contacts more easily visible.

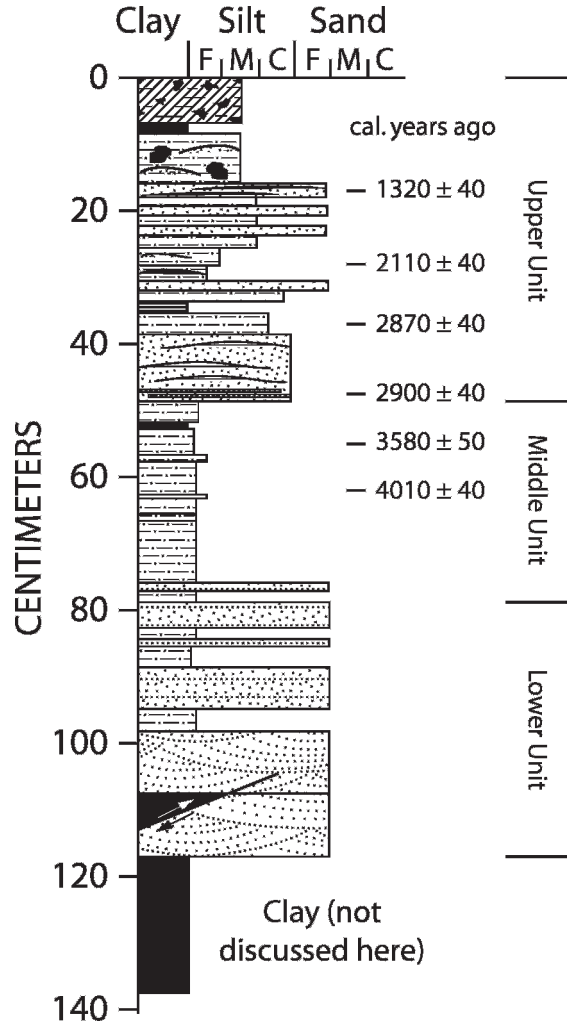

Figure 6. Sieving and pipette-withdrawal were used to determine the particle sizes of each significant bed in the Colonial Acres Cave (CAC) trench, and these results are the basis for this stratigraphic column. A clayey silt (48 to 75 cm) separates the lower sands (75 cm to 118 cm) from the younger sandy silts and silty sands (0 to 48 cm). Based upon AMS-^{14}C ages of charcoal (positions as indicated), deposition of the clayey silt ended at ~3,500 cal. years B.P., which we attribute to incision of the Greenbrier River below CAC. Ultimately, the trench was dug to a depth of 200 cm, which revealed soft clays (>118 cm) below the sand unit and a basal layer of river cobbles (not depicted). Unfortunately, repeated collapses of the lower trench face prevented detailed investigation of the clays and cobbles.

are excellently preserved and consist of laminated silts and sands, which have undergone minimal bioturbation (Figs. 5 and 6). However, the sedimentological record is censored. At present, the slackwater deposit is only inundated after river stage exceeds ~4 m and there are no high water marks correlative to individual slackwater beds because the most recent flood obliterated the high water mark of the previous flood, as that flood did to its predecessor's, ad infinitum. However, as will be shown, the censored record can be used to determine whether the cave was permanently or only intermittently flooded at particular points in time.

The slackwater sediments can be divided into three principle units: 0–47 cm, 47–78 cm, and >78 cm (Figs. 5–7). Short horizontal lines demarcate the boundaries between the units in Figure 5. The upper two units record very different hydrologic regimes. The capping unit of silts and sandy silts contains partially articulated bat bones along with other vertebrate bones and organic detritus. Deposition of these sediments began at ~3,500 cal. years B.P. and has continued to present. The bat bones demonstrate that the Greenbrier River has been below the observed slackwater

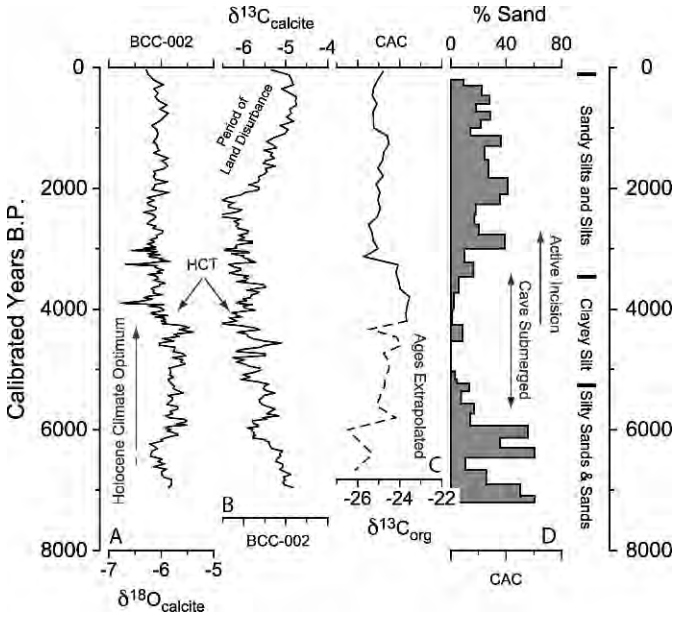

Figure 7. Paleoclimate proxies ($\delta^{18}O_{calcite}$ and $\delta^{13}C_{calcite}$) from stalagmite BCC-002 (A and B) are compared to data obtained from the Colonial Acres Cave (CAC) slackwater sediments (C and D). Note that sample ages from CAC are estimated below 4,000 cal. years B.P. using a sedimentation rate calculated for the upper, age-dated portion of the trench. And only six $\delta^{13}C_{org}$ values were obtained from CAC sediments below 5,000 cal. years B.P. Ignoring the period of land disturbance, $\delta^{13}C_{calcite}$ and $\delta^{13}C_{org}$ values were most enriched during the mid-Holocene and values decrease thereafter as the climate moistened (B and C). Submergence of CAC began prior to 5,000 cal. years B.P. and, assuming a low sedimentation rate for the clayey silts (see text), submergence probably began before the local Holocene Climatic Optimum (HCO)(A). Deposition of the clayey silt ended ~3,500 cal. years B.P. (D), and the overlying silts and sands contain abundant bat bones indicating incision of the river below the cave.

sediments since ~3,500 cal. years B.P. Today, there are extensive bedrock exposures in the channel banks and bed, and this bedrock channel morphology has probably existed for much of the last 3,500 years.

The clayey silts deposited prior to ~3,500 cal. years B.P. are devoid of bones and visible organic matter is rare. However, the clayey silts do contain insoluble cm-scale bedrock chips derived from thin claystone dikes in the cave ceiling. Paleozoic, coarsely crystalline marine fossils, such as blastoid thecas, are also present and derived from the host limestone. The coarsely crystalline fossils dissolve slower than the fine-grained limestone and stand in relief on existing cave walls and ceilings. Shale fragments and fossils found in the slackwater sediments fell or sank after the surrounding limestone was dissolved. Concentration of low solubility particles is a slow process and occurs when cave passages are permanently flooded and where sedimentation rates are slow (Reams, 1968; Springer et al., 1997). The corresponding depositional environment exists below low-water river surfaces and its products are known as backswamp or quietwater sediments (Springer et al., 1997; Bosch and White, 2003).

The clayey silts were deposited while the low-water surface of the Greenbrier River was higher than the cave room. In addition to the backwater sedimentological features, this conclusion is supported by the absence of terrestrial animal bones, desiccation features (e.g., mudcracks), and organic detritus such as has been carried into the cave by post-3,500 cal. years B.P. floodwaters. As an alternative hypothesis, all conduits connecting the cave and river could have been plugged during deposition of the clayey silts. This could have produced sustained backflooding. However, we reject this idea because of the improbability of every possible opening in a karstified riverbank being plugged such that a flooded cave could exist within meters of an open cliff. The simplest interpretation is that all openings were themselves permanently flooded, which would only be possible if base level were higher than present. Base-level rise is most commonly accomplished by sediment infilling a channel (aggradation).

Laminated and cross-bedded sands containing some visible organic detritus underlie the clayey silts (Figs. 6 and 7). Cross-bed orientations indicate that flow entered the room from the 210-m-long entrance passage and sediments prograded across the room floor. Currently, the floor of the first 100-m of the entrance passage consists of cross-bedded sands largely devoid of organic detritus, but overlain by woody flotsam. Presumably, the sands underlying the clayey silt in CAC were deposited in a manner similar to the modern sands, and were the product of episodic flooding above the low-water surface of the Greenbrier River.

In conclusion, the low-water surface of the Greenbrier River was below CAC during deposition of the lower sands, but subsequently aggraded above the cave (Fig. 8). The river re-incised below CAC at ~3,500 cal. years B.P. and has remained below the cave since then. BCC-002 and CAC values of $\delta^{13}C_{calcite}$ and $\delta^{13}C_{org}$, respectively, decrease after ~4,000 cal. years B.P. The enriched $\delta^{13}C_{calcite}$ and $\delta^{13}C_{org}$ values continue beyond the period of record, which suggests that deposition of the lower sands occurred during or prior to the HCO. Given the order of magnitude of the previously calculated sedimentation rate, deposition of the clayey silt probably began during the Early Holocene or the earliest part of the HCO. Thus, CAC slackwater sediments record a major aggradational event (≥4 m) in the Greenbrier River during the Early Holocene.

SUMMARY DISCUSSION

The Greenbrier River aggraded no later than the Early Holocene and may have begun aggrading during the Late Pleistocene. The implied increase in the sediment supply

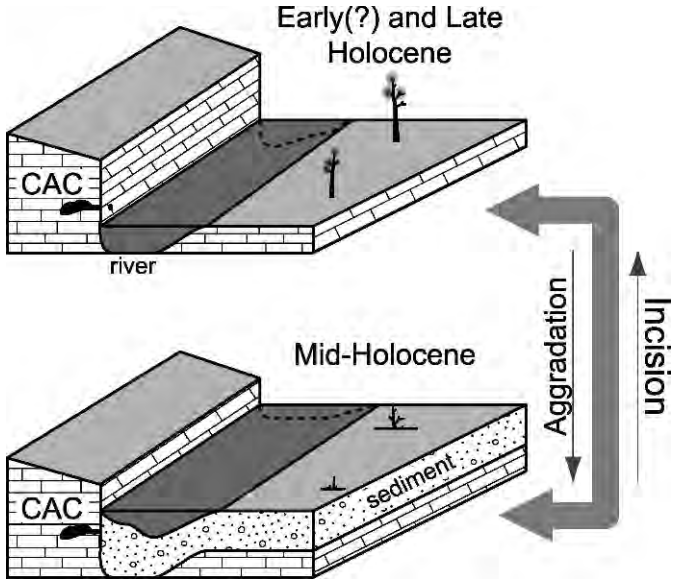

Figure 8. The sequence of events we interpret to have occurred begins with Colonial Acres Cave (CAC) lying above the Greenbrier River, which presumably had a bedrock channel morphology (upper diagram). Subsequently, the channel aggraded as a wetter Holocene climate allowed Pleistocene-age colluvium to be remobilized and carried into the river where transport capacity was initially less than sediment input, resulting in aggradation. The channel infilling may have created an alluvial channel morphology (bottom diagram). Eventually, the sediment wave was transmitted downstream and the river incised below CAC during the Late Holocene (upper diagram). This sequence of events is known to have occurred elsewhere in the Appalachians (Eaton et al., 2003).

may be the result of the Late Pleistocene-Holocene climatic transition. The Wisconsin Glaciation peaked ~20,000 cal. years B.P., and evidence for periglacial activity during the Wisconsin of the Appalachian and Blue Ridge Mountains is widespread (Gardner et al., 1991; Eaton et al., 2003; Mills, 2005; Nelson, et al., 2007). The associated pre-Holocene sedimentary deposits are commonly preserved at the bases of hillslopes where they are susceptible to remobilization by streams. The deposits reached valley bottoms via slope wash, solifluction, and gelifluction while climate was considerably cooler than present. The lower elevation limit for such periglacial activity at Mountain Lake, Virginia (50 km southeast of CAC) was ~800 m amsl (Nelson et al., 2007). Most ridges and mountaintops within the Greenbrier River watershed exceed that elevation, and well-developed periglacial landforms are present at 650 m amsl in the Buckeye Creek watershed.

Appalachian hillslope sediment production was enhanced by periglaciation during the Late Pleistocene (Gardner et al., 1991; Eaton et al., 2003; Mills, 2005), but regional palynology indicates that the Late Wisconsin climate was very dry (Kneller and Peteer, 1993). Therefore, it is entirely possible that the enhanced sediment production was not matched by an increase in the sediment transport capacity of regional streams and rivers. Under such a scenario, excess colluvium would have accumulated throughout much of the Greenbrier River watershed prior to the Holocene. The observed post-Pleistocene moistening of the region would have necessarily led to low-order streams remobilizing the accumulated regolith (cf. Eaton et al., 2003) and a large influx of sediment into the Greenbrier River. This sediment influx is probably the cause of the aggradational event recorded in CAC sediments.

We lack the means to establish the depth of infilling of the Greenbrier River channel at CAC. But the distinctive clayey silts associated with submergence are found 4 m above the low water surface of the modern Greenbrier River, which establishes a minimum depth of aggradation. Such infilling would have resulted in an alluvial channel morphology (Fig. 8), although bedrock exposure in pools cannot be ruled out. Significantly, the river began to incise through the accumulated sediments sometime during the Holocene Climatic Optimum (HCO) and incised below CAC by 3,500 cal. years B.P. Climate has moistened since the HCO (Figs. 4 and 7), which has presumably led to an increase in sediment transport capacity.

So, how will the Greenbrier River respond to Global Warming? Climate modelers predict (locally) decreasing runoff as Global Warming advances (Arnell, 2003). If we assume that decreasing runoff will lessen sediment transport capacity in the Greenbrier River, we must conclude that there is the potential for aggradation and morphological change. However, it is possible that heavy or extreme precipitation events may become more common as a result of Global Warming (Emori and Brown, 2005). If so, this could result in a net increase in transport capacity and no aggradation. Thus, it is premature to predict aggradation or incision.

Uncertainties about the future aside, the history of the Greenbrier River offers important insights into the long-term behavior of Appalachian rivers and hillslopes. Late Pleistocene climate variability resulted in significant channel infilling. The accumulated sediments were not fully excavated from the Greenbrier River channel until as late as 3,500 cal. years B.P., or roughly 16,000 years after the last glacial maxima (Webb, 1987). Interestingly, the Greenbrier River was already incised to its present elevation well before the last glacial maxima, and it is probable that very little net incision has occurred in tens of millennia. Incision may occur episodically during and immediately following interglacials, when precipitation totals are high or heavy precipitation events more common. This raises many questions concerning the usefulness of long-term incision rates calculated using paleomagnetic and cosmogenic isotopic data. These latter estimates require averaging incision over many hundreds to thousands of millennia (e.g., Springer et al., 1997; Anthony

and Granger, 2004; Anthony and Granger, 2006), so their estimates of actual millennial-scale incision rates may be off by many orders of magnitudes.

FUTURE DIRECTIONS

Stable isotopic records of paleoclimate from speleothems are rapidly becoming available throughout the world. As our study demonstrates, such records can be combined with traditional studies of slackwater stratigraphy to infer past effects of climate change on rivers. As such, there will soon be many opportunities to directly determine relationships between climate and hillslope and fluvial processes. However, such studies will be dependent upon fortuitously situated caves capable of recording the behavior of adjacent surface channels because surficial deposits are rapidly destroyed in many climatic settings (Kite et al., 2002; Springer, 2002). Combined with the subterranean origin of stalagmitic paleoclimate records, we foresee karst studies achieving prominent roles in geomorphology and climatology and encourage others to advance our methodology.

ACKNOWLEDGMENTS

The authors thank Tom Gardner and an anonymous reviewer for helpful suggestions that improved the manuscript. We thank Gene Turner for access to Buckeye Creek Cave and the West Virginia Association for Cave Studies for fieldwork assistance.

REFERENCES

Anthony, D.M., and Granger, D.E., 2004, A Late Tertiary origin for multilevel caves along the western escarpment of the Cumberland Plateau, Tennessee and Kentucky, established by cosmogenic ^{26}Al and ^{10}Be: Journal of Cave and Karst Studies, v. 66, p. 46–55.

Anthony, D.W., and Granger, D.E., 2006, A new chronology for the age of Appalachian erosional surfaces determined by cosmogenic nuclides in cave sediments: Earth Surface Processes and Landforms, v. 32, p. 874–887. doi: 10.1002/esp.1446.

Arnell, N.W., 2003, Effects of IPCC SRES emissions scenarios on river runoff: a global perspective: Hydrological Earth Systems Science, v. 7, p. 619–641.

Booth, R.K., Jackson, S.T., Forman, S.L., Kutzbach, J.E., Bettis, E.A. III, Kreigs, J., and Wright, D.K., 2005, A severe centennial-scale drought in midcontinental North America 4200 years ago and apparent global linkages: The Holocene, v. 15, p. 321–328.

Bosch, R.F., and White, W.B., 2003, Lithofacies and transport of clastic sediments in karstic aquifers, *in* Sasowsky, I.D., and Mylroie, J.E., eds., Studies of cave sediments, New York, Kluwer Academic and Plenum Press, p. 1–22.

Broecker, W.S., 1963, Preliminary evaluation of uranium series inequilibrium as a tool for absolute age measurement on marine carbonates: Journal of Geophysical Research 68, p. 2817–2834.

Bull, W.B., 1988, Floods; degradation and aggradation, *in* Baker, V.R., Kochel, R.C., and Patton, P.C., eds., Flood Geomorphology, New York, Wiley, p. 157–165.

Cheng, Hai, Edwards, R.L., Hoff, J., Gallup, C.D., Richards, D.A., and Asmerom, Y., 2000, The half-lives of uranium-234 and thorium-230: Chemical Geology, v. 169, no. 1–2, p. 17–33.

Dansgaard, W., 1964, Stable isotopes in precipitation: Tellus, v. 16, p. 436–468.

Dorale, J.A., Edwards, R.L., González, L., and Ito, E., 1998, Climate and vegetation history of the midcontinent from 75 to 25 ka: A speleothem record from Crevice Cave, Missouri, USA: Science, v. 282, p. 1871–1874.

Driese, S.G., Li, Z-H., and Horn, S.P., 2005, Late Pleistocene and Holocene climate and geomorphic histories as interpreted from a 23,000 ^{14}C yr B.P. paleosol and floodplain soils, southeastern West Virginia, USA: Quaternary Research, v. 63, p. 136–149.

Eaton, L.S., Morgan, B.A., Kochel, R.C., and Howard, A.D., 2003, Quaternary deposits and landscape evolution of the central Blue Ridge of Virginia: Geomorphology, v. 56, p. 139–154.

Edwards, R.L., Chen, J.H., and Wasserburg, G.J., 1987, ^{238}U–^{234}U–^{230}Th systematics and the precise measurement of time over the last 500,000 years: Earth and Planetary Science Letters, v. 81, p. 175–192.

Emori, S., and Brown, S.J., 2005, Dynamic and thermodynamic changes in mean and extreme precipitation under changed climate: Geophysical Research Letters, v. 32, no. L17706 p. doi: 10.1029/2005GL023272.

Gardner, T.W., Ritter, J.B., Shuman, C.A., Bell, J.C., Sasowsky, K.C., and Pinter, N., 1991, Stratified slope deposit in the Valley and Ridge Province of central Pennsylvania, USA: Sedimentology, stratigraphy, and geomorphic evolution: Permafrost and Periglacial Processes, v. 2, p. 141–162.

Hendy, C.H., 1971, The isotopic geochemistry of speleothems 1: The calculation of the effects of the different modes of formation on the isotopic composition of speleothems and their applicability as palaeoclimatic indicators: Geochimica et Cosmochimica Acta, v. 35, p. 801–824.

Kaplan, M.R., and Wolfe, A.P., 2006, Spatial and temporal variability of Holocene temperature in the North Atlantic region: Quaternary Research, v. 65, p. 223–231.

Kirby, M.E., Mullins, H.T., Patterson, W.P., and Burnett, A.W., 2002, Late glacial–Holocene atmospheric circulation and precipitation in the northeast United States inferred from modern calibrated stable oxygen and carbon isotopes: Geological Society of America Bulletin, v. 114, p. 1326–1340.

Kite, J.S., Gebhardt, T.W., and Springer, G.S., 2002, Slackwater deposits as paleostage indicators in canyon reaches of the central Appalachians: Reevaluation after the 1996 Cheat River Flood, *in* House, K., Webb, R., Baker, V., and Levish, D., eds., Ancient floods, modern hazards: Principles and applications of paleoflood hydrology: Water Science and Application Volume 5 (monograph), Washington, D.C., American Geophysical Union, p. 257–266.

Kneller, M., and Peteet, D.M., 1993, Late-Quaternary climate in the ridge and valley of Virginia, U.S.A.: changes in vegetation and depositional environment: Quaternary Science Reviews, v. 12, p. 613–628.

Knighton, D., 1998, Fluvial forms and processes: A new perspective, New York, Oxford University Press, 400 p.

Kundzewicz, Z.W., Mata, L.J., Arnell, N.W., Döll, P., Kabat, P., Jiménez, B., Miller, K.A., Oki, T., Senand, Z., and Shiklomanov, I.A., 2007, Freshwater resources and their management, *in* Parry, M.L., and Canziani, O.F., et al., eds., Climate Change 2007, Impacts, Adaptation and Vulnerability. Contribution of Working Group II to the Fourth Assessment Report of the Intergovernmental Panel on Climate Change, Cambridge, UK, Cambridge University Press, p. 173–210.

Lettenmaier, D.P., de Roo, A., and Lawford, R., 2006, Towards a capability for global flood forecasting: WMO Bulletin, v. 55, p. 185–190.

Li, Y.X., Yu, Z.C., and Kodama, K.P., 2007, Sensitive moisture response to Holocene millennial-scale climate variations in the Mid-Atlantic region, USA: The Holocene, v. 17, p. 1–6.

Maurer, E.P., Lettenmaier, D.P., and Mantua, N.J., 2004, Variability and potential sources of predictability of North American runoff: Water Resources Research, v. 40, no. W09306

McDermott, F., 2004, Palaeo-climate reconstruction from stable isotope variations in speleothems: A review: Quaternary Science Reviews, v. 23, p. 901–918.

Mills, H.H., 2005, Relative age dating of transported regolith and application to the study of landform evolution in the Appalachians: Geomorphology, v. 67, p. 63–96.

Montgomery, D.R., and Buffington, J.M., 1997, Channel-reach morphology in mountain drainage basins: Geological Society of America Bulletin, v. 109, p. 596–611.

Nelson, K.J.P., Nelson, F.E., and Walegur, M.T., 2007, Periglacial Appalachia: Palaeoclimatic significance of blockfield elevation gradients, eastern USA: Permafrost and Periglacial Processes, v. 18, p. 61–73.

Reams, M.W., 1968, Cave sediments and the geomorphic history of the Ozarks [PhD thesis], St. Louis, Mo., Washington University, 167 p.

Rozanski, K., Araguás-Araguás, L., and Gonfiantini, R., 1993, Isotopic patterns in modern global precipitation, *in* Swart, P.K., et al., eds., Climate Change in Continental Isotopic Records, Geophysical Monograph, Series, v. 78, Washington, D.C., American Geophysical Union, p. 1–36.

Schumm, S.A., 1973, Geomorphic thresholds and complex response of drainage systems, *in* Morisawa, M., ed., Fluvial geomorphology, Binghamton, New York State University Publications in Geomorphology, p. 299–310.

Shen, C.C., Edwards, R.L., Cheng, Hai, Dorale, J.A., Thomas, R.B., Moran, S.B., Weinstein, S.E., and Hirschmann, M., 2002, Uranium and thorium isotopic and concentration measurements by magnetic sector inductively coupled plasma mass spectrometry: Chemical Geology, v. 185, p. 165–178.

Springer, G.S., 2002, Caves and their potential use in paleoflood studies, *in* House, K., Webb, R., Baker, V., and Levish, D., eds., Ancient floods, modern hazards: Principles and applications of paleoflood hydrology, Water Science and Application Volume 5 (monograph), Washington, D.C., American Geophysical Union, p. 329–344.

Springer, G.S., Kite, J.S., and Schmidt, V.A., 1997, Cave sedimentation, genesis, and erosional history in the Cheat River Canyon, West Virginia: Geological Society of America Bulletin, v. 109, p. 524–532.

Springer, G.S., Rowe, H.D., Hardt, B., Edwards, R.L., and Cheng, Hai, 2008, Solar forcing of Holocene droughts in a stalagmite record from West Virginia in East-Central North America: Geophysical Research Letters, v. 35, no. L17703, doi: 10.1029/2008GL034971.

Stover, S.C., and Montgomery, D.R., 2001, Channel change and flooding, Skokomish River, Washington: Journal of Hydrology, v. 243, p. 272–286. doi: 10.1016/S0022-1694(00)00421-2.

Wang, Y.J., Cheng, Hai, Edwards, R.L., An, Z.S., Wu, J.Y., Shen, C.-C., and Dorale, J.A., 2001, a high-resolution absolute-dated Late Pleistocene monsoon record from Hulu Cave, China: Science, v. 294, no. 5550, p. 2345–2348.

Watts, W.A., 1979, Late Quaternary vegetation of central Appalachia and the New Jersey coastal plain: Ecological Monographs, v. 49, p. 427–469.

Webb, T. III., 1987, Climate change in eastern North America during the past 18,000 years: comparisons of pollen data with model results, *in* Ruddiman, W.F., and Wright, H.E., Jr., eds., The Geology of North America, v. K-3, Boulder, Colo., Geological Society of America, p. 447–462.

White, D.M., 2007, Reconstruction and analysis of Native American land use during the late Holocene [MS thesis], Athens, OH, Ohio University, 164 p.

Willard, D.A., Bernhardt, C.E., Korejwo, D.A., and Meyers, S.R., 2005, Impact of millennial-scale Holocene climate variability on eastern North American terrestrial ecosystems: pollen-based climatic reconstruction: Global and Planetary Change, v. 47, p. 17–35.

Wood, A.W., Maurer, E.P., Kumar, A., and Lettenmaier, D.P., 2002, Long range experimental hydrologic forecasting for the eastern U.S.: Journal of Geophysical Research, v. 107, no. D20, p. 4429, doi: 10.1029/2001JD000659.

F. Nozzoli, S. Bevilacqua, and L. Cavallari – The genesis of cave rings explained using empirical and experimental data. *Journal of Cave and Karst Studies,* v. 71, no. 2, p. 130–135.

THE GENESIS OF CAVE RINGS EXPLAINED USING EMPIRICAL AND EXPERIMENTAL DATA

F. Nozzoli[1], S. Bevilacqua[2], and L. Cavallari[2]

Abstract: A cave ring is a faint speleothem consisting in a thin circle on the floor symmetrically surrounding a water drop impact point. Two different mechanisms seem to be responsible for cave ring formation: the drop splash at the floor, for the splash rings, and the ejection of a secondary droplet during the fall, for the fall down rings. A systematic investigation of 67 speleothem rings discovered in five different caves in central Italy was conducted. The data show compatibility with a common nature for all the observed rings. For the observed rings, the hypothesis of a falling secondary droplet origin is confirmed and the hypothesis of a primary drop splash is rejected. The trajectory of a secondary droplet has been measured, and the collected data suggest that the secondary droplets originate from a primary drop breakup at a distance $y_0 = 142.7 \pm 7.2$ cm from the stalactite tip. Assuming this spontaneous breakup hypothesis, the velocities ratio $b = v_y/v_x = 25.5 \pm 1.6$ at the breakup time was measured. Finally, the collected ring data (5-cm- to 50-cm-diameter range) exhibit a negative curvature trajectory. The large departure from a gravity dominant parabolic trajectory suggests other forces, such as air friction or lift force, are at work on the small secondary droplets.

Introduction

A cave ring is a faint speleothem consisting of a thin circle on the cave floor symmetrically surrounding a water drop impact point. Depending on the water composition and the substrate, both positive or negative[3] rings were observed. Focusing on the more commonly occurring positive rings, the measured diameters range from a few centimeters to about two meters, depending on the height of the cave roof and on the formation mechanism. The ring width ranges from a few millimeters to a few centimeters and the surface of the calcite deposition ranges from a barely perceptible roughness to a ring thickness of a few centimeters (Hill and Forti, 1998; Torres Capote et al., 1991; Auler 1993; Montanaro, 1992). Perfectly circular rings are observed on flat floors, but when the floor slope increases, elliptical or elongated rings are observed with the major axis aligned with the dip direction. Formation survival[4] and visibility of a similar speleothem requires specific characteristics of the floor, such as the absence of strong water flows that could wash out the ring. Moreover, the rings are more easily revealed if a thin mud or dust film is covering a calcitic floor because of the increased contrast between clean and unclean areas.

Two different mechanisms appear to be responsible for cave ring formation. The first mechanism, capable of providing the larger observed rings (Hill and Forti, 1998), results from secondary droplets that are radially ejected after the primary drop splash on the floor. In this case, the secondary droplet velocity is related to the primary drop velocity at the impact point and is dependant on cave roof height and probably on the drop mass. The maximum bouncing distance of the secondary droplets is obtained when the ejection angle is 45°. The maximum bouncing distance determines the ring radius, and the random ejection direction of secondary droplets is responsible for the whole circle formation (Hill and Forti, 1998). In this article, we refer to rings generated with this mechanism as splash rings.

A different mechanism has been described for some smaller rings in the Grotta del Sorell cave in Sardinia (Montanaro, 1992). In this case, the ring is drawn by the superposition of many secondary droplets, but they are not ejected from the primary drop splash on the floor. In fact, the preliminary measurements of Montanaro showed that the secondary droplets originate near the roof, fall towards the floor, and retain an axial symmetry with respect to the primary drop trajectory. Montanaro postulated that the ejection of a secondary droplet was a result of a spontaneous breakup of the primary droplet after an approximate fall of two meters. The height of the breakup and the horizontal and vertical velocities of the droplet should be exactly constant to ensure a fixed ring radius, and the random ejection direction of the droplet is responsible for the whole circle formation. In the following, we refer to rings generated with this mechanism as fall down rings.

[3] The presence of negative rings on the gypsum floor at Lechuguilla Cave has been reported by Davis (2000).

[4] The rings can be quickly destroyed if stepped on during the cave exploration, and despite the lack of frequent observations of these speleothems, cave rings should be very common in many dry and richly decorated caves.

[1] Dipartimento di Fisica Università di Roma, Tor Vergata I-00133, Rome, Italy. Francesco.Nozzoli@roma2.infn.it

[2] Speleo Club Roma, via A. Doria - 79/F 00192, Rome, Italy. s.bevilacqua@speleoclubroma.org, cavallaripress@gmail.com

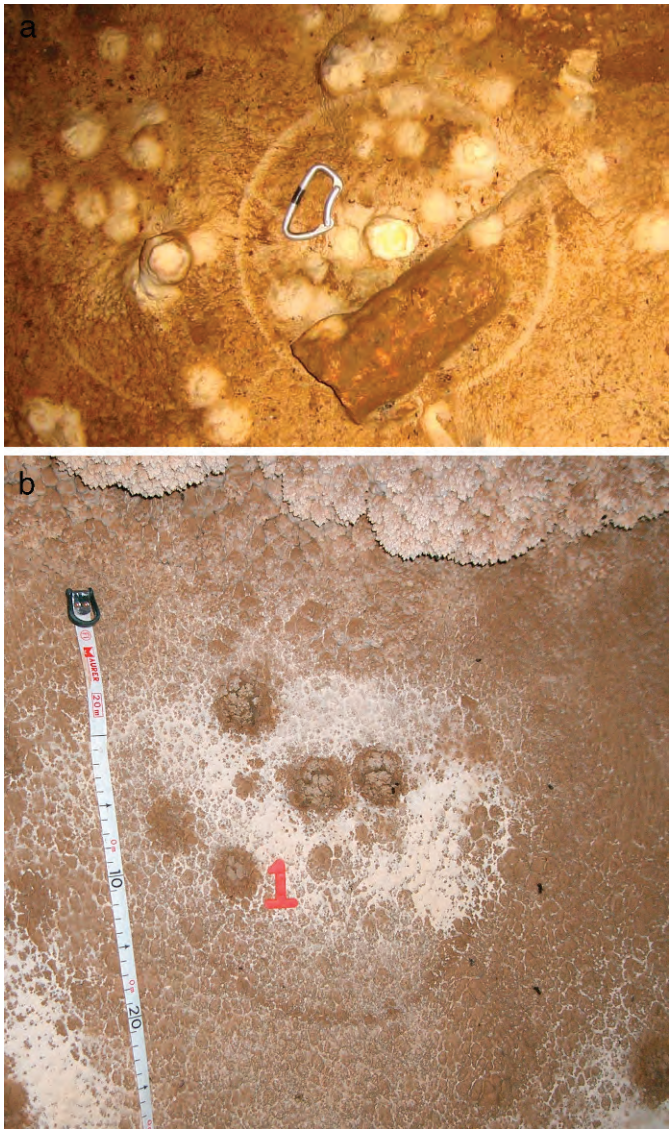

Figure 1. a): The most beautiful rings discovered in the Grotta Imbroglita Cave. b): Example of rings discovered in the dry lake of the Grotta del Secchio Cave.

For both cases, only qualitative results have been reported on the phenomenon. In particular, the second generation mechanism, which assumes the spontaneous breakup hypothesis, is very intriguing from an aerodynamic and fluid-dynamics point of view (see e.g., Joseph et al., 1999). Therefore, cave rings can also act as an ideal laboratory for additional investigations of Montanaro's postulated spontaneous breakup mechanism.

The Measured Sample

After the accidental discovery of some beautiful circles in the Grotta Imbroglita Cave (Fig. 1a), a systematic search for rings in various caves was pursued, providing a relatively large sample set (67 rings) distributed in five caves in central Italy. Forty-one new rings were discovered in four caves in the Lazio region (all located at a distance less than ~100 km from Rome) and five rings were artificially generated in the Grotta Imbroglita Cave (Table 1). Moreover, 21 rings were measured in the Grotta del Sorell Cave located on Sardinia Island. In this cave, more than one hundred rings are present that were previously investigated by Montanaro (1992). Interestingly, all these caves occur in very different karst areas, the caves are of different types, and the cave meteorology of each is dissimilar.

As general features, the observed rings were characterized by a barely perceptible roughness due to the calcite deposit, but were detected by the presence of a thin mud film covering the floor, where they provide a cleaner thin circular corona (Fig. 1a). An exception to this rule is evident in the Grotta del Secchio Cave where some circles have been found at the base of a small dry internal lake (this lake is full during rainy seasons). In this instance, the ring was somewhat darker as compared to the cave floor (Fig. 1b). All the observed rings are associated with a small central stalagmite, and the drop frequency of this primary drop was from ~0.1 Hz to less than $\sim 3\times10^{-4}$ Hz (e.g., no drops were falling within the one hour frequency of measurements). In addition, clear real-time evidence for a secondary droplet falling on the ring was never obtained during the ring observations.

Ring Measurements

For all the observed rings, the diameter and the distance from the central stalagmite and the generating stalactite (ring-height) were measured. Elliptical or elongated rings (e.g., rings on tilted cave floors) appear as perfect circles when observed from above so the minimum diameter was considered in the measurements because it is equal to the diameter of the projected circle.

For the case of incomplete circles, the radius from the central stalagmite was measured, which causes additional uncertainties for the correct estimation of the center. However, for all the measured rings, the larger uncertainty is provided by the pointing (and correct guess) of the generating stalactite on the roof. In fact, despite the use of a laser meter coupled to an air-bubble level, the exact targeting of the stalactite tip was, for all practical purposes, impossible, and fluctuations in the measured ring-height on the order of 15–20 cm (typical scale length for stalactites) were likely, as demonstrated by repeated measurements.

Artificial Rings

In order to understand the formation mechanism for the observed rings, some circles were artificially reproduced following the procedure developed by Montanaro (1992). In particular, wooden scaffolding was used in the Grotta Imbroglita Cave, and wooden tablets blackened with soot were placed at various heights over the original rings

Table 1. Cave ring sample distribution.

Cave	Cave Type	Altitude, m	Coordinates	Ring Position	Measured Rings
Grotta Imbroglita[a]	Tectonic cave	690	13°26′34″9 E 41°44′31″0 N	~50 m from entrance and ~−30 m deep	21 and 5 artificial
Pozzo l'Arcaro[b]	Tectonic cave	345	13°17′56″4 E 41°33′01″2 N	~50 m and ~−50 m deep from top entrance	1
Grotta dell'Inferniglio[c]	Active spring	510	13°09′21″6 E 41°53′26″1 N	~30 m from entrance	10
Grotta del Secchio[d]	Relic spring	750	13°08′05″ E 42°06′36″ N	~200 m from entrance	9
Grotta del Sorell (GEA)[e]	Sea cave	...	08°09′36″ E 40°34′24″ N	~100 m and +15 m from entrance	21

[a] 219La (Mecchia et al., 2003, p. 343). No air circulation.
[b] 340La (Mecchia et al., 2003, p. 343). Air circulation at entrances.
[c] 21La (Mecchia et al., 2003, p. 343). Completely submerged during rainy seasons.
[d] 575A (Mecchia et al., 2003, p. 343). Air circulation in the cave.
[e] 1580SA/SS (Montanaro, 1992). Rings already measured by Montanaro.

(Fig. 2a). After about 20 days, in vertical correspondence with an original ring on the cave floor, a new artificial ring was always present. The diameter of this new ring decreased with increasing height of the tablet.

To discriminate a splash ring from a fall down ring, some tablets were placed off center over the central stalagmites, and/or a hole was drilled in the tablets to allow the central drops to reach the cave floor. Therefore, because of the splash ring generating mechanism, no artificial rings were seen on the upper tablets and we were confident the observed circles are not a result of drop splash (Fig. 2b). Finally, for two different tablet heights we noted the formation of an additional and unexpected artificial ring without the corresponding circle on the cave floor. This suggests that the fall down ring mechanism could be common, but particular cave floor characteristics are necessary for ring detection.

DATA ANALYSIS

In order to quantitatively explore the ring features described by Montanaro (1992), all the circles data (ring-height vs. ring-radius) were plotted (Fig. 3a). Data from different caves and origin (natural/artificial) were coded by different markers and/or colors. A clear correlation of ring-height and ring-radius is shown by the data, which implies that the generating mechanism is the same for all the measured rings and that the final ring diameter depends only (or mainly) on the distance of the stalactite tip from its base (e.g., ring-height). It is worth noting that this property should not be expected a priori if, for example, the drop trajectory is dominated by some peculiar characteristics of the stalactite tip, or by drop mass, etc. On the basis of this result it is still puzzling that in the same cave only a few rings may be found among hundreds of stalactites, and it is not clear what phenomena cause some stalactites to generate rings.

The evidence that the measured circles are fall down rings and that the ring-radius is strongly correlated with the ring-height allows for additional interpretation of the plot in Figure 3a. In fact, because the ring-radius is the distance of the secondary drop impact point from the central stalagmite, the data points in the plot of Figure 3a follow the trajectory of secondary droplets in their motion planes. The parameters associated with the secondary drop trajectory are useful when evaluating the ring generation mechanism. Therefore, the data points have been fitted with a quadratic function

$$y = y_0 + br + ar^2 \quad (1)$$

where, y is the ring-height and r is the ring-radius. The parameters y_0, b, and a are physically related to some trajectory specifics:

1. $y_0 > 0$ represents the drop breakup distance, while the case of a null y_0 is related to a secondary drop ejected by the stalactite tip (e.g., no spontaneous breakup is necessary).
2. $b = v_y/v_x$ is the ratio of secondary droplet vertical velocity (v_y) over the horizontal velocity (v_x) at the breakup time.
3. a is related to the trajectory curvature and to the forces acting on the falling secondary droplets. In particular, a positive contribution is expected as a result of the force of gravity (see red curve in Fig. 3, a) although it is difficult to reliably evaluate the contribution of air friction (and/or air lift force) because it depends on the specifics of the drop geometry.

The black curve plotted in Figure 3a is the best-fit to all the data points (χ^2/dof = 1.3). Figure 3b shows the

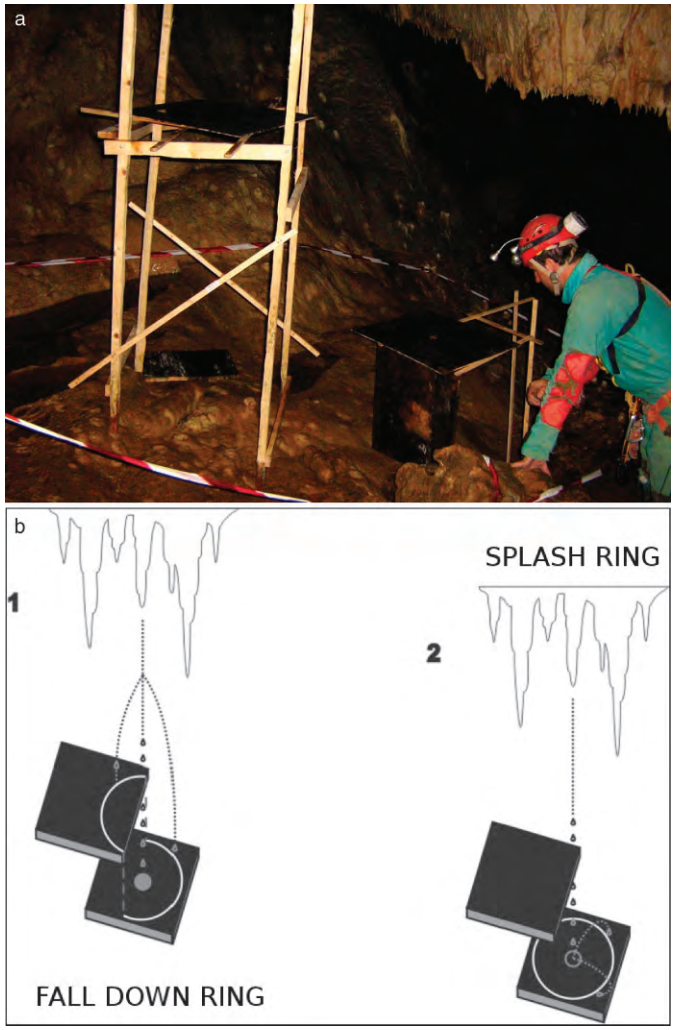

Figure 2. a): wooden scaffolding realized in the Grotta Imbroglita Cave. b): the formation of the ring on the upper tablet excludes the splash ring hypothesis.

distribution of Δh = ring-height − $y_{(\text{best fit})}$ and further demonstrates that the spread in the ring-height measurement (~15 cm) is mainly due to the imperfect pointing of the stalactite tips. From Figure 3a, the trajectory parameter values were determined to be $y_0 = 142.7 \pm 7.2$ cm, $b = 25.5 \pm 1.6$, and $a = -0.367 \pm 0.072$ cm^{-1}; and therefore, a non-null y_0 was measured with a statistical significance of about 20σ. The value of the curvature related parameter, a, is negative, with a statistical significance of about 5σ. The negative value for the curvature related parameter, a, was unexpected because, according to, Montanaro (1992), the trajectory curvature was described as positive (or it was simply assumed to be positive), as would be expected when gravity force is dominant as in the case for a falling drop (e.g., the red curve in Fig. 3a). However, the presence of a negative curvature was further demonstrated by the same analysis using only the artificial rings. In Figure 4, the 3σ confidence level allowed space for the y_0, b, a parameters is reported for the analysis of all data (dark area) or only for the artificial rings data (light area). The star indicates the best fit values of the y_0, b, a parameters.

Preliminary Mass Measurements

With an aim towards detecting evidence of the primary drop related to the ring generating mechanism, a preliminary drop mass measurement was pursued in the Grotta Imbroglita Cave. The mass of the primary drops from stalactites of four different rings was compared with the mass of drops from three stalactites that did not appear related to rings at floor level. Moreover, the drops were collected on the floor, and for ring related drops, the collector opening size was too small for collecting any possible secondary droplets[5]. The mass measurements are summarized in Table 2.

Only the most active stalactites were chosen for measurements. Therefore, relatively high dropping frequencies not representative of the stalactite population were measured. However, the difference between the dropping frequency for the two measured population samples given by

$$\Delta f = f_n - f_r = 0.25 \pm 0.26 \text{ Hz} \quad (2)$$

is still compatible with zero (f_n and f_r are the average dropping frequencies for no-ring drops and ring related drops, respectively).

Regarding the drop mass data, defining m_n and m_r as the average drop mass for no-ring drops and ring related drops, respectively, the difference is given by

$$\Delta m = m_n - m_r = 15.4 \pm 9.5 \text{ mg} \quad (3)$$

which is 1.6σ from zero. This result can be ascribed to statistical fluctuations. However, further primary drop mass data could be useful, in principle, for determining the average mass of the secondary droplets.

Discussion and Conclusions

Using the measurements of the 67 rings from the various caves, the qualitative features of the fall down ring speleothem class, originally recognized by Montanaro (1992), were confirmed. In particular, we can confidently reject the hypothesis that the observed circles occur as a result of drop splash at the cave-floor level. Moreover, for the first time, quantitative data were collected and analyzed, and the parameters for the trajectory for the hypothesized secondary droplets generating the rings were determined.

[5] We note that during these measurements, some extremely small droplets were felt on the operator's hands; their position would be comparable with the expected ring-radius, but no quantitative measurements of these droplets were possible for identifying these droplets as the ring generating droplets.

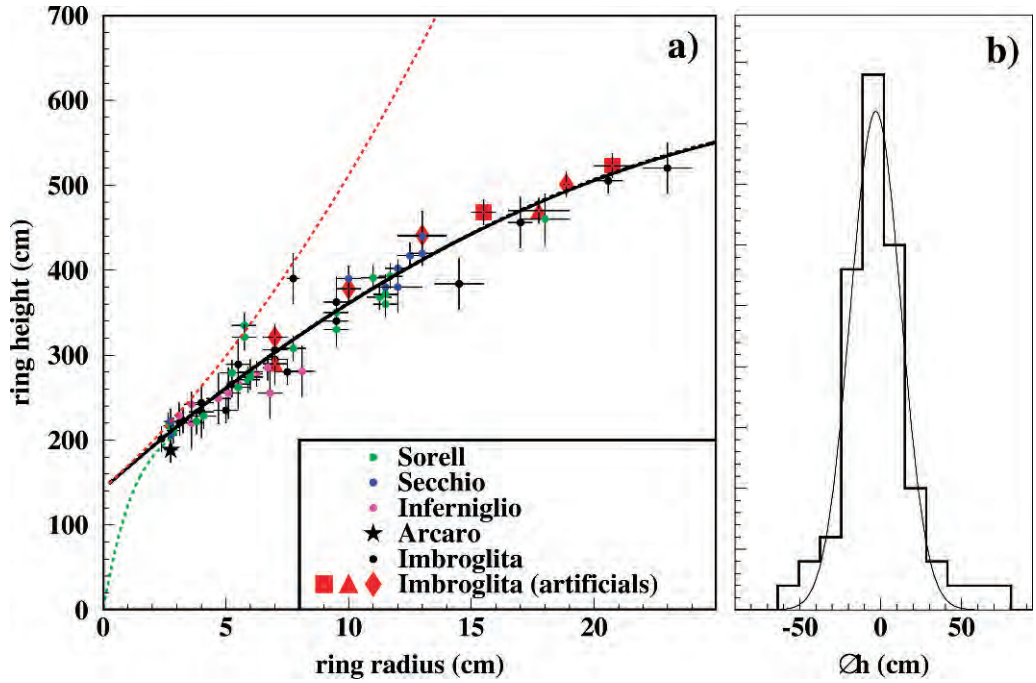

Figure 3. Plot a): Cave rings data points in the plane (ring-height vs. ring-radius); the stalactite tip is placed in the axis origin. The different color/markers refer to data of different caves. The red markers (squares, triangles, diamonds) refer to three different circles that have been artificially regenerated on wooden tablets at various heights from ground. Black curve is the quadratic best fit of all data points. Red dashed curve is the expected behavior assuming the spontaneous drop breakup hypothesis and negligible air friction on the drops. Green dashed curve is an example of possible model where the secondary droplet falls directly from the stalactite tip (e.g., no spontaneous drop breakup is necessary). Plot b): Distribution of Δh. The standard deviation of 15.6 cm obtained from the Gaussian fit is compatible with the spread due to the uncertainty in ring-height measurements.

The results suggest a nonzero value for y_0 (e.g., a spontaneous breakup mechanism of the primary drop should be active as hypothesized by Montanaro (1992)). The measured y_0 value (142.7 ± 7.2 cm) confirms the qualitative indication originally given by Montanaro (1992) (~2 m was given by Montanaro). Assuming the spontaneous breakup hypothesis, the velocities ratio $b = v_y/v_x = 25.5 \pm 1.6$ at the breakup time was determined, which is an interesting parameter for investigation of the hypothesized breakup phenomenon.

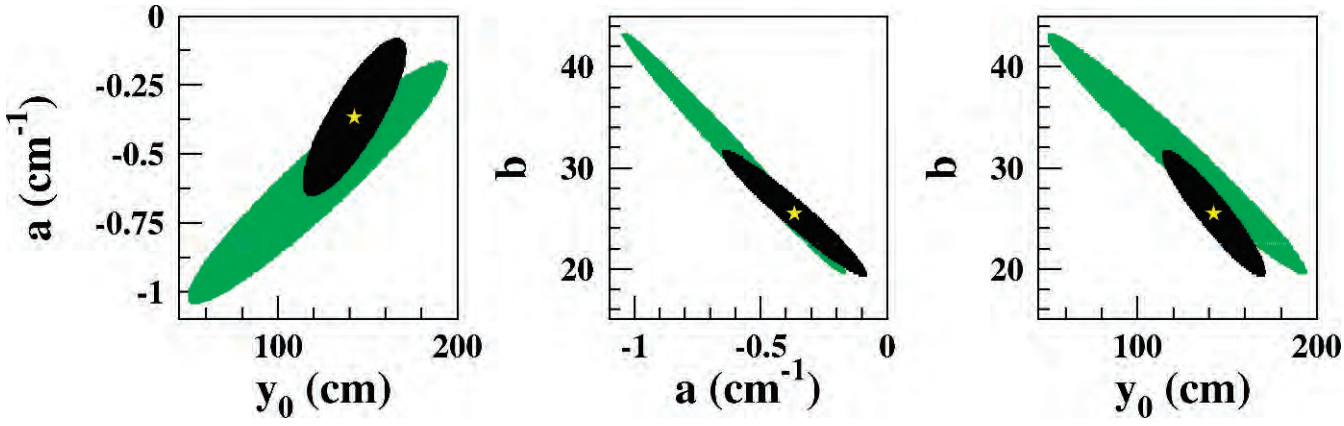

Figure 4. Allowed configurations at 3σ confidence level in the y_0, b, a parameter space for the analysis of all data (dark area) or only of artificial rings data (light area). The compatibility of the configurations allowed by the analysis of artificial rings with the ones allowed by the total data and confirms the trajectory parameter results and, in particular, the presence of a negative curvature. The star indicates the best fit values of the y_0, b, a parameters.

Table 2. Grotta Imbroglita Cave primary drop mass measurements.

Ring I.D.	Collected Drops	Average Drop Frequency, Hz	Average Drop Mass, mg
...	50	0.102 ± 0.004	102 ± 5
...	50	0.147 ± 0.006	93 ± 4
...	100	0.666 ± 0.013	110 ± 3
n. 4	50	0.119 ± 0.005	88 ± 4
n. 12	42	0.028 ± 0.001	97 ± 5
n. 19	40	0.063 ± 0.003	87 ± 5
n. 20	30	0.027 ± 0.002	81 ± 5

A third trajectory parameter $a = -0.367 \pm 0.072$ cm^{-1} was also determined. This parameter is related to the trajectory curvature and the collected data show a negative curvature trajectory. This observed trajectory feature is opposite that of the one described by Montanaro (1992), where a positive curvature was probably assumed as a result of dominance of the force of gravity on the secondary droplets.

The nature of the force driving this negative curvature trajectory is still unclear. However, the large departure from a gravity dominant parabolic trajectory (red curve in Figure 3a) suggests that other forces, such as air friction and/or lift force, are at work on the small secondary droplets. Alternatively, searching for and measurements of the trajectory features for small ring-radii (~2.5 cm) are very difficult because the primary drop splash on the cave floor would tend to wash out the small rings. Therefore, no data are available at present in this region, and departures from the extrapolated behavior cannot be excluded. This fact implies additional uncertainties on the measured y_0 value (because it is obtained by extrapolating the trajectory at the null radius) and also on the presence of the spontaneous drop breakup phenomenon. This is shown by the green curve in Figure 3a. In this example, an increasing curvature parameter at low ring-radius allows secondary drops falling directly from the stalactite tips. This example of trajectory does not require a spontaneous breakup of the primary drop and, with the present data, similar scenarios cannot be distinguished from previous ones.

Future measurements with a high speed camera should be able, in principle, to yield information about the secondary drop trajectory in this small ring-radius region. However, the final analysis would be much simpler (and cheaper) if very small rings can be found and measured in the future. For example, in Davis (2000), a small negative ring in gypsum is shown in Figure 18; this ring is described (or is assumed) to be a splash ring. A careful observation suggests, however, that the splash ring shown in Davis (2000) is actually two splash rings that overlap and that are most likely fall down rings. In fact, in the case of a splash ring, a 45° slope of the walls of the central hole and of the ring cuts should be expected. On the contrary, the central hole and the ring cut seem to be practically vertical as expected for fall down rings. The rings in Davis (2000) seem to be very small. Therefore, a further study of their nature and of their parameters (radius and stalactite tip distance) would be very useful as a check on the nature of the hypothesized spontaneous breakup phenomenon (see e.g., Joseph et al., 1999).

As a final conclusion, we recommend all cavers pay attention to the presence of cave rings and we encourage them to develop similar (or better) measurements on newly discovered rings. Particular importance should be directed to the small rings. Lastly, we note that we are available to assist with analyses of any data from new ring samples that may be discovered.

Acknowledgments

We thank all the following individuals who assisted with data collection: SCR: Rosa De Filippis, Silvia Caricati, Giovanni Mecchia, Maria Piro, Giorgio Pintus, Giovanna Politi, Maria Fierli, Massimiliano Re, Paola Fanesi, Stefano De Santis, Marco Lo Presti, Roberto Formica, Fabrizio Paoloni, Beatrice Paoloni, Francesca Cecaloni, Filippo Camerini; ASR86: Angelo Pompei; GSGM: Attilio Nini; GSV: Nicola Squicciarini; GEA: Giampiero Mulas, Pietro Serra, Massimo Siffu, Felice Moccia, Toni Castigliego, Zarini Ferrucio; GSS: Mauro Mucedda, Luca Montanaro. The authors are grateful to Luca Montanaro for insightful discussions and to Claudia Grasso for the text revision.

References

Auler, A., 1993, Les cercles de calcite flottante de le "Lapa do Bezzerra", (Sao Domingos, Golias, Bresil): Kartologia, v. 22, p. 55–56.

Davis, D.G., 2000, Extraordinary features of Lechuguilla Cave, Guadalupe Mountains, New Mexico: Journal of Cave and Karst Studies, v. 62, no. 2, p. 147–157.

Hill, C., and Forti, P., 1998, Cave minerals of the world (2nd ed.): Huntsville, Ala., National Speleological Society, 463 p.

Joseph, D.D., Belanger, J., and Beavers, G., 1999, Breakup of a liquid drop suddenly exposed to a high-speed airstream: International Journal of Multiphase Flow, v. 25, p. 1263–1303.

Mecchia, G., Mecchia, M., Piro, M., and Barbati, M., 2003, Le grotte del lazio: Regione lazio, collana verde dei parchi, Report 3 Serie Tecnica, 413 p.

Montanaro, L., 1992, Osservazioni sui "cerchi" della Grotta del Sorell: Boll. Gr. Speleol. Sassarese, v. 13, p. 21–22.

Torres-Capote, V., Jaimez-Salgade, E., and Marquez-Montera, V., 1991, Estudio litogenético preliminar de una nueva formaciòn: los circulos concéntricos recontructivos: Bol. Casimba, series 2, v. 3, no. 3, 68 p.

W.B. White, C. Vito, and B.E. Scheetz – The mineralogy and trace element chemistry of black manganese oxide deposits from caves. *Journal of Cave and Karst Studies,* v. 71, no. 2, p. 136–143.

THE MINERALOGY AND TRACE ELEMENT CHEMISTRY OF BLACK MANGANESE OXIDE DEPOSITS FROM CAVES

William B. White[1*], Carmen Vito[2], and Barry E. Scheetz[3]

Abstract: Free surface streams in caves and their surface infeeders often contain pebbles and cobbles coated with black manganese oxide minerals. Coating thicknesses vary from fractions of a millimeter to a few millimeters. In addition, a few caves contain loose masses of black oxide material. The results reported here are based on examination of 39 specimens and detailed chemical analyses of 18 of them. Most of the coatings are amorphous to x-rays, with at best, only a few broad diffraction lines. Infrared spectroscopy shows that most of the specimens are birnessite, with evidence for romanechite, ranceite, and pyrolusite in a few specimens. All specimens contain both iron and manganese, but the Mn/Fe ratio varies widely. Many specimens are enriched in Ba but depleted in Sr. The manganese and iron oxides contain the transition metals Co, Cu, Ni, V, and Zn in concentrations greater than 0.5 wt% in some specimens. Minor Cr and Mo also occur. Given the extremely low concentrations of these elements expected in freshwater streams in carbonate terrains, the manganese oxides exert a dramatic amplifying effect over the expected background. Manganese oxides appear to act as a dosimeter for heavy metals in karst waters.

Introduction

Stream cobbles, chert ledges, and other silica substrates exposed to free surface streams in limestone caves are frequently coated with a black substance usually labeled manganese oxide. In most localities, the coatings vary in thickness from fractions of a millimeter to a few millimeters. A few caves are known in which more massive black coatings or loose deposits many centimeters thick occur. As a caveat, it is not appropriate to label every black deposit seen in caves as manganese oxide. As noted by Hill (1982), soot from early explorer's torches, carbonized organic matter, and other black materials may occur. However, most black stream-bed coatings examined in this study have been identified as manganese oxide, and these coatings are the subject of the present paper.

The oxides of Mn^{3+} and Mn^{4+} display a very complex mineralogy, with many crystal structures and many variations in trace element chemistry (Post, 1999). Manganese oxide minerals are widely known from stream sediments, from soils, and from deep-sea nodules. Synthetic manganese oxides are important in technology, particularly as battery materials. It is generally agreed that the oxidation of the soluble Mn^{2+} to trivalent or tetravalent manganese in near surface environments is mediated by microorganisms. There is a very large body of earlier literature that has been reviewed by Tebo et al. (1997) and includes some quite recent work (Jürgensen et al., 2004).

For the most part, the manganese oxides that occur in caves are very poorly crystallized, thus making the identification of the mineral phase difficult. Birnessite has been identified as the most commonly occurring mineral (Moore, 1981; Kashima, 1983). Other manganese minerals that have been reported from caves, with identifications of varying degrees of confidence, include chalcophanite, cryptomelane, hausmannite, pyrolusite, rancieite, romanechite, and todorokite (Hill and Forti, 1997). Manganese oxides also occur in karst solution cavities (Jones, 1992). Manganese oxide deposits are listed among cave minerals of predominantly microbial origin (Northup and Lavoie, 2001; Spilde et al., 2005). Evidence for specific microorganisms has been provided by Peck (1986) and by Northup et al. (2003).

The present paper is concerned with manganese oxides as scavengers for transition (iron-group) metals in karst environments. Ore-quality concentrations of transition group metals are, of course, well known from marine manganese oxides (Burns and Burns, 1978). Deposition of metal-containing manganese oxides in a surface stream has been measured (Carpenter and Hayes, 1980). Cave deposits form in a fresh-water environment with relatively few sources for transition group metals. However, the few reported analyses (Moore, 1981; Peck, 1986; White et al., 1985) reveal metals such as zinc and nickel at the fractional percent level. Onac et al. (1997) reported high concentrations of rare earth elements in the manganese oxides in a cave in Romania. The present paper reports a more systematic investigation that reveals high concentrations of transition group elements in a variety of cave manganese deposits in the eastern and central United States.

* Corresponding author

[1] Materials Research Institute and Department of Geosciences, The Pennsylvania State University, University Park, PA 16802. wbw2@psu.edu
[2] 586 Harrison St., Hazleton, PA 18201
[3] Department of Civil and Environmental Engineering, The Pennsylvania State University, University Park, PA 16802

Table 1. Sources of specimens used for manganese oxide characterization.

Sample No.	Cave Name	Location	Sample Description
208	Weber Cave	Iowa	Loose black powder
209	Muenster Cave	Iowa	Loose black powder
214	Wind Cave	South Dakota	Brown earthy mass
271	Wind Cave	South Dakota	Brown dirt from geode
531	Mammoth Cave	Kentucky	Black coating on chert ledge
555	Parker Cave	Kentucky	Large pebbles with flaky brown coating
575	Jewel Cave	South Dakota	Thick massive black deposit in cave passage
580	Devil's Icebox	Missouri	Thick black coatings from stream passage
619	Mammoth Cave	Kentucky	2 mm coating on chert ledge
622	Snail Shell Cave	Tennessee	1 mm dull black coating on flowstone
627	Cumberland Caverns	Tennessee	Loose brown-black sooty material on chert
632	Tumbling Rock Cave	Alabama	0.2–0.5 mm coating on pebble
636	Priddy Cave	Kentucky	Thick coating on limestone chip in stream bed
639	Colossal Cave	Kentucky	Thin coating on chert
646	Anvil Cave	Kentucky	Black coating on sandstone pebble
650	Matt's Black Cave	West Virginia	3–5 mm massive black crust
82MM003	Jewel Cave	South Dakota	Loose black powder
96MM001	Hineman Cave	Pennsylvania	Soft black flowstone with orange bands

Experimental Methods

Sample Descriptions

A total of 39 specimens of black coatings and deposits were collected from caves, mostly in the eastern United States. Many of these were stream cobbles, either from active streams or from abandoned high-level cave passages. Many of the coatings were thin, fractions of a millimeter, so that it was not possible to physically remove sufficient sample for analysis. About half, 18 specimens, were either bulk deposits or were coatings of sufficient thickness that they could be sampled for analysis (Table 1). The samples are identified by their number in a master collection of cave material maintained by the senior author.

For those specimens of sufficient mass, milligram quantities of the oxide coatings were scraped off, care being taken to avoid contamination by the substrate and by sample handling. The manganese oxide coatings were soft enough to be easily removed. Bulk deposits could be sampled directly. Solid chips were ground in an agate mortar so that all initial samples were powders.

Characterization Methods

Textures and rough bulk compositions of the black coatings were measured using a scanning electron microscope equipped with an energy-dispersive X-ray detector (EDX). The EDX spectra confirmed that the coatings were indeed oxides of manganese and also revealed major elements such as Ca, Ba, Al, and Si.

X-ray diffraction was of limited value for phase identification because of the very small particle size and structural disorder within the samples. Infrared spectroscopy was more useful because it allowed comparison of the spectra of the cave deposits with the reference spectra established by Potter and Rossman (1979). All spectra were measured by the KBr pellet technique. One mg of sample was ground with 200 mg of KBr and vacuum cold-pressed into a compact disk that was then inserted into the spectrometer. Several older spectra were obtained from a Perkin-Elmer model 283 dispersive spectrometer. More recent spectra were obtained with a Nicolet Fourier transform spectrometer.

Samples for chemical analysis were dissolved in hydrochloric acid, and the resulting solutions analyzed for cations by DC plasma emission spectroscopy. The limit of detection for the method was 3 ppm with respect to the original solid sample.

Results

Chemical Characterization

Chemical analyses of the deposits are displayed for the powders and bulk specimens in Table 2 and for the coatings in Table 3. The analyses are reported as weight percent oxide with respect to the original solid sample. The total masses of the various component oxides do not add up to 100%, and some samples fall far short of 100%. There are three sources for this discrepancy. Most of the analyses were conducted on a few milligrams of material scraped from chert layers or sandstone stream cobbles. The scrapings were weighed and then dissolved in HCl. Excess silica would be included in the original weighing but not in the final solution injected into the DC plasma. This was confirmed by re-analyzing two of the bulk specimens (for which there was adequate sample) by a fusion technique that took the entire sample into solution. Sample 214

Table 2. Chemical analyses of massive and loose powder deposits. All compositions in wt%.

	Sample Number							
Oxide	82MM003	209	575	627	208	96MM001	214	271
Al_2O_3	0.23	0.11	0.63	11.3	0.21	1.89	0.71	0.39
B_2O_3	0.054	0.046	0.013	0.029	0.031	0.081	0.023	0.025
BaO	7.73	1.84	8.83	0.3	5.13	0.18	0.96	0.31
CaO	8.17	7.69	2.52	1.63	5.11	3.67	4.68	4.71
CoO	0.26	0.22	0.3	0.36	0.21	0.11	0.003	0.005
Cr_2O_3	0.038	0.039	0.007	0.13	0.009	0.01	0.021	0.01
CuO	0.51	0.045	0.17	0.044	0.04	0.056	0.083	0.018
Fe_2O_3	0.68	0.95	3.29	33	0.82	21.5	9.53	3.06
K_2O	0.65	0.13	0.36	0.085	0.37	0.082	0.16	0.15
MgO	2.11	2.39	1.15	3.13	2.4	1.08	0.69	0.21
MnO_2	67.39	64.94	58.82	13.72	53.92	24.63	8.47	4.17
MoO_3	0.052	0.044	0.05	0.12	0.051	0.036	0.038	0.035
Na_2O	0.46	0.24	0.29	0.88	0.69	0.28	0.072	0.098
NiO	0.66	0.37	0.43	0.28	0.76	0.49	0.13	0.069
SiO_2	0.33	0.36	0.24	1.38	0.33	1.66	0.66	0.61
SrO	0.2	0.006	0.18	0.15	0.049	0.011	0.03	0.003
TiO_2	0.006	0.015	0.052	0.34	0.015	0.003	0.047	0.006
V_2O_5	0.72	0.014	0.94	0.28	0.014	0.025	0.092	0.034
ZnO	0.14	1.87	0.091	0.39	1.37	0.068	0.072	0.023
ZrO_2	0.1	<0.003	<0.003	0.19	<0.003	<0.003	<0.003	<0.003
Total	90.49	81.32	78.36	67.74	71.53	55.87	26.47	13.78

Table 3. Chemical analyses of coatings. All concentrations in wt%.

	Sample Number									
Oxide	531	580	555	650	619	622	636	646	632	639
Al_2O_3	6.62	2.47	5.76	3.8	7.56	4.68	2.77	7.44	9.97	1.54
B_2O_3	0.014	<0.003	0.017	0.026	0.071	0.035	0.019	0.023	0.048	0.032
BaO	0.64	0.278	0.72	0.77	0.44	0.45	1.62	0.26	0.24	0.31
CaO	20.5	5.71	4.09	4.76	4.34	5.82	10.7	2.06	3.26	1.96
CoO	0.074	0.06	0.08	0.13	0.036	0.065	0.18	0.57	0.18	0.11
Cr_2O_3	0.038	<0.003	0.006	0.067	0.047	0.046	0.1	0.081	0.062	0.067
CuO	0.56	0.029	0.024	<0.003	<0.003	<0.003	0.004	0.013	<0.003	0.011
Fe_2O_3	4.09	3.25	5.86	3.19	6.58	4.23	2.59	2.48	4.67	1.72
K_2O	0.13	0.39	0.14	0.21	0.12	0.27	0.31	0.06	0.049	0.078
MgO	1.37	0.7	0.96	0.79	0.93	0.64	0.86	0.47	0.44	0.47
MnO_2	20.46	45.34	31.49	34.06	20.22	25.12	20.95	20.95	17.65	8.99
MoO_3	0.052	0.036	0.044	0.081	0.03	0.031	0.12	0.1	0.074	0.078
Na_2O	0.099	0.3	0.082	0.15	0.13	0.12	0.24	0.16	0.12	0.13
NiO	0.98	0.094	0.22	0.15	0.15	0.038	0.13	1.3	0.62	0.11
SiO_2	1.67	0.14	0.75	0.47	1.26	0.54	0.16	0.13	0.38	0.27
SrO	0.072	0.027	0.047	0.048	0.067	0.031	0.057	0.029	0.047	0.026
TiO_2	0.072	0.011	0.055	0.076	0.078	0.041	0.11	0.091	0.1	0.088
V_2O_3	0.037	0.067	0.035	0.15	0.071	0.072	0.24	0.21	0.14	0.17
ZnO	0.17	1.56	0.33	0.077	0.18	0.021	0.085	1.58	0.18	0.056
ZrO_2	0.17	<0.003	<0.003	0.041	<0.003	0.026	0.22	0.081	0.053	0.066
Total	57.82	60.47	50.71	49.05	42.31	42.27	40.46	37.73	33.28	16.29

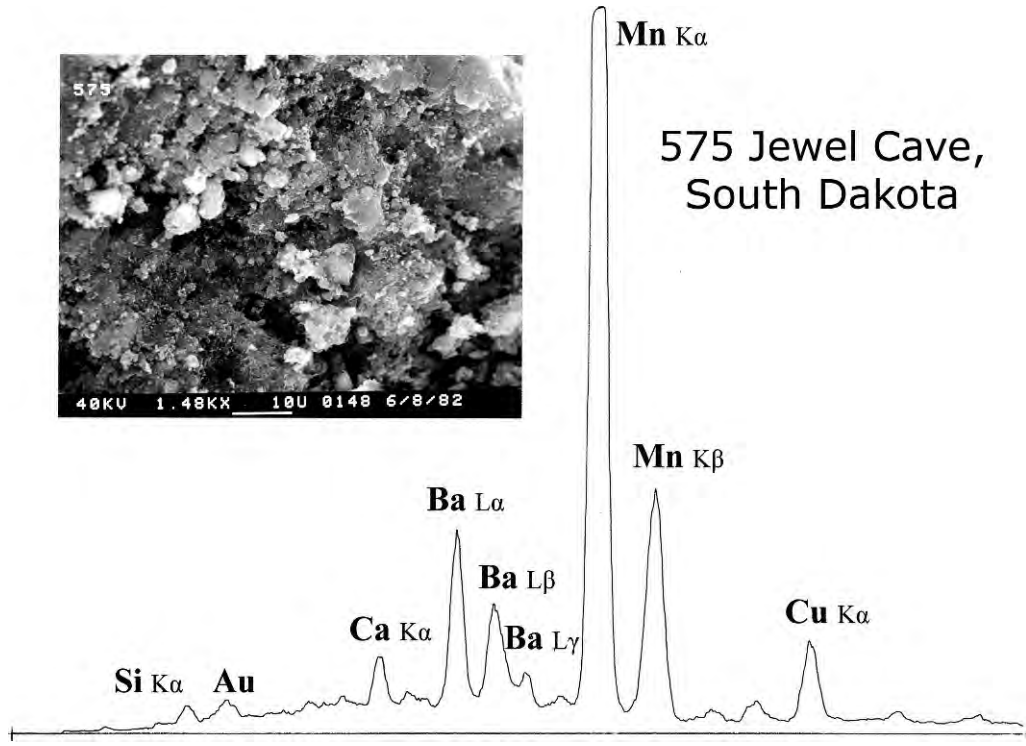

Figure 1. SEM image and EDX spectrum of specimen 575 from Jewel Cave, South Dakota. Note that this sample is exceptionally barium-rich. The EDX spectrum is a plot of X-ray intensity versus X-ray energy. Characteristic lines for various elements are labeled.

contained 41.0 wt% SiO_2, compared with 0.66% in the acid solution. Sample 580 contained 12.3% SiO_2 by fusion, compared with 0.14% in the acid solution. The second source of discrepancy is that most of the samples are hydrated to some extent, but the results were calculated only as the oxides and did not account for either OH^- or bound water. The third, and minor, source is that a few samples contain some carbonate that is taken into solution along with the manganese oxide, but the CO_2 component does not appear in the analysis, although Ca does. Tables 2 and 3 contain the original analytical data. Further interpretation was based on elemental concentrations that were normalized to the sum of oxide components given at the bottoms of the tables.

Thermogravimetric analysis was conducted on four of the samples (214, 575, 580, and 650) from ambient to 1000 °C. There was a continuous mass loss of 15–20% up to 700 °C, above which the weight remained constant. 5–10% of the mass loss occurred below 150 °C and likely represents water and easily decomposed hydrates.

Structural Characterization

SEM images of two samples are superimposed on their X-ray emission spectra (Figs. 1 and 2). The Jewel Cave sample (575) is a thick, massive deposit that occupies the floor of one small passage to a depth of at least tens of centimeters. The laboratory sample was several centimeters thick and free of extraneous contamination. The SEM image reveals little structure at the micrometer scale. This locality had been previously examined by Moore (1981), who identified the mineral as hollandite, a conclusion consistent with the high Ba concentration shown in the EDX spectrum. The Mammoth Cave sample (531) was taken from a several-millimeters-thick layer that had been deposited on a chert ledge just above the floodwater zone. The SEM image reveals a granular structure with individual particles about 3–5 μm in diameter. The appearance of Al and Si in the EDX spectrum suggests contamination by silica and silicate minerals in the coating itself; not all contamination is due to the substrate. SEM images of two additional samples, both loose powders from cave floors, (Fig. 3) show a filimentary structure that may indicate a microbial origin. Well-crystallized manganese oxides do occasionally appear in caves, for example, romanèchite from Corkscrew Cave, AZ, which gives a sharp X-ray powder pattern (Onac et al., 2007).

Infrared spectra of two bulk samples display the expected features of manganese oxides (Fig. 4). The Muenster Cave, IA sample (209) was a loose powder; the Jewel Cave sample was a massive, consolidated chunk. The broad bands at 3280 and 3400 cm^{-1} are the stretching modes of OH groups. The band at 1610 is the H_2O bending mode, which shows that at least some of the OH is H_2O. The intense band at 465 and the group of bands centered at

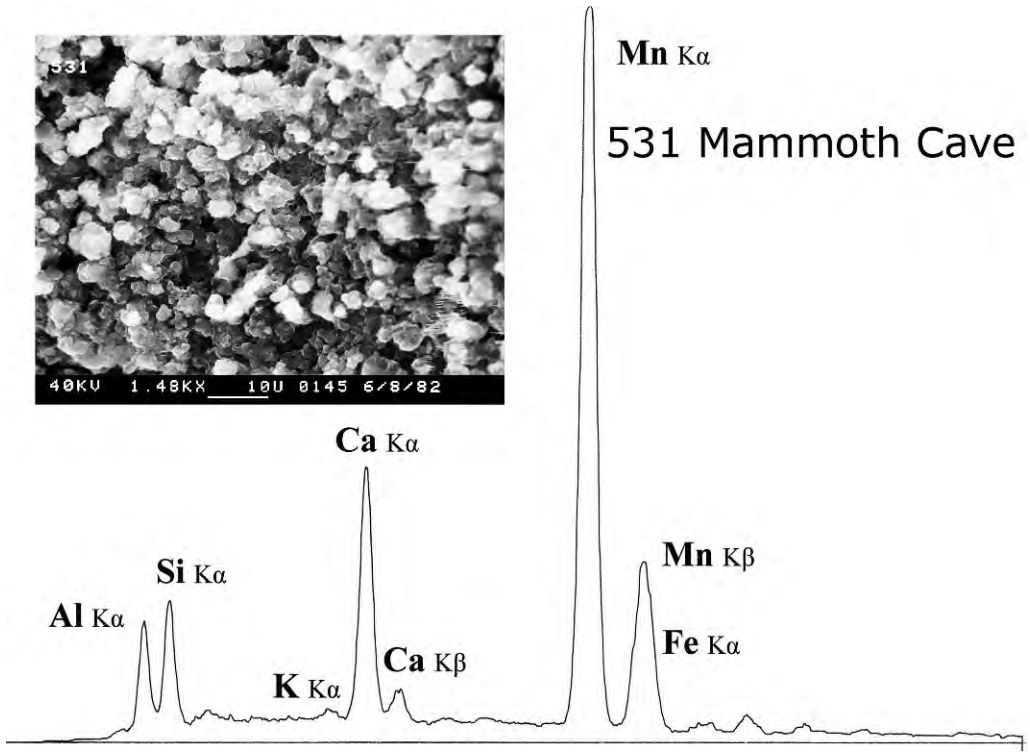

Figure 2. SEM image and EDX spectrum of specimen 531 from Mammoth Cave, Kentucky.

525 cm^{-1} are the stretching modes of the MnO_6 octahedra that are the fundamental building blocks of the manganese oxide mineral structures.

Infrared spectra also reveal the presence of mineral contaminants (Fig. 5). Specimen 214 contains a great deal of silica, which appears in the IR spectrum as the intense band at 1030 cm^{-1}. The weaker bands at 795, 772, and 690 cm^{-1} identify the contaminant mineral as quartz. Specimen 531 contains both silica and carbonate, the latter producing the strong absorption at 1425 cm^{-1}.

Examination of the Mn-O stretching mode on the four samples in Figures 4 and 5 and three additional spectra (only the Mn-O band) in Figure 6 makes clear that the manganese mineral coatings deposited in cave environments have distinctly different structures. The cave samples, as cold water deposits, are crystallized only at

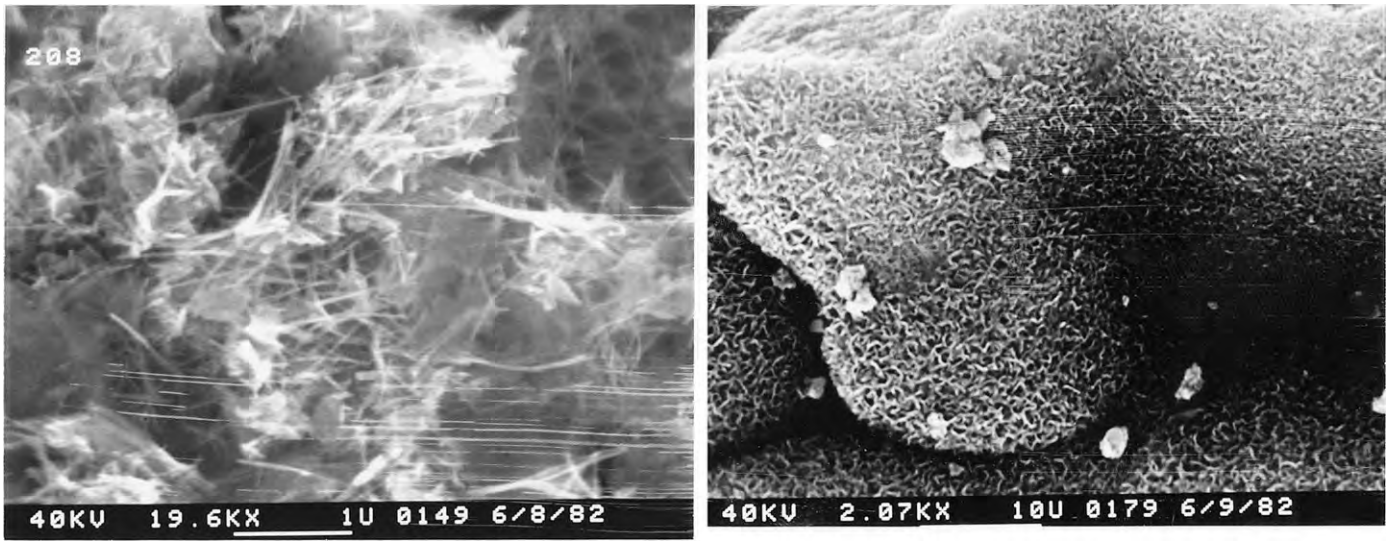

Figure 3. SEM images. Left: sample 208, Weber Cave, Iowa, showing filimentary structure. Right: sample 209, Muenster Cave, Iowa, showing crenulated surface structure.

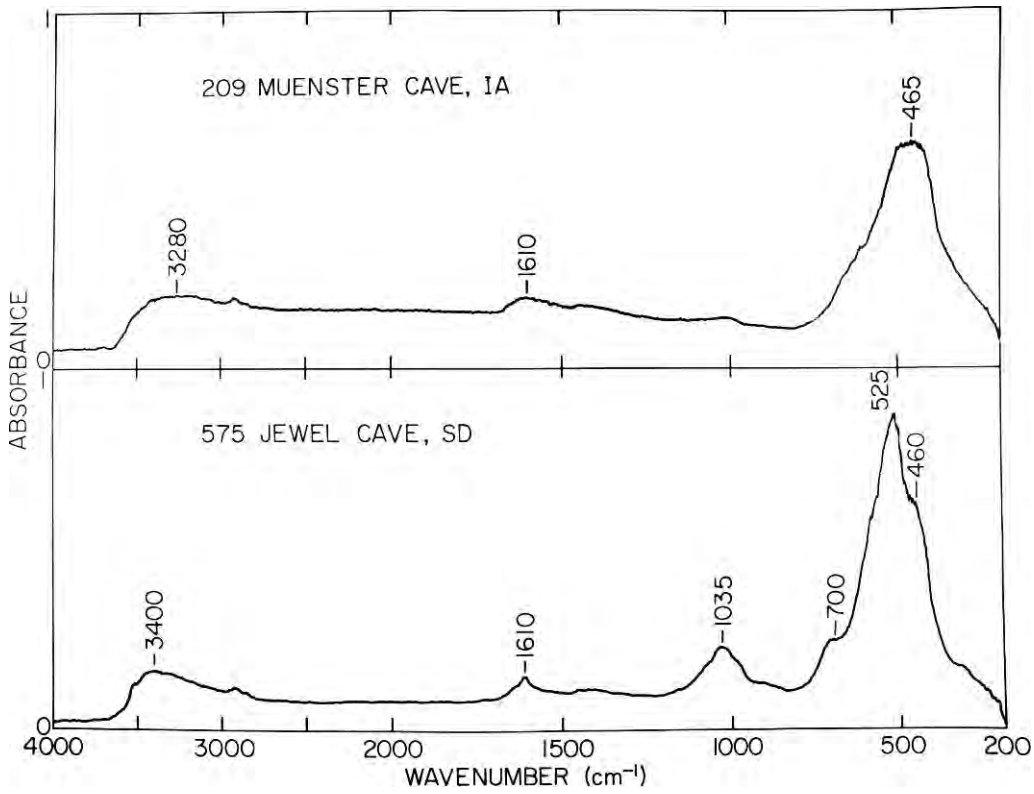

Figure 4. Infrared spectra of two phase-pure manganese oxides.

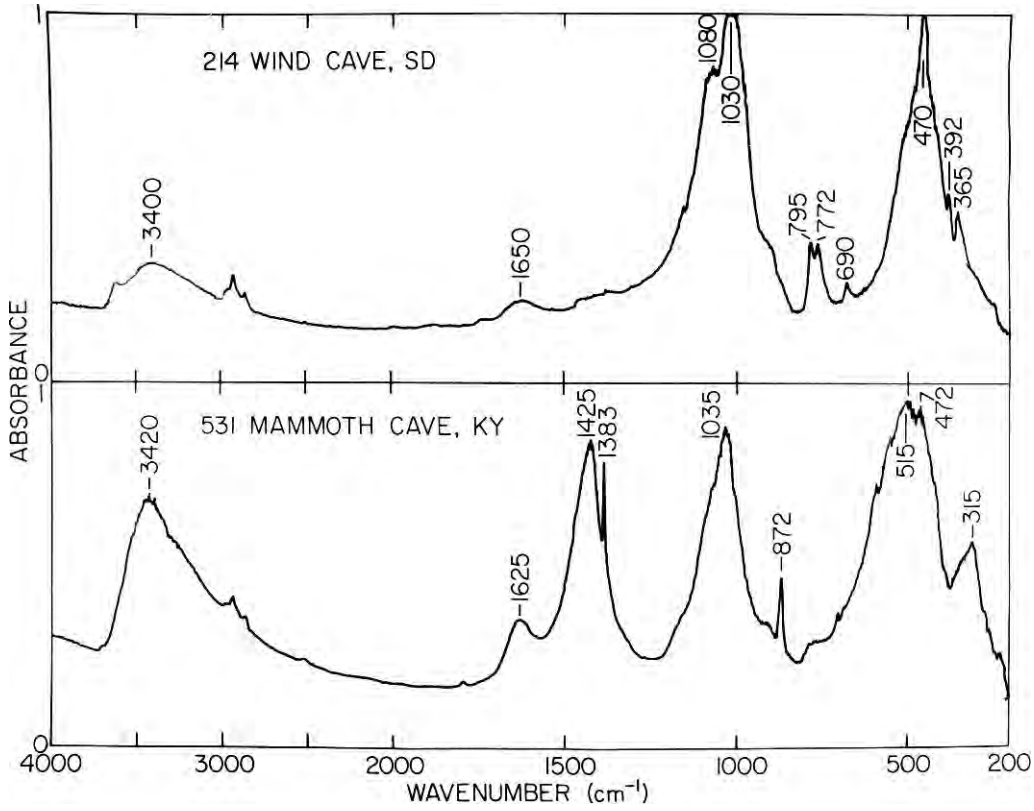

Figure 5. Infrared spectra of two contaminated manganese oxides.

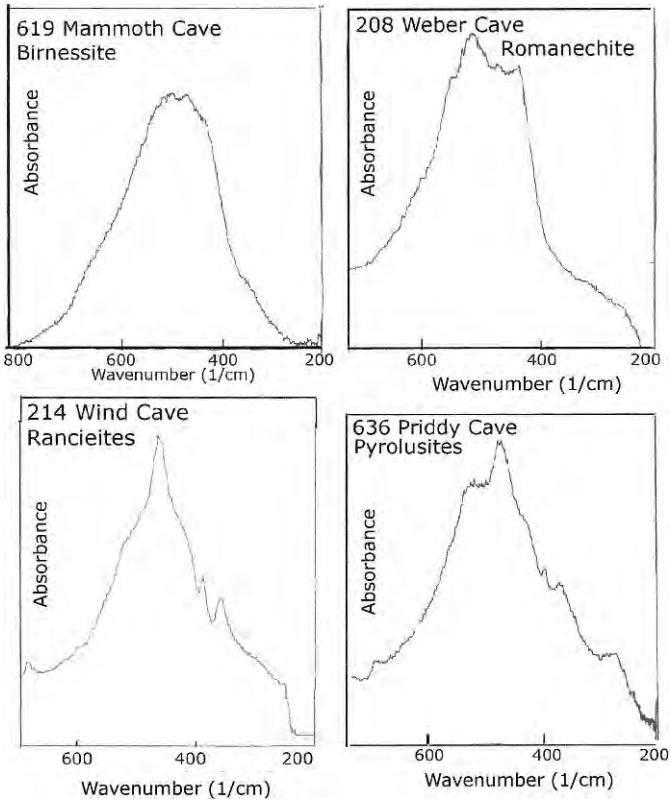

Figure 6. Infrared spectra of the Mn-O stretching region of four manganese oxides.

the nano-scale so that their X-ray diffraction patterns are essentially featureless. Tentative interpretation of the IR spectra of 14 of the 18 samples gives mineral identifications of eight birnessites, one romanechite, two rancieites, and three pyrolusites.

Heavy Metal Chemistry in Cave Manganese Oxide Minerals

Iron/Manganese Relations

There is a rough correlation between iron and manganese in the deposits (Fig. 7). All of the Mn-rich deposits and coatings contain at least some Fe. There appears to be a gap between Fe-rich Mn deposits and three samples that might be called Mn-containing iron deposits.

Alkaline Earth Relations

Normalized concentrations of BaO, SrO, CaO, and MgO are displayed in Figure 8. The high Ca concentration is expected, since Ca is a component of many of the manganese oxide minerals and the deposits examined all formed from carbonate waters. Many of the samples are Ba-rich, with BaO concentrations between 1 and 10 wt%. What is surprising is that Sr seems to be strongly suppressed. Concentrations of SrO range from less than 0.01 wt% to, at most, a few tenths of a percent, almost two

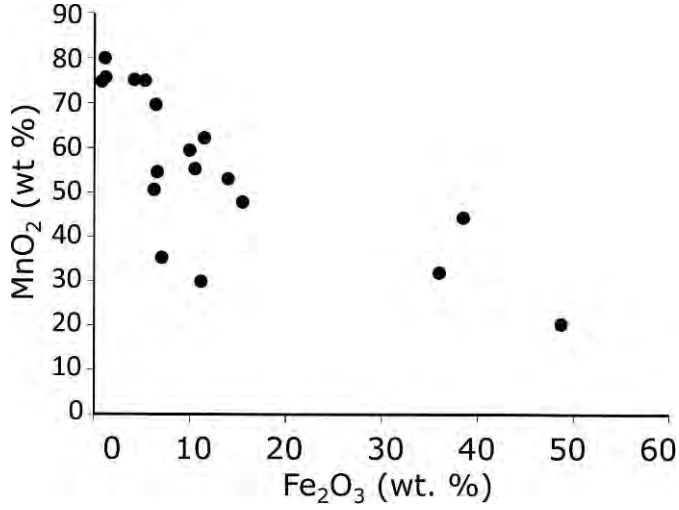

Figure 7. Plot of iron versus manganese content. Iron is calculated as Fe_2O_3 and manganese as MnO_2. Both are expressed as a percentage of the final sum of analyzed constituents.

orders of magnitude less than BaO. Carbonate mineral deposits in caves (speleothems), usually composed of calcite or aragonite, contain more Sr than Ba.

Transition Metal Relations

Cave Mn deposits, like ocean floor nodules and other stream Mn deposits, contain substantial quantities of transition metals (Fig. 9). Of the seven trace metals plotted in Figure 9, CoO, NiO, V_2O_5, and ZnO are present in some samples at concentrations greater than one wt%. The samples represent a range of localities, mostly in the eastern United States. The cave streams from which the samples were taken are mostly in the headwaters of their associated drainage basins. Background concentrations of transition metals in the streams are not known for any of the localities and, indeed, the streams are no longer present in many of the cave passages.

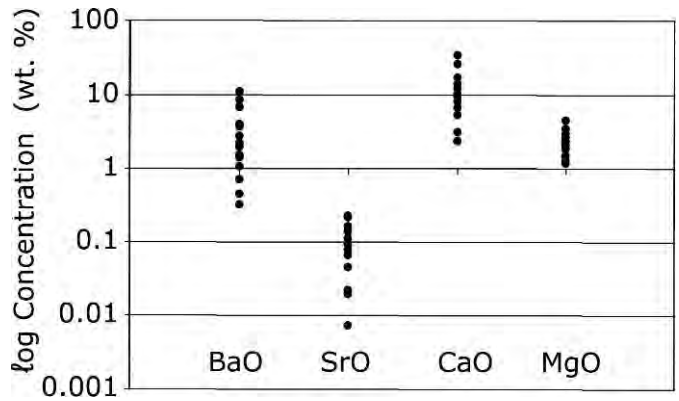

Figure 8. Distribution of alkaline earth elements calculated as the oxides.

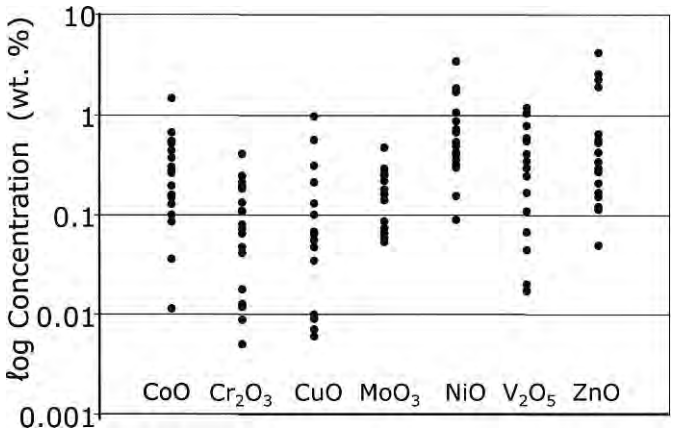

Figure 9. Distribution of the transition elements Co, Cr, Cu, Mo, Ni, V, and Zn.

Analyses of transition metals in freshwater surface streams are rare, and the few observed concentrations are highly variable. Such sparse data as are available suggest that transition metal concentrations would be expected to be in the range of a few parts per billion. At the high end are elements such as V and Zn in the range of tens of parts per billion. At the low end, is Co at fractions of a parts per billion. Yet Co appears in the Mn-deposits at concentrations from 0.01 to 1 wt% (10^5 to 10^7 ppb). The Mn-oxide minerals in general, and birnessite (δ-MnO_2) in particular, are extremely effective adsorbers of transition metals. The enhancement factors between the background concentration in the cave streams or groundwater and the concentration in the deposits are on the order of 10^6. There is the possibility that the concentrations of transition metals in manganese oxides reflect the concentrations in the surface environment. If this should prove to be the case, the manganese oxides would act as a dosimeter for other metals in the environment.

Conclusions

Black coatings on stream cobbles and on chert ledges commonly found in limestone caves were shown to consist of very poorly crystalline manganese oxides. Mineral identification by infrared spectroscopy suggests birnessite to be the most common phase. Complete chemical analyses were obtained for 18 specimens. Among the alkaline earth elements, the concentration of Ba is enhanced, while the concentration of Sr is suppressed. The transition metals Co, Cr, Cu, Mo, Ni, V, and Zn were found in most of the manganese deposits at concentrations in the fractional percent to percent range. Manganese oxides are deposited in caves from freshwater streams that often sink into the cave system from headwaters on nearby non-carbonate rocks. Comparison of the concentrations of transition metals found in the deposits with expected concentrations in the source streams suggests an enhancement factor on the order of 10^6.

Acknowledgements

We are grateful to Ms. Catherine A. Chess and Ms. Nichole Wonderling, who measured the infrared spectra. Chemical analyses were performed at Penn State's Materials Characterization Laboratory by Mr. Scott D. Atkinson. The early stages of this investigation were supported by the Cave Research Foundation. Field assistance was provided by James R. Fisher and Elizabeth L. White. The samples from Weber and Muenster Caves, Iowa were contributed by Stewart Peck. The Devil's Icebox Cave sample was collected by George H. Deike.

References

Burns, V.M., and Burns, R.G., 1978, Post-depositional metal enrichment processes inside manganese nodules from the North Equatorial Pacific: Earth and Planetary Science Letters, v. 39, p. 341–348.

Carpenter, R.H., and Hayes, W.B., 1980, Annual accumulation of Fe-Mn oxides and certain associated metals in a stream environment: Chemical Geology, v. 29, p. 249–259.

Hill, C.A., 1982, Origin of black deposits in caves: National Speleological Society Bulletin, v. 44, p. 15–19.

Hill, C.A., and Forti, P., 1997, Cave Minerals of the World (second edition): Huntsville, National Speleological Society, 463 p.

Jones, B., 1992, Manganese precipitates in the karst terrain of Grand Cayman, British West Indies: Canadian Journal of the Earth Sciences, v. 29, p. 1125–1139.

Jürgensen, A., Widmeyer, J.R., Gordon, R.A., Bendell-Young, L.I., Moore, M.M., and Crozier, E.D., 2004, The structure of the manganese oxide on the sheath of the bacterium *Leptothrix discophora*: An XAFS study: American Mineralogist, v. 89, p. 1110–1118.

Kashima, N., 1983, On the wad-minerals from the cavern environment: International Journal of Speleology, v. 13, p. 67–72.

Moore, G.W., 1981, Manganese deposition in caves, *in* Proceedings of the 8th International, Congress of Speleology, Bowling Green, KY, p. 642–644.

Northup, D.E., and Lavoie, K.H., 2001, Geomicrobiology of caves: A review: Geomicrobiology Journal, v. 18, p. 199–222.

Northup, D.E., Barns, S.M., Yu, L.E., Spilde, M.N., Schelble, R.T., Dano, K.E., Crossey, L.J., Connolly, C.A., Boston, P.J., Natvig, D.O., and Dahm, C.N., 2003, Diverse microbial communities inhabiting ferromanganese deposits in Lechuguilla and Spider Caves: Environmental Microbiology, v. 5, p. 1071–1086.

Onac, B.P., Pedersen, R.B., and Tysseland, M., 1997, Presence of rare-earth elements in black ferromanganese coatings from Vântului Cave (Romania): Journal of Cave and Karst Studies, v. 59, p. 128–131.

Onac, B.P., Hess, J.W., and White, W.B., 2007, The relationship between the mineral composition of speleothems and mineralization of breccia pipes: Evidence from Corkscrew Cave, Arizona, USA: The Canadian Mineralogist, v. 45, p. 1177–1188.

Peck, S.B., 1986, Bacterial deposition of iron and manganese oxides in North American caves: National Speleological Society Bulletin, v. 48, p. 26–30.

Post, J.E., 1999, Manganese oxide minerals: Crystal structures and economic and environmental significance: Proceedings of the National Academy of Sciences, v. 96, p. 3447–3454.

Potter, R.M., and Rossman, G.R., 1979, The tetravalent manganese oxides: identification, hydration, and structural relationships by infrared spectroscopy: American Mineralogist, v. 64, p. 1199–1218.

Spilde, M.N., Northup, D.E., Boston, P.J., Schelble, R.T., Dano, K.E., Crossey, L.J., and Dahm, C.N., 2005, Geomicrobiology of cave ferromanganese deposits: A field and laboratory investigation: Geomicrobiology Journal, v. 22, p. 99–116.

Tebo, B.M., Ghiorse, W.C., van Waasbergen, L.G., Siering, P.L., and Caspi, R., 1997, Bacterially mediated mineral formation: Insights into manganese(II) oxidation from molecular genetic and biochemical studies: Reviews in Mineralogy, v. 35, p. 225–266.

White, W.B., Scheetz, B.E., Atkinson, S.D., Ibberson, D., and Chess, C.A., 1985, Mineralogy of Rohrer's Cave, Lancaster County, Pennsylvania: National Speleological Society Bulletin, v. 47, p. 17–27.

J.E. Birdwell and A.S. Engel – Variability in terrestrial and microbial contributions to dissolved organic matter fluorescence in the Edwards Aquifer, Central Texas. *Journal of Cave and Karst Studies,* v. 71, no. 2, p. 144–156.

VARIABILITY IN TERRESTRIAL AND MICROBIAL CONTRIBUTIONS TO DISSOLVED ORGANIC MATTER FLUORESCENCE IN THE EDWARDS AQUIFER, CENTRAL TEXAS

JUSTIN E. BIRDWELL[1*] AND ANNETTE SUMMERS ENGEL[2]

Abstract: Most cave and karst ecosystems are believed to be dependent on an influx of allochthonous organic carbon. Although microbes are largely responsible for the fate of dissolved organic matter (DOM) in karst, the role of microbes in chemosynthetic (autochthonous) production and processing of DOM has received limited attention. Chromophoric dissolved organic matter (CDOM) is the fraction of DOM that absorbs ultraviolet and visible light, and differences in the fluorescence spectral characteristics of humic-like (terrigenous) and protein-like (microbially-derived) CDOM allow for tracing the relative contributions of allochthonous or autochthonous carbon sources, respectively, in water. We investigated CDOM in karst-aquifer well and spring waters along the fresh- to saline-water transition zone of the Edwards Aquifer, Central Texas, over a four year period. The groundwater fluorescence spectral characteristics were distinct from those generally observed in surface waters and soil porewaters. The dominant source of organic carbon in the aquifer waters may be a product of chemolithoautotrophic primary production occurring in situ. It is possible that the absence of a strong terrestrial CDOM signature may be due to filtering effects in the epikarst or rapid utilization by heterotrophs in the aquifer. Our results indicate that intense recharge following periods of drought may influence the intensity of microbial activity, either due to an influx of DOM or nutrients from the surface that was not quantified by our analyses or because of increased in situ autotrophic activity, or both. The variable contributions of allochthonous and autochthonous DOM during and after recharge events call into question whether karst aquifer ecosystems are necessarily dependent on allochthonous organic matter.

INTRODUCTION

For most karst aquifers, meteoric water enters the subsurface from the surface (e.g., at sinkholes, fractures), moves for some distance underground in conduit- or in diffuse-flow systems, and often resurges at the surface as diffuse or spring discharge (White, 1988). The surface-derived water can carry with it a signature of its origin, including particulate and dissolved organic matter (DOM) from plant and soil material, but also anthropogenic contaminants. As a direct result of this hydrological connectivity between the surface and subsurface, karst aquifers are one of the most susceptible habitat types to disturbance due to their responsiveness to changes in the surface-water balance and possible contaminant release (e.g., Chen et al., 2001; Butscher and Huggenberger, 2009). In recent years, climatic conditions and widespread urbanization have led to increased stress on karst aquifer systems, which can be important drinking water sources due to their potential for significant permeability and porosity.

One way to monitor water quality and ecosystem integrity for management and conservation purposes is by evaluating the nature and behavior of DOM (Spizzico et al., 2005; Green et al., 2006). DOM is important in the global carbon cycle and ecosystem nutrient balance, as well as in the transport of trace metals and organic contaminants in natural and engineered systems (e.g., McKnight et al., 1992; Johnson and Amy, 1995). DOM is found throughout the biosphere as a complex mixture of freely dissolved and aggregated organic molecules at various stages of chemical, physical, or biological compositional change from parent compounds; the sum of these processes is known as diagenesis (e.g., Peuravuori and Pihlaja, 2004). Unfortunately, there have been limited investigations on the nature of DOM in karst (e.g., Baker and Genty, 1999; Farnleitner et al., 2005; Green et al., 2006; Einsiedl et al., 2007).

Chromophoric (also known as colored) dissolved organic matter (CDOM) is the fraction of DOM that

* Corresponding Author

[1] Cain Department of Chemical Engineering, Louisiana State University, Baton Rouge, LA 70803, jbirdw1@tigers.lsu.edu

[2] Department of Geology and Geophysics, Louisiana State University, Baton Rouge, LA 70803, aengel@lsu.edu

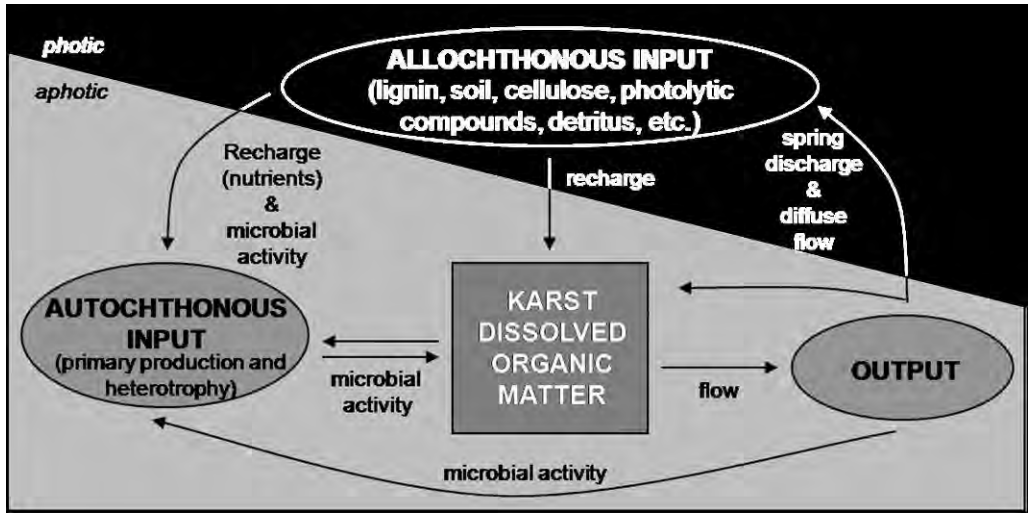

Figure 1. Schematic representation of dissolved organic matter (DOM) in karst aquifers based on the surface and subsurface being hydrologically connected. For this study, the square box represents the karst aquifer, which is sampled via wells, and the composition and nature of DOM at a specific point in time within the karst aquifer. Organic matter in the aquifer can be sourced from allochthonous and/or autochthonous inputs. Allochthonous input can enter the aquifer directly; this material is often processed by microbes and may take on a signature of autochthonous input. Some DOM may remain in the aquifer system because of in situ physical, chemical, or microbiological breakdown (i.e., diagenesis). Freshwater springs are one type of output from the aquifer system, whereby the DOM from the aquifer will mix with, and potentially become part of, an allochthonous input source at another location.

absorbs ultraviolet (UV) and visible light and represents a wide range of structures within the compositional range of DOM. Essentially, CDOM is what causes the pale yellow to brown color of filtered natural water (i.e., water not containing suspended particles like clays). The absorbance and fluorescence properties of CDOM, measured at natural abundance concentrations via spectroscopic methods, can provide information on the nature of the DOM present in a water sample, as well as DOM parent materials. By measuring the fluorescent properties of CDOM, it is possible to distinguish between DOM derived from terrestrial sources, which are dominated by the degradation products of photosynthetic primary production, and other microbial sources, which are characterized by fluorescent amino acids (McKnight et al., 2001). Various modes of degradation can affect CDOM characteristics, including photodegradation due to exposure to UV radiation from the sun and biodegradation through microbial heterotrophic metabolism. Fluorescence can also be used to identify the presence of various types of contaminants, such as polycyclic aromatic hydrocarbons (combustion byproducts) and fluorescent brightening agents (often present in wastewater and sewage).

In uncontaminated natural waters, two types of CDOM fluorophores are typically observed and are manifested as humic-like and protein-like peaks or features in collected fluorescence spectra (Baker and Lamont-Black, 2003; Chen et al., 2003; Hudson et al., 2007). Humic substances, primarily fulvic acids, are the dominant component of DOM in most surface waters. These materials represent a large fraction of the total dissolved organic carbon (DOC) because their refractory nature and high solubility allow them to accumulate in solution (Frimmel, 1998). In general, humic-like fluorescence is a term used to describe spectral features that resemble those of isolated humic and fulvic acids, while the term protein-like fluorescence applies to spectral peaks attributed to the fluorescent amino acids tryptophan and tyrosine. Although both fluorophore types absorb and are excited by UV light (240–360 nm), humics emit primarily in the violet to near-green wavelengths (400–500 nm), which is attributed to complex photophysical interactions between quinone-like structures from degraded terrestrial material, such as lignin (Ariese et al., 2004; Del Vecchio and Blough, 2004; Cory and McKnight, 2005; Boyle et al., 2009; Cook et al., 2009), In contrast, microbially-derived CDOM emits in the UVB to UVA wavelength range (300–380 nm). In karst, CDOM spectral features are expected to be derived from several sources, including material brought into the system by surface recharge, wind, speleothem drip-waters, or as guano, produced from microbial processing of allochthonous material within the aquifer, and in situ microbial activity (e.g., Griebler and Lueders, 2008) (Fig. 1).

Healthy aquatic environments contain high concentrations of microbial biomass (e.g., Whitman et al., 1998, Griebler and Lueders, 2008). In the absence of allochthonous input, autochthonous CDOM produced by microbial activity is the dominant form of DOM in groundwater,

which is supported from examinations of CDOM that possess a relatively greater portion of biologically labile materials relative to surface waters, including polysaccharides, alkyl alcohols, aldehydes, ketones, and amides that are produced in situ (Leenheer, 1981). However, except for some studies of CDOM in groundwater (Baker and Lamont-Black, 2003), cave drip waters (e.g., Baker and Genty, 1999), and the open ocean (Murphy et al., 2008) that identified significant protein-like fluorescence associated with microbial activity, there have been few investigations of systems where terrigenous DOM sources or photosynthetically-driven microbial activity are lacking (e.g., McKnight et al., 2001). It is clear that fluorescence signatures indicative of microbial activity are often not observed in water samples because biomolecules are more susceptible to enzymatic attack relative to more refractory fulvic acids (e.g., Moran and Hodson, 1990; Claus et al., 1999; Ogawa et al., 2001; Hertkorn et al., 2002; Yamashita and Tanoue, 2003; Anesio et al., 2004; Judd et al., 2006).

Therefore, our current understanding of the nature and behavior of CDOM primarily derived from microbes and microbial activity is limited. These issues make investigating the relative contribution of different sources of organic matter in caves and karst aquifers unique. In cave and karst settings, it is clear that water from the surface contributes to the majority of recharge. Organic matter from terrestrial sources is expected to enter into these waters via leaching from vadose soils and epikarst. In addition, subsurface environments are devoid of sunlight, and therefore two important processes in the terrestrial carbon cycle (photosynthesis and photodegration) do not directly affect DOM in these systems. Because of the combination of distinct CDOM signature anticipated for surface-derived recharge and the lack of photophysical processes in caves and karst, any CDOM produced in situ, for example by chemolithoautotrophic microbial activity, should possess fluorescent characteristics that are readily distinguishable.

In this study, our goal was to characterize CDOM from fresh and saline water sampled from the karstic Edwards Aquifer in Central Texas, one of the most spatially extensive, permeable, and productive aquifers in the United States (e.g., Hovorka et al., 1995; Sharp and Banner, 1997). Based on what is known of aquifer geochemistry, hydrology, and microbiology, we hypothesized that allochthonous CDOM input would be distinguishable from an autochthonous CDOM generated by in situ microbial activity, and that microbial signatures would be more prevalent than terrestrial signatures in the deep, more saline portions of the aquifer. Additionally, the samples were available over a four-year window that included periods of severe drought and intense recharge in the Edwards Aquifer region. This allowed for an assessment of the potential use of fluorescence to examine changes in CDOM sources during and following climatic events that might perturb the subsurface hydrology and ecosystem.

MATERIALS AND METHODS

THE EDWARDS AQUIFER

The Edwards Aquifer is located in south-central Texas and extends across a narrow, 8- to 60-km-wide tract approximately parallel to the Balcones Fault Zone that arcs from north of the city of Austin to south of the city of Brackettville. The aquifer is within extensively karstified Cretaceous carbonate rock units, with a predominant groundwater flow path from southwest to northeast (e.g., Hovorka et al., 1995; Groscehen and Buszka, 1997; Kuniansky et al., 2001; Lindgren et al., 2004). The aquifer is subdivided into different segments based on discharge sites and regional structural controls, as well as by water type. In general, recharge to the aquifer takes place where limestone outcrops in the recharge zone along the Balcones Fault Zone and on the Edwards Plateau in the contributing zone (Fig. 2) (Lindgren et al, 2004). Edwards Plateau soils are mollisols that support grasses, savanna vegetation, and some trees; these terrigenous sources would be expected to contribute soil humics and photosynthetically-derived organic material, like lignin and cellulose, to the aquifer. In comparison, regional soils are generally described as thin and stony and have been characterized as dominantly calcareous, clayey, and loamy (e.g., Musgrove and Banner, 2004).

Downdip of the recharge and contributing zones, the aquifer is artesian and is predominately freshwater, with total dissolved solids (TDS) of 1000 mg L^{-1} or less (Groscehen and Buszka, 1997). Permeability within the freshwater zone is multimodal and varies over eight orders of magnitude, with a significant percentage of the porosity represented by a complex network of fractures (fracture flow), macroscopic caves, and underground solution-enlarged features (conduit flow) (Hovorka et al., 1995). Natural freshwater discharges from the artesian zone along faults, including at San Pedro Springs, Comal Springs, and San Marcos Springs, from southwest to northeast, respectively (Fig. 2).

TDS values in excess of 1000 mg L^{-1} constitute saline water, and the transition between the freshwater and saline-water zone, locally known as the bad-water line (Schultz, 1993), trends parallel to the Balcones Fault Zone, and is encountered at depth and downdip of the freshwater (Fig. 2). The saline-water zone has high concentrations of hydrogen sulfide (H_2S) as a result of leakage of brine and H_2S gas from oil-fields along the eastern edge of the aquifer (e.g., Sharp and Banner, 1997). Although there is still much to be learned about the saline-water zone, flow is hypothesized to be in tight fractures or through intercrystalline or intergranular porosity (matrix flow) (e.g., Hovorka et al., 1995). The freshwater–saline-water interface is generally stable through time, although historical data from times of regional drought indicate that saline water may have discharged from freshwater springs and

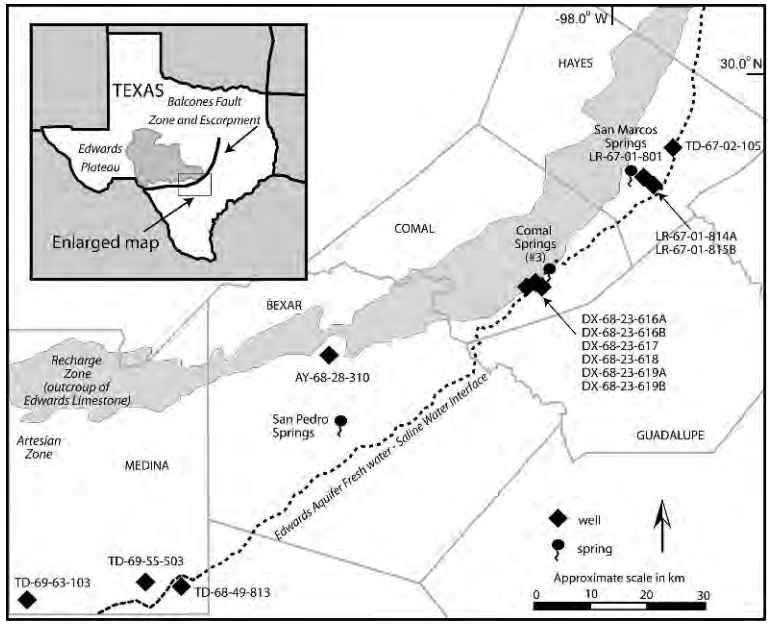

Figure 2. Detailed Edwards Aquifer sampling locations in Central Texas. The freshwater and saline water transition zone line is based on Groscehen and Buszka (1997) and recent estimates from Edwards Aquifer Authority online reports (http://www.edwardsaquifer.org/).

that there is possible updip movement of the transition zone (e.g., Harden, 1968; Perez, 1986).

The classic model for karst development in carbonates involves carbonic acid dissolution, where carbon dioxide (CO_2) is sourced from infiltrating meteoric water and dissolution is focused at a local to regional base level. This would imply that most karst development takes place at or above the water table. However, for the Edwards Aquifer, karstification due to carbonic acid is juxtaposed with the possibility of dissolution within the saline-water zone that some have suggested is due to abiotic or microbial sulfide oxidation to sulfuric acid (e.g., Grubbs, 1991; Schindel et al., 2000; Randall, 2006; Engel and Randall, 2008). It is unclear how much of Edwards Aquifer development may be a result of this type of process or to what extent microbes influence the nature of porosity and permeability between the fresh and saline-water zones.

Sample Acquisition and Geochemical Characterization

We focused our investigation during a time period extending from May 2005 to April 2009, and only in Hayes, Comal, Bexar, and Medina counties. We collected water from wells drilled into the Edwards Aquifer carbonates within the saline-water zone and at freshwater springs (Table 1; Fig. 2). When collected from wells, water was purged a minimum of one well volume prior to sample acquisition (purge volumes depended on well volumes). Grab samples were collected at springs. Physiochemical properties were measured immediately in the field using standard electrode methods (e.g., APHA, 1998), including temperature and pH on an Accumet AP62 meter with a double junction electrode (Accumet, Fisher Scientific, USA), and TDS and temperature on a YSI-85 meter (YSI Inc., Yellow Springs, OH, USA). Dissolved hydrogen sulfide was measured in the field using the methylene blue colorimetric method on a portable V-2000 multi-analyte photometer (CHEMetrics, Inc., Calverton, VA, USA) (APHA, 1998). Alkalinity, as total titratable bases, here dominated by bicarbonate, although acetate can also be high in some saline waters (Groscehen and Buszka, 1997), was determined in the field from a filtered sample by titration to pH 4.3 (APHA, 1998). Each water sample was filtered simultaneously into HDPE bottles through a 0.45-μm Whatman glass fiber filter (GF/F, precombusted at 500 °C) and a 0.2-μm polyvinylidene-fluoride membrane (PVDF) filter (Millipore, Bedford, Mass.). Filtered water was stored on ice for transport and maintained at 4 °C until analysis, at which point samples were brought to room temperature (~22 °C).

Fluorescence Spectroscopy

Fluorescence measurements on samples from May 2005, January 2007, and June 2007 were made using a SPEX Fluorolog-3 spectrofluorometer (Jobin Yvon, Edison, NJ, USA). Spectra for samples from March 2008 and April 2009 were made using a SPEX Fluoromax-4 spectrofluorometer. Identical settings were used with both instruments. Slits for both excitation and emission monochromators were set to 5 nm, and a 0.1 second integration time was used. Analyses were done in a 1-cm quartz cuvette at room temperature (22 °C). Instrument stability was

Table 1. General descriptions of Edwards Aquifer water samples, including well depth, either as the depth interval of the open-hole (^{O}) or the screened interval depths (^{S}), and total dissolved solids (TDS), dissolved sulfide concentrations, and total alkalinity.

Sampling Site Name	Well Number	Collection Period	Well Depth (m)	Temp (°C)	pH	TDS (mg L^{-1})	Sulfide (mg L^{-1})	Alkalinity (mg L^{-1})
Paradise Alley well	DX-68-23-616A	May 2005	209–224^{S}	23.6	7.20	1140	3.5	233
Paradise Alley well	DX-68-23-616A	Jan. 2007		23.0	7.80	1559	0	199
Paradise Alley well	DX-68-23-616A	June 2007		25.0	7.23	1149	3.3	253
Paradise Alley well	DX-68-23-616A	March 2008		25.4	7.25	1159	4.6	266
Paradise Alley well	DX-68-23-616A	April 2009		24.3	7.25	1443	4.2	327
Comal Spring #3		Jan. 2007		23.3	7.18	372	0	250
Comal Spring #3		March 2008		23.1	7.07	302	0	248
LCRA field deep well	DX-68-23-617	June 2007	214–226^{S}	25.0	7.31	369	0	271
LCRA field deep well	DX-68-23-617	March 2008		25.2	7.03	373	0	262
LCRA field shallow well	DX-68-23-618	June 2007	166–180^{S}	24.5	7.46	438	0.3	239
LCRA field shallow well	DX-68-23-618	March 2008		23.9	7.50	459	0.3	235
Girl Scout shallow well	DX-68-23-619A	June 2007	185–198^{S}	24.9	7.32	375	trace	289
Girl Scout deep well	DX-68-23-619B	June 2007	228–240^{S}	24.4	7.42	353	trace	229
Sonterra well #8	AY-68-28-310	May 2005	103–373^{O}	26.0	7.40	990	trace	219
Aquarena Golf Course well	LR-67-01-814A	Jan. 2007	154–169^{S}	22.0	6.87	12,440	38.5	290
Aquarena Hotel spring	LR-67-01-801	June 2007		21.6	7.12	401	0	331
South Medina well	TD-69-63-103	June 2007	801–1038^{O}	38.9	7.31	366	trace	223
Farm well	TD-69-55-503	June 2007	137–610^{O}	27.7	7.26	332	0	240
SE Medina well	TD-68-49-813	June 2007	783–973^{O}	41.4	7.16	817	5.9	346

Table 2. Fluorescence characteristics of Edwards Aquifer water samples, including maximum emission intensity (I_{max}), maximum emission wavelength ($\lambda_{Em,\ max}$), maximum excitation wavelength ($\lambda_{Ex,\ max}$), FI, and HIX (letters in parenthesis by Sampling Site Names correspond to spectra labels in Fig. 4).

Sampling Site Name	I_{max} (RU)	$\lambda_{em,\ max}$ (nm)	$\lambda_{ex,\ max}$ (nm)	FI	HIX
Paradise Alley well (a)	3.4	395	240	2.16	4.30
Paradise Alley well (c)	3.3	395	240	2.14	3.48
Paradise Alley well (e)	37.0	340	270	1.93	0.39
Paradise Alley well (i)	2.0	382.5	240	2.01	5.00
Paradise Alley well (l)	1.7	385	240	1.90	2.98
Comal Spring #3	1.0	412.5	240	1.79	4.33
Comal Spring #3 (j)	0.8	415	240	1.74	2.93
LCRA field deep well	12.5	305	240	1.58	1.15
LCRA field deep well (l)	1.6	435	240	1.51	9.03
LCRA field shallow well (g)	16.0	342.5	240	1.84	0.62
LCRA field shallow well (k)	1.6	375	240	1.75	3.40
Girl Scout shallow well	10.5	307.5	240	1.54	1.12
Girl Scout deep well (f)	3.7	340	275	1.90	0.55
Sonterra well #8 (b)	2.2	395	250	2.65	2.52
Aquarena Golf Course well (d)	2.7	397.5	240	2.38	2.72
Aquarena Hotel spring (h)	10.5	342.5	240	1.90	0.61
South Medina well	16.5	337.5	275	1.72	0.17
Farm well	3.9	310	240	1.92	0.24
SE Medina well	4.6	305	240	2.41	0.51

determined using the Raman peak of deionized water excited at 348 nm with emission monitored at 395 nm (position of Raman peak indicated by the white circle in Fig. 3, panel a). Raman intensities were consistent during each session, with values varying less than 2% between runs on both instruments. Samples were analyzed in signal/reference mode with the fluorescence emission intensity normalized to the intensity of the xenon lamp at the particular excitation wavelength applied. Absorbance spectra for May 2005, January 2007, and June 2007 samples were collected using a double-beam UV-3101PC spectrophotometer (Shimadzu Corporation, Kyoto, Japan), while spectra for those samples from March 2008 and April 2009 were collected using a double-beam Lambda-850 spectrophotometer (Perkin Elmer, Waltham, Mass.). For both instruments, absorbance spectra were obtained using a 1-cm quartz cuvette over the range of 200–700 nm with deionized water as the reference.

Excitation-emission matrix (EEM) fluorescence spectra were obtained by collecting a series of forty-three emission scans (λ_{Em} = 250–550 nm, 2.5-nm steps) at 5-nm excitation wavelength (λ_{Ex}) intervals between 240 and 450 nm. An EEM spectrum provides a fluorescence spectral signature of a sample containing CDOM within the UV and visible range of the electromagnetic spectrum. Examples of EEM spectra are shown in Figure 3 (panels a, b, and e–h) and Figure 4. Spectral corrections for primary and secondary inner filter effects were made using absorbance spectra (Lakowicz, 1999). Raman scattering was mitigated by subtracting a blank spectrum collected on pyrogen-free deionized water from each corrected EEM. Rayleigh scattering effects were edited from each spectrum following correction and blank subtraction. Differences between uncorrected and corrected EEMs can be seen by comparing panels a and b of Figure 3 and the effects on individual emission scans are illustrated in panels c and d. EEM contour plots were assembled by combining the individual emission spectra using SigmaPlot 10 (Systat Software, Inc., San Jose, CA, USA). Each contour line represents between 5% and 10% of the maximum emission intensity, depending on the number of contour lines shown.

CDOM spectra are often described in terms of characteristic peaks that have been identified in studies of surface waters from a wide range of environments. The system described by Coble (1996) is one of the most commonly used for discussing CDOM fluorescent features. The peaks include UVC-excited humics (peak A, $\lambda_{Ex} \leq$ 260 nm. λ_{Em} = 400–460 nm), UVA-excited humics (peak C, λ_{Ex} =320–360 nm, λ_{Em} = 420–460 nm), marine humics (peak M, λ_{Ex} = 290–310 nm, λ_{Em} = 370–410 nm), tyrosine-like (peak B, λ_{Ex} = 275 nm, λ_{Em} = 305 nm) and tryptophan-like (peak T, λ_{Ex} = 275 nm, λ_{Em} = 340 nm). The locations of these peaks are illustrated in Figure 3, panel b.

Two diagnostic metrics based on specific emission scans were used to assess ecologically relevant properties of the CDOM in the aquifer samples. The Zsolnay Humification Index (HIX) (Zsolnay et al., 1999) is used to estimate the degree of CDOM humification, which can be considered an indicator of DOM bioavailability within a natural system because highly humified organic substances are expected to

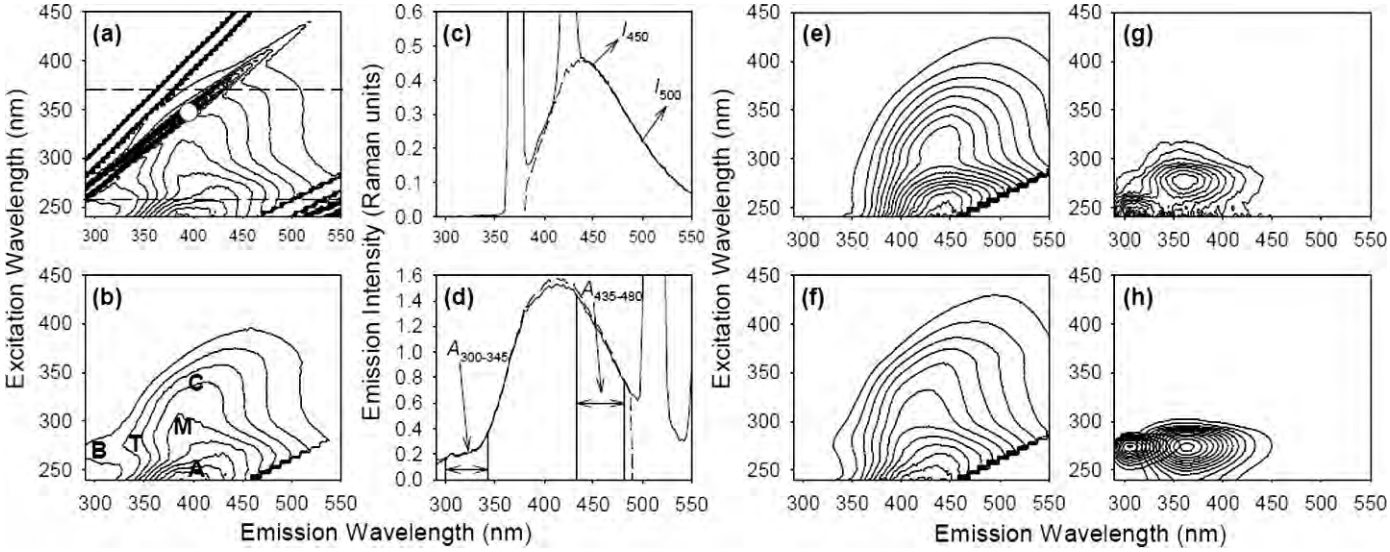

Figure 3. Overview of fluorescence excitation-emission matrices (EEMs) and scans along with corrected spectra of surface water fulvic acids and biological fluorophore standards. (a) Uncorrected EEM spectrum for Paradise Alley well water (March 2008) showing scattering bands relating to (from upper left to lower right) 1st order Rayleigh, 1st order Raman, 2nd order Rayleigh and 2nd order Raman; dashed lines indicate positions of emission scans for the Humification Index (HIX) (bottom) and Fluorescence Index (FI) (top); white circle indicates position of the reference Raman peak ($\lambda_{Ex} = 348$ nm, $\lambda_{Em} = 395$ nm). (b) Corrected EEM spectrum for Paradise Alley well water (March 2008) following inner filter effect corrections, removal of Raman scattering by DI water blank subtraction and editing to remove Rayleigh scattering bands. Positions of Coble (1996) peak designations indicated by letters A, C, M, T and B (see Results section for details). (c) Uncorrected (solid line) and corrected (dashed line) emission scan for FI calculation (intensities at 450 and 500 nm indicated by arrows). (d) Uncorrected (solid line) and corrected (dashed line) emission scan for HIX calculation (integration areas indicated). (e) Suwannee River fulvic acid EEM spectrum (terrestrial humic-like standard). (f) Pony Lake fulvic acid EEM spectrum (microbial humic-like standard). (g) EEM spectrum of tryptone (protein-like standard). (h) EEM spectra of the fluorescent amino acids tyrosine (left peak) and tryptophan (right peak).

be less labile, and therefore, persist in the environment longer than substances with a low degree of humification (Zsolnay et al., 1999; Ohno, 2002). Soil and terrestrially-derived CDOM is expected to have higher HIX values than CDOM from microbial sources. The HIX was calculated by dividing the sum of the emission intensities between 435 and 480 nm by the sum of the intensities between 300 and 345 nm with excitation at 254 nm. The McKnight Fluorescence Index (FI) (McKnight et al., 2001) was used to assess the relative contributions of allochthonous (terrestrially-derived material) and autochthonous (microbial material produced in situ) CDOM. FI values are determined from an emission scan with excitation at 370 nm by calculating the ratio of the emission intensity at 450 nm to that at 500 nm (McKnight et al., 2001). In a study of fulvic acids derived from terrestrial and microbial sources, McKnight et al. (2001) determined that FI values of 1.4 or less indicated CDOM of terrestrial origin, while values of 1.9 or higher corresponded to microbially-derived CDOM. Moreover, when applied to filtered whole water samples, similar diagnostic values resulted (McKnight et al., 2001). Examples of the emission scans used to calculate these indices are shown in panels c (FI) and d (HIX) of Figure 3.

STANDARDS AND MODEL COMPOUNDS FOR FLUORESCENCE SPECTROSCOPY

A set of reference fluorescence spectra was obtained to represent CDOM from different environments and compounds whose fluorescence characteristics are similar to CDOM spectral features observed in other studies. Samples from the International Humic Substances Society (IHSS) served as proxies for dissolved humic substances derived from terrestrial plants (Suwannee River fulvic acid, Georgia, USA, IHSS catalog #2S101F) and photosynthetic microorganisms (Pony Lake fulvic acid, Antarctica, IHSS catalog # 1R109F). Other standards included L(-) tryptophan (Acros Organics, Thermo Fisher Scientific, Inc., NJ, USA) and L(-) tyrosine (Acros Organics). Tryptone (Fisher Bioreagents, Fisher Scientific, Inc., NJ, USA), a casein digest commonly used as an additive in microbial culture media, was included to obtain a protein-like signature. All comparison samples were prepared to concentrations of ~10 mg carbon L^{-1} using pyrogen-free deionized water. Corrected EEM spectra for these materials are shown in Figure 3 (panels e–h) and illustrate the different regions of the excitation-emission fluorescence landscape occupied by humic-like

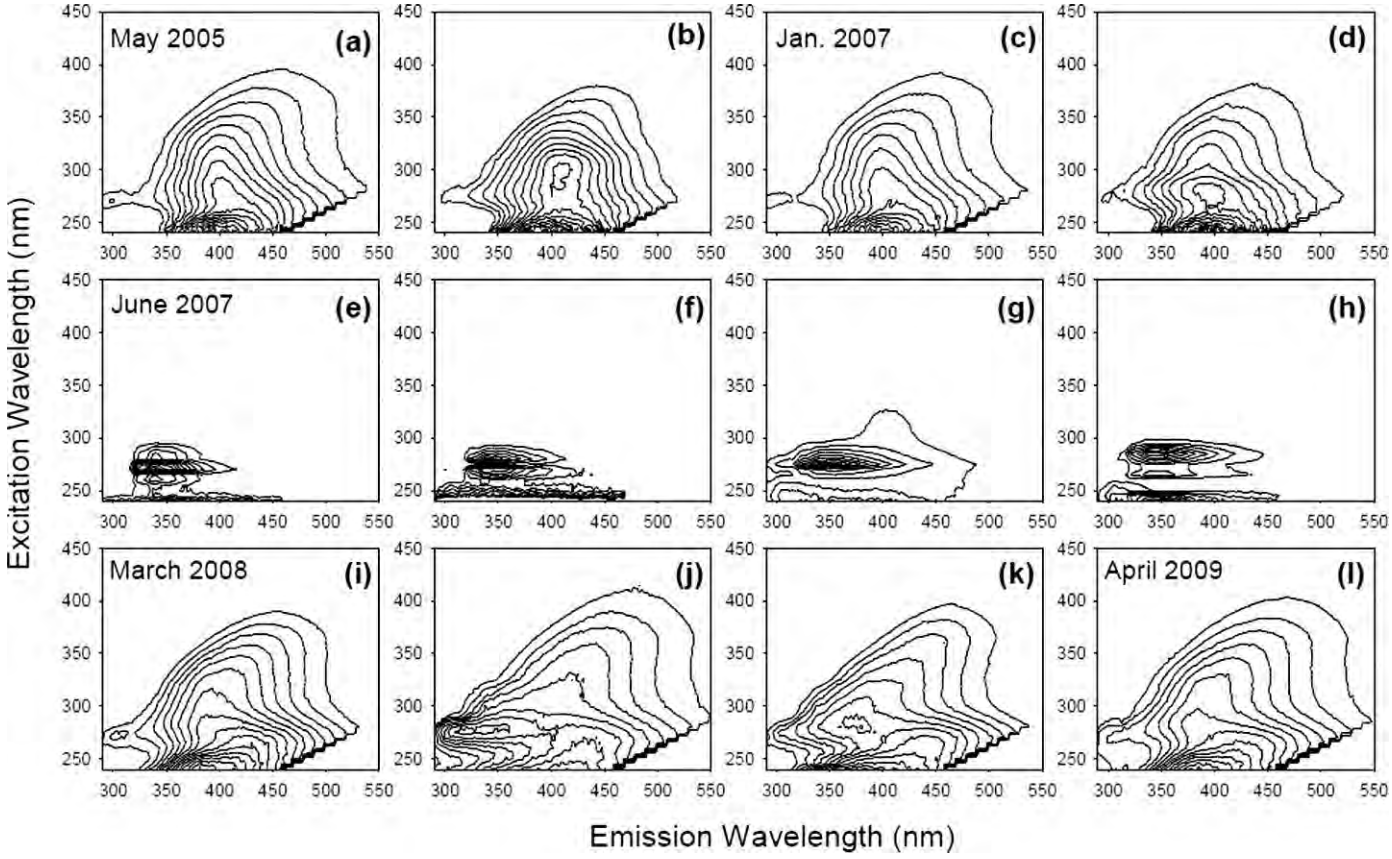

Figure 4. EEM spectra of various waters from sampling sites in the Edwards Aquifer, Central Texas; see Table 2 for sample information and correspondence to panel letter.

(Fig. 3, panels e and f) and protein-like (Fig. 3, panels g and h) fluorophores.

Hydrological and Drought Data for the Edwards Aquifer

Climatic and hydrologic extremes of Central Texas lead to significant fluctuation in annual recharge to the aquifer, primarily in response to variation in regional precipitation. To compare the fluorescence characteristics of aquifer-water samples to hydrological conditions relevant to recharge, data were obtained from online databases maintained by local and federal agencies charged with monitoring important aspects of the hydrology of Edwards Aquifer. We used the Palmer Drought Severity Index (PDSI) (Palmer, 1965) for Texas Divisions 6 and 7 to assess the relative availability of recharge water for the Edwards Aquifer system. The National Oceanic and Atmospheric Administration, through the Climate Prediction Center, publishes PDSI data for specific regions throughout the United States[1]. Division 6 encompasses the Edwards Plateau (i.e., recharge and contributing zones) and Division 7 contains the locations of the wells and discharge springs. The PDSI is based on a water balance approach, taking into account precipitation and soil moisture supply. PDSI values below zero correspond to drier than normal conditions and values below −4 indicate extreme drought.

For a direct indicator of water storage in the aquifer, we used information on well levels and spring flow rates, as well as the estimated annual net extraction or influx of aquifer water, during the study period. Water levels for three regional wells and the flow rates for two springs were acquired from Edwards Aquifer Authority (EAA) reports and online data[2] (Schindel, 2008). We focused on well-level data from the Hondo Index Well, Medina County, and flow-rate data for Comal Springs, Comal County, which were representative of the others. Annual total recharge to, and discharge from, the Edwards Aquifer for most of the study period was found in a recent report from the EAA (Schindel, 2008). Net annual water influx or extraction from the aquifer was calculated for 2005, 2006, and 2007 using these values.

Statistical Analyses

Student's t-test (2-tail, type 2) analyses were performed to assess whether FI, HIX, and emission maximum wavelength ($\lambda_{Em,\ Max}$) values determined for samples

[1] http://www.cpc.noaa.gov/products/monitoring; ftp://ftp.ncdc.noaa.gov/pub/data/cirs/

[2] http://www.edwardsaquifer.org/pages/waterlevels_sa.asp

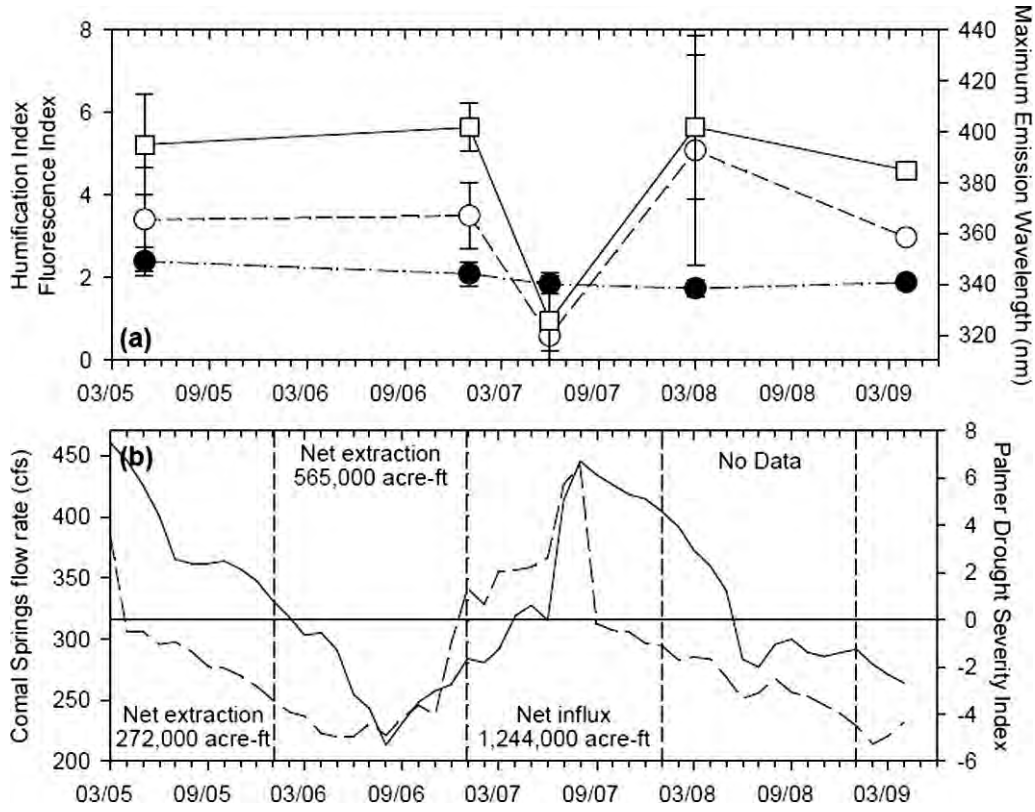

Figure 5. (a) Average values of Fluorescence Index (●, dash-dot line), Humification Index (○, dashed line) and Emission Maximum wavelength (□, solid line) values for each sampling period (error bars represent standard deviation). (b) Discharge flow rate (cubic feet per second, cfs) for Comal Springs, Comal County, Texas (solid line), and Palmer Drought Severity Index (PDSI) for Division 7 (as defined by the National Climate Data Center), Texas (dashed line), from 2005 through April 2009.

collected during the four sampling events were significantly correlated. Calculations were made using Microsoft Excel (Redmond, WA). *P*-values below 0.05 were considered indicative of significant differences between the measured and calculated fluorescence parameters determined during each sampling period. Statistical comparison was not possible for the April 2009 sampling event, as water could only be obtained from a single well.

RESULTS

CHARACTERIZATION OF CHROMOPHORIC DISSOLVED ORGANIC MATTER

Maximum fluorescence emission intensities (I_{Max}) of CDOM in Edwards Aquifer samples were between 1 and 40 Raman Units (RU) (Table 2). The EEM spectra contained many of the characteristic peaks observed in other studies of marine and terrestrial CDOM (Fig. 3, panel b). The dominant features in the CDOM spectra for water samples collected during May 2005, January 2007, March 2008, and April 2009 were peaks A and M, with some samples containing contributions from peaks C, T, and B. The June 2007 samples were dominated by peak T, which had fluorescent intensities that were an order of magnitude higher than any other feature present. It should be noted that the fluorescence response of CDOM is sensitive to pH and temperature; however, this was not an issue for the aquifer waters, which all had circumneutral pH and moderate temperatures that were not significantly different among the sampling times (Table 1).

FLUORESCENCE INDICES

Average values and standard deviations for HIX, FI, and $\lambda_{Em,\ Max}$ determined for each sampling event are shown in Figure 5a. The two fluorescence indices, HIX and FI, provide a clear contrast among the reference materials and the well and spring waters (Table 2). The IHSS reference fulvic acids had HIX values greater than 25. The HIX value for tryptone was 0.05. All but one of the Edwards Aquifer water samples from May 2005, January 2007, March 2008, and April 2009 had HIX values of 5 or lower and none of the June 2007 samples had values greater than 1.2. FI values are rarely lower than ~1.0, and the highest reported values are less than ~3.0 (McKnight et al., 2001). As an example of typical surface water humic substances, Suwannee River fulvic acid exhibited a FI value of 1.25, while for tryptone, the value was 2.45. Pony Lake fulvic acid, representing the most humified portion of

the DOM from a lake dominated by photosynthetic microbial activity, had a FI of 1.52. FI values for samples collected in May 2005 and January 2007 were the highest observed and were generally greater than 2, while those from June 2007, March 2008, and April 2009 were between 1.5 and 2. *P*-values determined for comparisons of HIX and $\lambda_{Em,\ Max}$ values for the May 2005, January 2007, and March 2008 sampling events were all $\geq$0.37, while comparisons of those samples to the HIX and $\lambda_{Em,\ Max}$ from the June 2007 samples yielded *P*-values $<$0.001. These results indicate that the fluorescent properties of the June 2007 samples were significantly different than the other sampling periods. For the FI data, the *P*-values were 0.37 between May 2005 and January 2007 and 0.50 between June 2007 and March 2008; all other comparisons had *P*-values between 0.01 and 0.12. These results indicate that there were not significant differences in FI among the different sampling times. While statistical testing was not possible for the April 2009 sample from the Paradise Alley well, it was very similar to the sample collected from that site in March 2008, but with a 40% lower HIX value.

Drought and Recharge Data

The PDSI values for Division 7 from May 2005 through April 2009 indicate that the region experienced variable drought conditions until August 2006 (Fig. 5b). Similar conditions also existed for Division 6 (data not shown). Lower discharge rates at Comal Springs and lower well levels at the Hondo Creek Index well (data not shown), corresponded with PDSI values that were indicative of drought conditions. From August 2006 until September 2007 the region experienced wetter conditions, leading to greater spring discharge and higher (positive) PDSI values. The summer of 2007 had the most intense wetting in both Divisions 6 and 7, and many places in the two regions experienced major flood events. Since September 2007, the Divisions have had lower PDSI values, indicating worsening drought conditions (Fig. 5b).

The net volume of water entering or being extracted from the Edwards Aquifer system was calculated from recharge and discharge estimates, as a way to assess whether net removal of water from the aquifer could exacerbate drought effects on the subsurface ecosystem. During 2005 and 2006, estimated net volumes of 33,551 and 69,692 hectare meter (272,000 and 565,000 acre-feet) of water were removed from the aquifer, respectively. In 2007, the aquifer system had a net estimated recharge of 153,446 hectare meter (1,244,000 acre-feet) of water. These estimates are consistent with trends in the PDSI, well level, and spring discharge data for the same periods.

Discussion

In this study, we set out to characterize the nature of CDOM in freshwater and saline water from the karstic Edwards Aquifer in Central Texas, both from the standpoint of understanding the relative contributions of terrigenous and autochthonous (e.g., microbial) CDOM to the aquifer, but also from the viewpoint of determining if there would be different CDOM sources because of variability in surface hydrology that could contribute to, or perturb, the aquifer ecosystem. We used fluorescence spectral characteristics of CDOM to characterize the relative contributions of organic matter into the Edwards Aquifer from May 2005 through April 2009. Regardless of being freshwater or saline water, the FI and HIX values determined for the water samples indicate that the CDOM present in the aquifer waters has a significant microbial component and does not possess a signature indicative of DOM dominated by soil or other surface sources. The high FI values indicate that most of the CDOM is likely of microbial origin, though some sites had values that suggest a mixture of terrestrial and microbial sources. The low HIX values from the water samples are consistent with fluorescent, water soluble, extracellular substances excreted by microorganisms or organic matter extracted from plant biomass and animal manure (Zsolnay et al., 1999; Ohno and Bro, 2006; Hunt and Ohno, 2007; Ohno et al., 2007). The lack of humification implies that much of the CDOM is labile and likely to be an active constituent in the local carbon cycle. This supports the suggestion by Simon et al. (2007) that there must be significant DOM processing in subsurface environments, as well as the results from Einsiedl et al. (2007) indicating that DOM transformation in karst is rapid and occurs on the order of decades, unlike many soil organic matter pools that persist for centuries (e.g., Trumbore, 1997).

Collectively, the results are not surprising, as CDOM in cave drip waters (e.g., Baker and Genty, 1999) has been linked to microbial activity and Goldscheider et al. (2006) recently concluded that DOM in karst lacked a significant plant- or soil-derived humic signature. However, in addition to the general indices, the overall patterns of CDOM fluorescence spectral features from our work suggest that recharge into different portions of the aquifer may have had a significant impact on the subsurface ecosystem. These results are unique. Samples from May 2005, January 2007, March 2008, and April 2009 were all from times of low recharge and regional drought (Fig. 5a–b) and shared similar humic-like spectral characteristics that had shorter maximum emission wavelengths, compared to spectra for reference humic substances like Suwannee River and Pony Lake fulvic acids (Fig. 3e–f). Hence, although the fulvic acid data do not necessarily differentiate between allochthonous or autochthonous DOM, we attribute the fulvic acid-like fluorescence to a humic substance that is primarily derived from heterotrophic processing of other types of DOM. The shorter wavelengths could also be due in part to the lack of exposure to solar radiation.

In contrast, nearly all of the June 2007 fresh and salinewater samples, which corresponded to a period of

high precipitation and recharge to the aquifer (Fig. 5b), had intense tryptophan peaks and fluorescence intensities in the other peak areas that were comparable to those observed from the other sampling times. The signature indicates that there was an increase in microbial activity because of autochthonous DOM produced by chemolithoautotrophs, along with in situ heterotrophy, or because of a combination of in situ processes and surface infiltration. Based on the fluorescence spectra, any possible contribution of surface DOM appears to be small relative to the in situ production, as the average FI values from the June 2007 data set indicate persistent microbial CDOM influences (Fig. 5a). It is possible that an influx of water from the surface could have stimulated microbial activity because of nutrient input, leading to an increase in the observed intensity of a microbial CDOM signature. But, it seems unlikely that surface recharge would transport DOM with other dissolved nutrients to the sampled aquifer depths, so another possible explanation for the variability is that terrestrial organic carbon did infiltrate into the subsurface but that most of the DOM was sequestered in the epikarst and shallower portions of the aquifer. The results are not conclusive enough to support either explanation for the June 2007 data set, as it is possible that a combination of processes occurred concomitantly. The samples collected in March 2008 and April 2009 contained prominent tryptophan-like peaks with similar intensities to those from May 2005 and January 2007, as well as more pronounced features in the peak C area. The intensity of the biological peak could represent baseline microbial activity, although at a much lower level than observed in the June 2007 samples. The presence of the more pronounced peak C feature suggests that some terrestrial CDOM did enter the aquifer waters during the period of greater recharge (December 2006 through September 2007), which is consistent with the slightly lower FI values observed in the June 2007 and March 2008 datasets.

The average FI values were nearly constant throughout the entire sampling period because the relative distribution of allochthonous and autochthonous CDOM in the wells does not vary significantly. The implication is that, even when there is an influx of surface water, terrestrial CDOM is not likely to become the dominant DOM fraction in the aquifer waters (as sampled from the wells). The differences in spectral features and indices between the low and high recharge periods are directly related to the appearance of an intense tryptophan peak in most of the samples from June 2007. This spectral change could not be the result of wastewater contamination or some other surface source of amino acid fluorescence. We propose that the shift in CDOM fluorescence properties is due to changes in climatic conditions and related changes in the hydrological properties and ecological conditions in the aquifer at the wells and springs, which may lead to an increase in microbial activity in the aquifer. If this conjecture is correct, then these results support that cave and karst ecosystems, even at significant depth in karst aquifers, are influenced by disturbances such as recharge events.

CONCLUSIONS

Karst aquifers are an exceptional type of groundwater system where the subsurface can be in direct hydrological communication with the surface. However, based on this and other recent studies, it is becoming increasingly apparent that the link between the surface and subsurface may also be blurred in karst. The most significant finding from our study is that CDOM in the Edwards Aquifer groundwater carries a signature suggestive of being sourced primarily from microbial activity. We understand that aquifer recharge rarely occurs over the entire spatial scale of the recharge area, and therefore epikarstic flow in one area may rapidly flush through the system, whereas another part of the aquifer may receive less or no infiltration. This makes it difficult to estimate recharge, and so it is possible that we did not sample locations that might be influenced more directly by terrigenous organic matter contributions. There are also many questions related to how much material, including organic carbon, infiltrates into the Edwards Aquifer through the epikarst, or how organic matter is temporarily stored, and even retarded, in the unsaturated zone. The physical nature of the epikarst should cause highly variable flow path interconnectiveness, as well as geochemically diverse aqueous- and gas-phase input (Musgrove and Banner, 2004; Taucer et al., 2005). Consequently, ecosystems that develop in karst aquifers must sustain themselves through times of limited epikarstic input (i.e., recharge), as well as survive times of intense and extreme input.

Another important result from our study is that the persistent signatures of microbial CDOM in the aquifer call into question the dependence of karst aquifer ecosystems on terrigenous carbon because there may be processes interfering with communication with the surface, even following extreme recharge events. In the absence of significant contributions of allochthonous DOM and because photosynthesis is not possible in the aquifer, the source of CDOM that we identified is associated with microbial processing of (chemolitho)autotrophically-produced organic matter (Randall, 2006). Cave and karst waters can have high microbial cell abundances, and there has been significant effort to understand the types of microbial processes, including autotrophy, in cave and karst systems (e.g., Sarbu et al., 1996; Sarbu et al., 2000; Simon et al., 2003; Farnleitner et al., 2005; Goldscheider et al., 2006; Opsahl and Chanton, 2006; Simon et al., 2007; Porter et al., 2009), although not in the Edwards Aquifer (Engel and Randall, 2008). The issue of microbial contributions to the ecosystem carbon cycle may indicate a significant departure from our current understanding of karst aquifer ecosystem dynamics (e.g., Pronk et al., 2006),

whereby differences in the nature and composition of DOM between surface and karst groundwater have been attributed to retention (selective or not) of terrigenous DOM by soil as water percolates into the subsurface, biotic molecular transformation of terrestrial inputs, or in situ microbial production (e.g., Einsiedl et al., 2007). In conclusion, scientists who manage karst aquifers for water quality and resource allocation should consider future work developing methods to discriminate between differences in DOM due to epikarstic filtering and in situ primary productivity linked to microbial diversity.

ACKNOWLEDGEMENTS

We thank G. Schindel and other scientists at the Edwards Aquifer Authority for access to wells and field assistance and J. Waugh and D. Mahula from the San Antonio Water System, who also assisted in field work. The authors thank R. Cook, M. Lowry, I. Warner, and E. D'Sa for equipment access. C. Schulz and S.A. Engel assisted in field data collection and analyses, and K. Brannen, B. Donnelley, and S. White helped with laboratory analyses. The manuscript benefited from insightful comments provided by K. Lavoie, C. Wicks, and two anonymous reviewers. The research was funded by Louisiana Board of Regents Support Fund (contracts LEQSF (2006-09)-RD-A-03).

REFERENCES

Anesio, A.M., Hollas, C., Granéli, W., and Laybourn-Perry, J., 2004, Influence of humic substances on bacterial and viral dynamics in freshwaters: Applied and Environmental Microbiology, v. 70, p. 4848–4854.

APHA, 1998, (American Public Health Association) Standard methods for the examination of water and wastewater, 20th ed., U.S. EPA, APHA, American Water Works Association, and the Water Environment Federation, 1220 p.

Ariese, F., van Assema, S., Gooijer, C., Bruccoleri, A.G., and Langford, C.H., 2004, Comparison of Laurentian fulvic acid luminescence with that of the hydroquinone/quinone model system: Evidence from low temperature fluorescence studies and EPR spectroscopy: Aquatic Sciences, v. 66, p. 86–94.

Baker, A., and Genty, D., 1999, Fluorescence wavelength and intensity variations of cave waters: Journal of Hydrology, v. 217, p. 19–34.

Baker, A., and Lamont-Black, J., 2003, Fluorescence of dissolved organic matter as a natural tracer of ground water: Ground Water, v. 39, p. 745–750.

Boyle, E.S., Guerriero, N., Thiallet, A., Del Vecchio, R., and Blough, N.V., 2009, Optical properties of humic substances and CDOM: Relation to structure: Environmental Science and Technology, v. 43, p. 2262–2268.

Butscher, C., and Huggenberger, P., 2009, Modeling the temporal variability of karst groundwater vulnerability, with implications for climate change: Environmental Science and Technology, v. 43, p. 1665–1669.

Chen, C.-C., Gillig, D., and McCarl, B.A., 2001, Effects of climatic change on a water dependent regional economy: A study of the Texas Edwards Aquifer: Climatic Change, v. 49, p. 397–409.

Chen, W., Westerhoff, P., Leenheer, J.A., and Booksh, K., 2003, Fluorescence excitation-emission matrix regional integration to quantify spectra for dissolved organic matter: Environmental Science and Technology, v. 37, p. 5701–5710.

Claus, H., Gleixner, G., and Filip, Z., 1999, Formation of humic-like substances in mixed and pure cultures of aquatic microorganisms: Acta Hydrochimica et Hydrobiologica, v. 27, p. 200–207.

Coble, P., 1996, Characterization of marine and terrestrial DOM in seawater using excitation-emission matrix spectroscopy: Marine Chemistry, v. 51, p. 325–346.

Cook, R.L., Birdwell, J.E., Lattao, C.V., and Lowry, M., 2009, A multi-method comparison of Atchafalaya Basin surface water organic matter samples: Journal of Environmental Quality, v. 38, p. 702–711.

Cory, R.M., and McKnight, D.M., 2005, Fluorescence spectroscopy reveals ubiquitous presence of oxidized and reduced quinones in dissolved organic matter: Environmental Science and Technology, v. 39, p. 8142–8149.

Del Vecchio, R., and Blough, N.V., 2004, On the origin of the optical properties of humic substances: Environmental Science and Technology, v. 38, p. 3885–3891.

Einsiedl, F., Hertkorn, N., Wolf, M., Frommberger, M., Schmitt-Kopplin, P., and Koch, B.P., 2007, Rapid biotic molecular transformation of fulvic acids in a karst aquifer: Geochimica et Cosmochimica Acta, v. 71, p. 5474–5482.

Engel, A.S., and K.W. Randall, 2008, Microbially enhanced carbonate dissolution in karst aquifers, *in* Sasowsky, I.D., Feazel, C.T., Mylroie, J.E., Palmer, A.N., and Palmer, M.V., eds., Karst from recent to reservoirs: Karst Waters Institute Special Publication 14, p. 52–56.

Farnleitner, A.H., Wilhartitz, I., Ryzinska, G., Kirschner, A.K.T., Stadler, H., Burtscher, M.M., Hornek, R., Szewzyk, U., Herndl, G., and Mach, R.L., 2005, Bacterial dynamics in spring water of alpine karst aquifers indicates the presence of stable autochthonous microbial endokarst communities: Environmental Microbiology, v. 71, p. 3003–3015.

Frimmel, F.H., 1998, Characterization of natural organic matter as major constituents in aquatic systems: Journal of Contaminant Hydrology, v. 35, p. 201–216.

Goldscheider, N., Hunkeler, D., and Rossi, P., 2006, Review: Microbial biocenoses in pristine aquifers and an assessment of investigative methods: Hydrogeology Journal, v. 14, p. 926–941.

Green, R.T., Painter, S.L., Sun, A., and Worthington, S.R.H., 2006, Groundwater contamination in karst terranes: Water Air and Soil Pollution, v. 6, p. 157–170.

Griebler, C., and Lueders, T., 2008, Microbial biodiversity in groundwater ecosystems: Freshwater Biology, v. (Articles online in advance of print), p. 1–29. doi: 10.1111/j.1365-2427.2008.02013.x.

Groscehen, G.E., and Buszka, P.M., 1997, Hydrogeologic framework and geochemistry of the Edwards Aquifer saline-water zone, south-central, Texas, U.S. Geological Survey Water-Resources Investigation 97-4133, 47 p.

Grubbs, A.G., 1991, Sulfur bacteria and the deep phreatic environment of the Edwards Aquifer [abs.]: Bulletin of the National Speleological Society, v. 53, 41 p.

Harden, R.W., 1968, Review of water quality changes in the Edwards Reservoir, especially near the bad water line — file memo, William F. Guyton and Associates, 23 p.

Hertkorn, N., Claus, H., Schmitt-Kopplin, P.H., Perdue, E.M., and Filip, Z., 2002, Utilization and transformation of aquatic humic substances by autochthonous microorganisms: Environmental Science and Technology, v. 36, p. 4334–4345.

Hovorka, S.D., Mace, R.F., and Collins, E.W., 1995, Regional distribution of permeability in the Edwards aquifer, San Antonio, Texas, Edwards Aquifer Underground Water Conservation District Report No. 93-17-FO, 128 p.

Hudson, N., Baker, A., and Reynolds, D., 2007, Fluorescence analysis of dissolved organic matter in natural, waste and polluted waters — A review: River Research and Applications, v. 23, p. 631–649.

Hunt, J.F., and Ohno, T., 2007, Characterization of fresh and decomposed dissolved organic matter using excitation-emission matrix fluorescence spectroscopy and multiway analysis: Journal of Agricultural and Food Chemistry, v. 55, p. 2121–2128.

Johnson, W.P., and Amy, G.L., 1995, Facilitated transport and enhanced desorption of polycyclic aromatic hydrocarbons by natural organic matter in aquifer sediments: Environmental Science and Technology, v. 29, p. 807–817.

Judd, K.E., Crump, B.C., and Kling, G.W., 2006, Variation in dissolved organic matter controls bacterial production and community composition: Ecology, v. 87, p. 2068–2079.

Kuniansky, E.L., Fahlquist, L., and Ardis, A.F., 2001, Travel times along selected flow paths of the Edwards Aquifer, Central Texas, *in* Proceedings, U.S. Geological Survey Karst Interest Group, USGS Water-Resources Investigations Report 01-4011, p. 69–77.

Lakowicz, J.R., 1999, Principles of fluorescence spectroscopy, 2nd ed., New York, Plenum Publishing, 725 p.

Leenheer, J.A., 1981, Comprehensive approach to preparative isolation and fractionation of DOC from natural waters and wastewaters: Environmental Science and Technology, v. 15, p. 587–592.

Lindgren, R.J., Dutton, A.R., Hovorka, S.D., Worthington, S.R.H., and Painter, S., 2004, Conceptualization and simulation of the Edwards Aquifer, San Antonio Region, Texas, U.S. Geological Survey, Scientific Investigations Report 2004-5277, 154 p.

McKnight, D.M., Bencala, K.E., Zellweger, G.W., Aiken, G.R., Feder, G.L., and Thorn, K.A., 1992, Sorption of dissolved organic carbon by hydrous aluminum and iron oxides occurring at the confluence of Deer Creek with the Snake River, Summit County, Colorado: Environmental Science and Technology, v. 26, p. 1388–1396.

McKnight, D.M., Boyer, E.W., Westerhoff, P.K., Doran, P.T., Kulbe, T., and Andersen, D.T., 2001, Spectrofluorometric characterization of dissolved organic matter for indication of precursor organic material and aromaticity: Limnology and Oceanography, v. 46, p. 38–48.

Moran, M.A., and Hodson, R.E., 1990, Bacterial production on humic and nonhumic components of dissolved organic carbon: Limnology and Oceanography, v. 35, p. 1744–1756.

Murphy, K.R., Stedmon, C.A., Waite, T.D., and Ruiz, G.M., 2008, Distinguishing between terrestrial and autochthonous organic matter sources in marine environments using fluorescence spectroscopy: Marine Chemistry, v. 108, p. 40–58.

Musgrove, M., and Banner, J.L., 2004, Controls on the spatial and temporal variability of vadose dripwater geochemistry: Edwards Aquifer, central Texas: Geochimica et Cosmochimica Acta, v. 68, p. 1007–1020.

Ogawa, H., Amagai, Y., Koike, I., Kaiser, K., and Benner, R., 2001, Production of refractory dissolved organic matter by bacteria: Science, v. 292, p. 917–920.

Ohno, T., 2002, Fluorescence inner-filtering correction for determining the humification index of dissolved organic matter: Environmental Science and Technology, v. 36, p. 742–746.

Ohno, T., and Bro, R., 2006, Dissolved organic matter characterization using multiway spectral decomposition of fluorescence landscapes: Soil Science Society of America Journal, v. 70, p. 2028–2037.

Ohno, T., Chorover, J., Omoike, A., and Hunt, J., 2007, Molecular weight and humification index as predictors of adsorption for plant- and manure-derived dissolved organic matter to goethite: European Journal of Soil Science, v. 58, p. 125–132.

Opsahl, S.P., and Chanton, J.P., 2006, Isotopic evidence for methane-based chemosynthesis in the Upper Floridan Aquifer food web: Oecologia, v. 150, p. 89–96.

Palmer, W.C., 1965, Meteorological drought, research paper no. 45, United States Weather Bureau, Washington, DC, 58 p.

Perez, R., 1986, Potential updip movement of saline water in the Edwards Aquifer, San Antonio, Texas, U.S. Geological Survey Water-Resources Investigation Report 86-4032, 21 p.

Peuravuori, J., and Pihlaja, K., 2004, Preliminary study of lake dissolved organic matter in light of nanoscale supramolecular assembly: Environmental Science and Technology, v. 38, p. 5958–5967.

Porter, M.L., Engel, A.S., Kane, T.C., and Kinkle, B.K., 2009, Productivity-diversity relationships from chemolithoautotrophically based sulfidic karst systems: International Journal of Speleology, v. 38, p. 27–40.

Pronk, M., Goldscheider, N., and Zopfi, J., 2006, Dynamics and interaction of organic carbon, turbidity and bacteria in a karst aquifer system: Hydrogeology Journal, v. 14, p. 473–484.

Randall, K.W., 2006, Assessing the potential impact of microbes in the Edwards and Trinity Aquifers of Central Texas [M.S. thesis], Louisiana State University, 115 p.

Sarbu, S.M., Kane, T.C., and Kinkle, B.K., 1996, A chemoautotrophically based cave ecosystem: Science, v. 272, p. 1953–1955.

Sarbu, S.M., Galdenzi, S., Menichetti, M., and Gentile, G., 2000, Geology and biology of Grotte di Frasassi (Frasassi Caves) in Central Italy, an ecological multi-disciplinary study of a hypogenic underground karst system, *in* Wilkens, H., Culver, D., and Humphreys, S., eds., Ecosystems of the World: Subterranean Ecosystems, Volume 30, Oxford, Elsevier Science, p. 361–381.

Schindel, G.M., 2008. Edwards Aquifer Authority hydrological data report for 2007, Report no. 08-02, 235 p.

Schindel, G.M., Worthington, S.R.H., and Veni, G., 2000, An overview of the San Antonio segment of the Edwards (Balcones Fault Zone) Aquifer in south-central Texas [abs.]: Journal of Cave and Karst Studies, v. 62, p. 197.

Schultz, A.L., 1993, Defining the Edwards Aquifer freshwater/saline-water interface with geophysical logs and measured data-San Antonio to Kyle, Texas, San Antonio, Texas, Edwards Underground Water District Report 93-06, 81 p.

Sharp, J.M., and Banner, J.L., 1997, The Edwards Aquifer: A resource in conflict: GSA Today, v. 7, p. 1–9.

Simon, K.S., Benfield, E.F., and Macko, S.A., 2003, Food web structure and the role of epilithic biofilms in cave streams: Ecology, v. 84, p. 2395–2406.

Simon, K.S., Pipan, T., and Culver, D.C., 2007, A conceptual model of the flow and distribution of organic carbon in caves: Journal of Cave and Karst Studies, v. 69, p. 279–284.

Spizzico, M., Lopez, N., and Sciannamblo, D., 2005, Analysis of the potential contamination risk of groundwater resources circulating in areas with anthropogenic activities: Natural Hazards and Earth System Sciences, v. 5, p. 109–116.

Taucer, P.I., Munster, C.L., Wilcox, B.P., Shade, B., Dasgupta, S., Owens, M.K., and Mohanty, B., 2005, Large plot tracing of subsurface flow in the Edwards Aquifer epikarst, *in* Beck, B.F., ed., Sinkholes and the Engineering and Environmental Impacts of Karst, 10th Multidisciplinary Conference San Antonio, Texas, p. 207–215. doi 10.1061/40796(177)22.

Trumbore, S.E., 1997, Potential responses of soil organic carbon to global environmental change, *in* Proceedings of the National Academy of Science of the US, v. 94, p. 8284–8291.

White, W.B., 1988, Geomorphology and Hydrology of Karst Terrains, Oxford, Oxford University Press, 464 p.

Whitman, W., Coleman, D.C., and Wiebe, W.J., 1998, Prokaryotes: The unseen majority, *in* Proceedings of the National Academy of Sciences USA, v. 95, p. 6578–6583.

Yamashita, Y., and Tanoue, E., 2003, Chemical characterization of protein-like fluorophores in DOM in relation to aromatic amino acids: Marine Chemistry, v. 82, p. 255–271.

Zsolnay, Á., Baigar, E., Jimenez, M., Steinweg, B., and Saccomandi, F., 1999, Differentiating with fluorescence spectroscopy the sources of dissolved organic matter in soils subjected to drying: Chemosphere, v. 38, p. 45–50.

GUIDE TO AUTHORS

The *Journal of Cave and Karst Studies* is a multidisciplinary journal devoted to cave and karst research. The *Journal* is seeking original, unpublished manuscripts concerning the scientific study of caves or other karst features. Authors do not need to be members of the National Speleological Society, but preference is given to manuscripts of importance to North American speleology.

LANGUAGES: The *Journal of Cave and Karst Studies* uses American-style English as its standard language and spelling style, with the exception of allowing a second abstract in another language when room allows. In the case of proper names, the *Journal* tries to accommodate other spellings and punctuation styles. In cases where the Editor-in-Chief finds it appropriate to use non-English words outside of proper names (generally where no equivalent English word exists), the *Journal* italicizes them. However, the common abbreviations i.e., e.g., et al., and etc. should appear in roman text. Authors are encouraged to write for our combined professional and amateur readerships.

CONTENT: Each paper will contain a title with the authors' names and addresses, an abstract, and the text of the paper, including a summary or conclusions section. Acknowledgments and references follow the text.

ABSTRACTS: An abstract stating the essential points and results must accompany all articles. An abstract is a summary, not a promise of what topics are covered in the paper.

STYLE: The *Journal* consults The Chicago Manual of Style on most general style issues.

REFERENCES: In the text, references to previously published work should be followed by the relevant author's name and date (and page number, when appropriate) in parentheses. All cited references are alphabetical at the end of the manuscript with senior author's last name first, followed by date of publication, title, publisher, volume, and page numbers. Geological Society of America format should be used (see http://www.geosociety.org/pubs/geoguid5.htm). Please do not abbreviate periodical titles. Web references are acceptable when deemed appropriate. The references should follow the style of: Author (or publisher), year, Webpage title: Publisher (if a specific author is available), full URL (e.g., http://www.usgs.gov/citguide.html) and date when the web site was accessed in brackets; for example [accessed July 16, 2002]. If there are specific authors given, use their name and list the responsible organization as publisher. Because of the ephemeral nature of websites, please provide the specific date. Citations within the text should read: (Author, Year).

SUBMISSION: Effective July 2007, all manuscripts are to be submitted via AllenTrack, a web-based system for online submission. The web address is http://jcks.allentrack2.net. Instructions are provided at that address. At your first visit, you will be prompted to establish a login and password, after which you will enter information about your manuscript (e.g., authors and addresses, manuscript title, abstract, etc.). You will then enter your manuscript, tables, and figure files separately or all together as part of the manuscript. Manuscript files can be uploaded as DOC, WPD, RTF, TXT, or LaTeX. A DOC template with additional manuscript specifications may be downloaded. (Note: LaTeX files should not use any unusual style files; a LaTeX template and BiBTeX file for the *Journal* may be downloaded or obtained from the Editor-in-Chief.) Table files can be uploaded as DOC, WPD, RTF, TXT, or LaTeX files, and figure files can be uploaded as TIFF, EPS, AI, or CDR files. Alternatively, authors may submit manuscripts as PDF or HTML files, but if the manuscript is accepted for publication, the manuscript will need to be submitted as one of the accepted file types listed above. Manuscripts must be typed, double spaced, and single-sided. Manuscripts should be no longer than 10,000 words plus tables and figures, but exceptions are permitted on a case-by-case basis. Authors of accepted papers exceeding this limit may have to pay a current page charge for the extra pages unless decided otherwise by the Editor-in-Chief. Extensive supporting data will be placed on the *Journal*'s website with a paper copy placed in the NSS archives and library. The data that are used within a paper must be made available. Authors may be required to provide supporting data in a fundamental format, such as ASCII for text data or comma-delimited ASCII for tabular data.

DISCUSSIONS: Critical discussions of papers previously published in the *Journal* are welcome. Authors will be given an opportunity to reply. Discussions and replies must be limited to a maximum of 1000 words and discussions will be subject to review before publication. Discussions must be within 6 months after the original article appears.

MEASUREMENTS: All measurements will be in Systeme Internationale (metric) except when quoting historical references. Other units will be allowed where necessary if placed in parentheses and following the SI units.

FIGURES: Figures and lettering must be neat and legible. Figure captions should be on a separate sheet of paper and not within the figure. Figures should be numbered in sequence and referred to in the text by inserting (Fig. x). Most figures will be reduced, hence the lettering should be large. Photographs must be sharp and high contrast. Color will generally only be printed at author's expense.

TABLES: See http://www.caves.org/pub/journal/PDF/Tables.pdf to get guidelines for table layout.

COPYRIGHT AND AUTHOR'S RESPONSIBILITIES: It is the author's responsibility to clear any copyright or acknowledgement matters concerning text, tables, or figures used. Authors should also ensure adequate attention to sensitive or legal issues such as land owner and land manager concerns or policies.

PROCESS: All submitted manuscripts are sent out to at least two experts in the field. Reviewed manuscripts are then returned to the author for consideration of the referees' remarks and revision, where appropriate. Revised manuscripts are returned to the appropriate Associate Editor who then recommends acceptance or rejection. The Editor-in-Chief makes final decisions regarding publication. Upon acceptance, the senior author will be sent one set of PDF proofs for review. Examine the current issue for more information about the format used.

ELECTRONIC FILES: The *Journal* is printed at high resolution. Illustrations must be a minimum of 300 dpi for acceptance.

Journal of Cave and Karst Studies

Volume 71 Number 2 August 2009